

In compliance with the  
Canadian Privacy Legislation  
some supporting forms  
may have been removed from  
this dissertation.

While these forms may be included  
in the document page count,  
their removal does not represent  
any loss of content from the dissertation.



**University of Alberta**

A Molecular Dissection of the Forkhead Domain in FOXC1, a Transcription  
Factor Mutated in Axenfeld-Rieger Malformations

By

Ramsey Saleem



A thesis submitted to the Faculty of Graduate Studies and Research in partial  
fulfilment of the requirements for the degree of Doctor of Philosophy.

In

Medical Sciences – Medical Genetics

Edmonton, Alberta  
Fall, 2003



National Library  
of Canada

Bibliothèque nationale  
du Canada

Acquisitions and  
Bibliographic Services

Acquisisitons et  
services bibliographiques

395 Wellington Street  
Ottawa ON K1A 0N4  
Canada

395, rue Wellington  
Ottawa ON K1A 0N4  
Canada

*Your file* *Votre référence*  
*ISBN: 0-612-88042-7*  
*Our file* *Notre référence*  
*ISBN: 0-612-88042-7*

The author has granted a non-exclusive licence allowing the National Library of Canada to reproduce, loan, distribute or sell copies of this thesis in microform, paper or electronic formats.

L'auteur a accordé une licence non exclusive permettant à la Bibliothèque nationale du Canada de reproduire, prêter, distribuer ou vendre des copies de cette thèse sous la forme de microfiche/film, de reproduction sur papier ou sur format électronique.

The author retains ownership of the copyright in this thesis. Neither the thesis nor substantial extracts from it may be printed or otherwise reproduced without the author's permission.

L'auteur conserve la propriété du droit d'auteur qui protège cette thèse. Ni la thèse ni des extraits substantiels de celle-ci ne doivent être imprimés ou autrement reproduits sans son autorisation.

# Canada

**University of Alberta**

**Library Release Form**

**Name of Author:** Ramsey Saleem

**Title of Thesis:** A Molecular Dissection of the Forkhead Domain in FOXC1, a Transcription Factor Mutated in Axenfeld-Rieger Malformations.

**Degree:** Doctor of Philosophy

**Year this Degree Granted:** 2003

Permission is hereby granted to the University of Alberta Library to reproduce single copies of this thesis and to lend or sell such copies for private, scholarly or scientific research purposes only.

The author reserves all other publication and other rights in association with the copyright in the thesis, and except as herein before provided, neither the thesis nor any substantial portion thereof may be printed or otherwise reproduced in any material form whatever without the author's prior written permission.

*July 14, 2003.*

University of Alberta

Faculty of Graduate Studies and Research

The undersigned certify that they have read, and recommend to the Faculty of Graduate Studies and Research for acceptance, a thesis entitled **A Molecular Dissection of the Forkhead Domain in FOXC1, a Transcription Factor Mutated in Axenfeld-Rieger Malformations** submitted by Ramsey Saleem in partial fulfillment of the requirements for the degree of Doctor of Philosophy in Medical Sciences – Medical Genetics.

Date

July 14, 2003

## **Abstract**

The developmental disease Axenfeld-Rieger malformation is thought to arise from defects in the migration and differentiation of neural crest cells. Individuals with Axenfeld-Rieger malformation present with dysgenesis of the anterior segment of the eye and have a 50% increase in the risk of developing glaucoma, a progressively blinding condition. Axenfeld-Rieger malformation is genetically heterogeneous with mutations in FOXC1 underlying Axenfeld-Rieger malformations mapping to human chromosome 6p25. FOXC1 is a member of the FOX family of developmentally important transcription factors, characterized by the presence of the forkhead domain, a highly conserved DNA binding motif. To date, all FOXC1 missense mutations reported occur within the forkhead domain. These missense mutations provided an opportunity to understand the functional significance of individual amino acids within the forkhead domain in a biologically relevant manner, as they are disease causing in humans. It was found that these missense mutations caused specific disruptions to FOXC1 with respect to protein stability, nuclear localization, DNA binding affinity, and DNA binding specificity. All of the missense mutations tested had the net effect of reducing the transactivation capacity of FOXC1.

A second line of investigation was undertaken to further probe the structure of the FOXC1 forkhead domain. Using predictions based on computational modeling of the FOXC1 forkhead domain, several of the forkhead domain residues studied in the missense mutation analyses were converted individually to positive, negative, or neutrally charged amino acids, perturbing

the forkhead domain to different degrees, depending on both the position and charge of the converted amino acid.

These experiments have provided a detailed analysis of several key residues within the highly conserved forkhead domain of FOXC1. I have generated a body of experimental data demonstrating how amino acids within the forkhead domain function to provide the correct structural organization of the forkhead domain, localize FOXC1 to the nuclei of cells, and establish and regulate FOXC1-DNA interactions. Given the limited topological variation of forkhead domains, due to the high conservation of residues, models of forkhead domain function derived from these data may be relevant to other members of the FOX family of transcription factors.

## **Acknowledgements**

I would like to thank the entire laboratory of Dr. Michael Walter for all their assistance and friendship. In particular I would like to thank Dr. Michael Walter for his mentoring and intellectual contributions and Dr. Fred Berry for intellectual and experimental collaborations. I would also like to thank Drs. Richard Wozniak and Marcello Marelli for their initial guidance in the process of doing rigorous science and implanting a firm skepticism of data in me. Thank you to the members of my committee, Drs. Richard Rachubinski and Moira Glerum, for their time and help. Finally, thank you to Jacqueline for her love and support, Alan and Maureen for always being there for us, my Dad and my Mom, both for so many things, my brothers, 70 Sunshine Divine, and all my squash partners. Go forth and multiply.

## Table of Contents

### List of Tables

### List of Figures

### List of Abbreviations

<b>INTRODUCTION</b>	<b>1</b>
<b>Locus and Expression</b>	<b>1</b>
Expression of Foxc1 in the somites and presomitic mesoderm.	2
Cardiac expression of Foxc1.	7
Urogenital expression of Foxc1	10
Ocular expression of Foxc1	10
<b>Clinical Description</b>	<b>11</b>
Affected ocular tissues in AR malformation share a neural crest lineage.	12
Axenfeld-Rieger Malformation	15
Management and Counselling	18
<b>Identification of the gene and mutational spectrum</b>	<b>19</b>
<b>FOXC1 Animal Model Studies</b>	<b>20</b>
The Congenital Hydrocephalus mouse	20
Foxc1 <sup>lacZ</sup> and ch homozygous nulls have severe developmental defects	26
Foxc1 <sup>lacZ</sup> and ch heterozygotes have ocular defects similar to Axenfeld-Rieger malformations	33
Foxc1 and Foxc2 are important regulators of somitogenesis and cardiovascular development	36
<b>Developmental Pathogenesis</b>	<b>39</b>
<b>Forkhead Domain Structure</b>	<b>47</b>
<b>The Transactivation Domains</b>	<b>52</b>
<b>Rationale for Project</b>	<b>55</b>
<b>RESULTS</b>	<b>58</b>
<b>FOXC1 localization and delineation of Nuclear Localization Signals</b>	<b>58</b>
<b>Analysis of FOXC1 Missense Mutations</b>	<b>61</b>
Expression and mutagenesis of FOXC1	61

The FOXC1 I87M mutation results in reduced protein levels.	64
Subcellular Localization	69
Electrophoretic Mobility Shift Assays (EMSAs)	74
<b>FOXC1</b>	<b>77</b>
The binding specificity of the FOXC1 I126M mutation is altered	80
Transactivation assays	83
Some FOXC1 missense mutation transactivation defects can be restored by addition of an exogenous DNA binding domain	86
<b>Charge conversion studies at key forkhead domain residues</b>	<b>92</b>
FOXC1 expression is impaired by mutations at I87	92
Subcellular localization of charge conversion mutants	95
Charge conversion mutations differentially perturb the DNA binding capacity of FOXC1	99
Amino acids in $\alpha$ -helix 3 of the FHD regulate FOXC1 DNA binding specificity.	100
Transactivation Assays	103
<b>Helix 4 Alanine Mutagenesis Studies</b>	<b>108</b>
<b>Helix 1 Disruption Studies</b>	<b>117</b>
<b>DISCUSSION</b>	<b>123</b>
<b>Identification of Nuclear Localization Signals within the FOXC1 FHD</b>	<b>123</b>
<b>Analysis of the Region Preceding <math>\alpha</math>-Helix 1</b>	<b>124</b>
<b>Analysis of Altered Amino Acids within <math>\alpha</math>-Helix 1</b>	<b>127</b>
I87 is a key residue in the stability of the FOXC1 molecule	127
L86 functions to organize the FHD in such a manner that FOXC1 is transcriptionally competent	128
I91 is a key residue in the organization of the FHD with respect to nuclear localization and transcription	131
<b>Analysis of Loop/Helix4 Region</b>	<b>133</b>
<b>Analysis of Key Residues within Helix 3</b>	<b>137</b>
I126 is involved in FHD organization with respect to localization, transactivation, and DNA binding specificity	137
R127 is a key residue of the FHD with respect to FOXC1 function	139
S131 severely perturbs FOXC1 DNA binding capacity	142
Helix-3 Summary	142
<b>Architecture of other Helix-Turn-Helix DNA-binding Domains</b>	<b>143</b>

<b>Genotype and Phenotype Correlations</b>	<b>148</b>
<b>Future Directions</b>	<b>151</b>
<b>Conclusions</b>	<b>154</b>
<b>EXPERIMENTAL PROCEDURES</b>	<b>157</b>
Plasmid construction and mutagenesis	157
Cell transfection and Co-transfection Assays	160
Protein Extraction and Western Analysis	160
Immunofluorescence	161
Northern Analysis	161
Electrophoretic Mobility Shift Assay (EMSA)	162
Dual Luciferase Assay	162
Phosphorylation prediction	163
DNA modeling	163
<b>REFERENCES</b>	<b>164</b>

## LIST OF TABLES

Table 1. Summary of Human Mutations Reported in FOXC1.	21
Table 2. Summary of Genes affected by Foxc1 (Foxc2) deletions.	41
Table 3. The FOXC1 binding site and variant oligonucleotides.	77
Table 4. Summary of molecular defects caused by missense mutations in FOXC1.	90
Table 5. Summary of subcellular localization of wild type and converted FOXC1 molecules.	97
Table 6. Summary of the molecular consequences of conversion of these critical amino acid positions to an alanine, glutamic acid, or lysine residue.	108
Table 7. Primers used for site directed mutagenesis.	156
Table 8. Primers used for degenerate site directed mutagenesis.	157

## LIST OF FIGURES

Figure 1. Protein sequence alignment of human FOXC1 and murine Foxc1.	3
Figure 2. Expression of FOXC1 mRNA in the somites of the developing mouse.	5
Figure 3. Cardiovascular expression in Foxc1 lacZ mice.	8
Figure 4. Three waves of neural crest derived mesenchyme invade the developing eye.	13
Figure 5. Clinical features of Axenfeld–Rieger malformations.	16
Figure 6. A schematic showing the position of disease-causing, missense mutations within the FOXC1 forkhead domain.	24
Figure 7. Analysis of Mice Homozygous for Foxc1 lacZ.	27
Figure 8. Kidney and ureter abnormalities in newborn mice homozygous for Foxc1 <sup>ch</sup> .	31
Figure 9. Axenfeld Rieger-like malformations seen in Foxc1 mutant mice.	34
Figure 10. Structure of the forkhead domain.	48
Figure 11. Position of FOXC1 disease-causing missense mutations studied herein, relative to FHD secondary structures.	50
Figure 12. FOXC1 transactivation domains.	53
Figure 13. The FOXC1 NLS resides in the FHD.	59
Figure 14. Residues in the FOXC1 FHD are sufficient for nuclear	62

localization.	
Figure 15. Western blot analysis of both recombinant FOXC1 and FOXC1 containing missense mutations.	65
Figure 16. The I87M mutation leads to a reduction in FOXC1 protein levels.	67
Figure 17. Missense mutations can perturb the nuclear localization of FOXC1.	70
Figure 18. Nuclear localization signals and the positions of the missense mutations relative to the FHD secondary structures.	75
Figure 19. FOXC1 missense mutations can disrupt the DNA-binding capacity of FOXC1.	78
Figure 20. Effect of FOXC1 missense mutations on DNA-binding specificity.	81
Figure 21. FOXC1 is an activator of transcription, a function disrupted by missense mutations.	84
Figure 22. The addition of an exogenous DNA binding domain can restore transactivation capacity in some FOXC1 missense mutations.	87
Figure 23. Conversion of I87 to an alanine, glutamate, or lysine residue reduces protein levels of FOXC1.	92
Figure 24. A, E, and K conversions in the FOXC1 FHD differentially disrupt the nuclear localization of FOXC1.	95
Figure 25. FOXC1 A, E, and K mutations disrupt the DNA-binding capacity of FOXC1 to different extents depending on position and	100

charge.

Figure 26. Conversion of R127 to an alanine or lysine residue alters the binding specificity of FOXC1. 103

Figure 27. Disruption of transactivation of a luciferase reporter construct by FOXC1 A/E/K proteins. 105

Figure 28. A schematic of the FHD, indicating the position of the amino acids converted in the  $\alpha$ -helix 4 studies. 109

Figure 29. Conversion of amino acids in Helix 4 of the FHD do not perturb FOXC1 DNA binding. 111

Figure 30. Conversion of amino acids in helix 4 of the FHD does not alter the DNA binding specificity of FOXC1. 113

Figure 31. The conversion of L86 to a proline severely disrupts FOXC1 localization and DNA binding capacity 117

Figure 32. Transactivation studies with FOXC1 L86P. 119

Figure 33. The topology of the FHD with the function of specific regions indicated. 142

## LIST OF ABBREVIATIONS

BD – binding domain

C – cytoplasmic

*ch* – congenial hydrocephalus

DAPI – 4, 6-diamidino-2-phenyl-indole

dpc – days post coitum

*dyl* – dysgenic lens

EMSA – Electrophoretic mobility shift assay

FHD – Forkhead domain

FOX – Forkhead Box

GFP – green fluorescent protein

HTH – helix-turn-helix

KDa – kilodaltons

L-DOPA – L-dihydroxyphenylalanine

N – nuclear

N + C – nuclear and cytoplasmic

NLSs – nuclear localization signals

NMR – nuclear magnetic resonance

PSM – presomitic mesoderm

SDS-PAGE – sodium dodecyl sulfate polyacrylamide gel electrophoresis

TK – thymidine kinase

TM – trabecular meshwork

Tyr – Tyrosinase

## **Introduction**

When a 110 amino acid, monomeric DNA-binding domain was first identified as a region of almost perfect homology between the *Drosophila melanogaster* protein *Fork head* and rat Hepatocyte Nuclear Factor 3 (HNF3) proteins (Weigel and Jackle 1990), it became clear that this domain would define a new family of transcription factors. Since this time, more than 135 genes have been identified in a wide range of species, from yeast to humans, that contain the forkhead domain (FHD), the defining motif of the FOX (Forkhead Box) family. Members of the FOX family are involved in a variety of developmental processes, including embryogenesis, tissue-specific cell differentiation, cell cycle regulation, and cell signalling cascades. In addition to these cellular processes, FOX genes are involved in aberrant biological events such as tumorigenesis (Carlsson and Mahlapuu 2002; Kaufmann and Knochel 1996).

## **Locus and Expression**

*FOXC1* (previously referred to as FREAC3 and FKHL7) is a member of the FOX family of transcription factors. *FOXC1* is a single exon gene, located at 6p25 in the human genome. The 1659-bp open reading frame encodes a protein 553 amino acids in length. *FOXC1* is expressed in multiple fetal and adult tissues, as determined by Northern blot analysis (Mears et al. 1998; Nishimura et al. 1998; Pierrou et al. 1994). A 3.9-4.5 kb mRNA is detected with the highest expression in adult kidney, heart, peripheral blood leukocytes, prostate, and in fetal kidney. An alternative transcript 3.4-4.0 kb in size is detected in fetal

kidney, likely generated by differential polyadenylation (Mears et al. 1998; Nishimura et al. 1998; Pierrou et al. 1994). PCR analysis detects *FOXC1* in human fetal craniofacial RNA and in human adult iris (Mears et al. 1998).

*Foxc1* (formerly *Mfl* and *Fkh1*) is the murine homologue of human *FOXC1*. At the amino acid level the forkhead domains of human *FOXC1* and murine *Foxc1* are identical, and outside the forkhead domain the proteins are 92% identical (Figure 1). Adult expression of murine *Foxc1* is seen in multiple tissues, with the exception of liver (Hiemisch et al. 1998; Nishimura et al. 1998). The highest expression of mouse *Foxc1* is found in heart, kidney, adrenal gland, and brain, as determined by RNase protection assays (Hiemisch et al. 1998). Embryonically, *Foxc1* expression has been studied extensively. A significant advance to these studies was the generation of a mouse carrying a *LacZ* disruption of *Foxc1* (*Foxc1<sup>lacZ</sup>*), which allows analysis of *Foxc1* promoter activity by staining for  $\beta$ -galactosidase (Kume et al. 1998).

#### *Expression of Foxc1 in the somites and presomitic mesoderm.*

Embryonic expression of *Foxc1* is seen in the entire non-notochordal mesoderm including the prechordal plate (Sasaki and Hogan 1993). Between 7.5-9.0 days post coitum (dpc), *Foxc1* is first expressed in the developing embryo in the presomitic mesoderm (PSM) and somites (Hiemisch et al. 1998; Sasaki and Hogan 1993). Interestingly, immunohistochemistry experiments show that by 9.5 dpc *Foxc1* protein in the presomitic mesoderm forms a gradient from low levels in the posterior PSM to high levels in the anterior PSM (Figure 2)

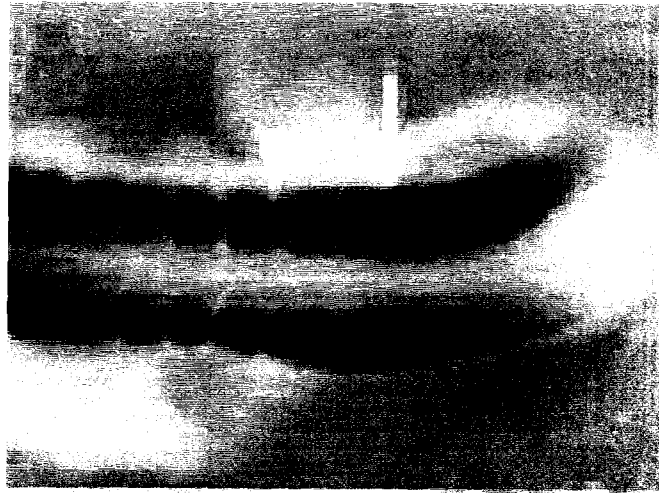
**Figure 1. Protein sequence alignment of human FOXC1 and murine Foxc1.**

The forkhead domain is bounded by the box. The human and mouse sequences show 97% identity with 100% identity in the forkhead domain itself. Human FOXC1 is 553 amino acids in length.



**Figure 2. Expression of *Foxc1* mRNA in the somites of the developing mouse.**

Expressed mRNA was detected by whole-mount *in situ* hybridization of day 9.5 embryos. *Foxc1* is strongly expressed in the presomitic mesoderm and somites. The arrowheads indicate the boundary between the newly forming somites (S0) and the formed somite (S1), while the arrows indicate the regions of highest *Foxc1* expression. Adapted from (Kume et al. 2001).



(Kume et al. 2001). Transverse sections at the PSM level also detect the highest levels of *Foxc1* RNA closest to the neural tube, forming a dorsal-ventral gradient (Kume et al. 2000). Expression of the zebrafish homologue of *FOXCI*, *foxc1a*, is seen in the developing somites of zebrafish (Topczewska et al. 2001; Topczewska et al. 2001). As somitogenesis proceeds, it becomes evident that *Foxc1* is also required for skeletal development, where it is expressed by 11.5-12.5 dpc in the condensing mesenchyme of the vertebrae and forelimbs (Hiemisch et al. 1998; Kume et al. 1998).

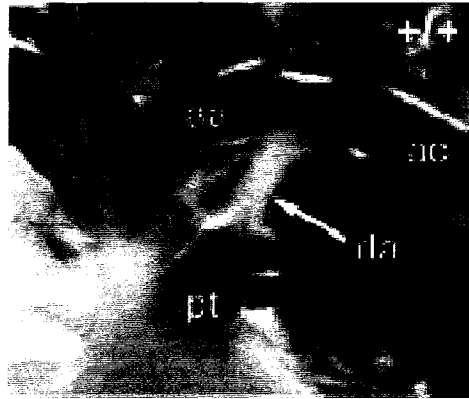
#### *Cardiac expression of Foxc1.*

*Foxc1* is involved in early cardiac development (Figure 3). Between 7.5-9.0 dpc *Foxc1* is first seen in the developing embryo in the first branchial arches (Hiemisch et al. 1998; Sasaki and Hogan 1993). *Foxc1* is also weakly expressed during early embryogenesis in the endocardium, the dorsal portion of the pericardial peritoneal canal (Swiderski et al. 1999), the pharyngeal arch system, and endothelium of the heart (Winnier et al. 1999). There is robust expression of *Foxc1* in the heart at 10.5-11.5 dpc, as the valves and septae form, with expression in the mesenchyme and endothelium of the aortic arches at 10.5 dpc (Winnier et al. 1999). By 11.5-13 dpc *Foxc1* is expressed in the mesenchyme surrounding all arterial vessels, the mesenchyme of each leaflet of the semilunar valves, the future spiral septum outflow tract, the future atrial septum, the endocardial cushion tissue of the heart, and the semilunar, tricuspid, and mitral valves. *Foxc1* is also expressed uniformly throughout the smooth muscle of the

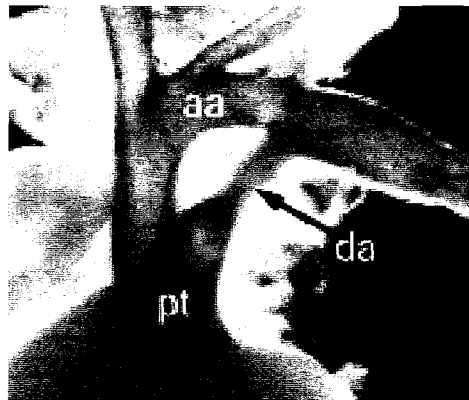
**Figure 3. Cardiovascular expression in *Foxc1 lacZ* mice.**

Shown are newborn hearts with the atria, veins, and nerves removed for better viewing of the aortic arch. (A) Wild-type heart in which ink injection reveals the aortic arch (aa), pulmonary trunk (pt), and descending aorta (ao) and the complete closure of the ductus arteriosus (da). (B) Normal *Foxc1 lacZ*<sup>+/-</sup> heart, where expression of *Foxc1* can be seen in the aortic arch, the pulmonary trunk and descending aorta. The heart has been stained in whole mount for lacZ activity to show *Foxc1 lacZ* expression. *Foxc1 lacZ* expression is down regulated in the closed ductus arteriosus. Figure adapted from (Winnier et al. 1999).

**A.**



**B.**



pulmonary trunk (Swiderski et al. 1999; Winnier et al. 1999). Swiderski et al. (Swiderski et al. 1999) also found expression of *Foxc1* in the venous valve, the trabeculated region of the ventricular wall, the aortic and pulmonary valves, and the septum primum. By 15 dpc there is a general decrease in *Foxc1* expression but there was still a persistence of signal in the atrial septum, and in the venous, mitral, tricuspid, aortic, and pulmonary valves (Swiderski et al. 1999). *Foxc1* expression is still present in adult mouse cardiac tissue in the aorta, the pulmonary trunk, the endocardium, and the smooth muscle and endothelium of the coronary vessels (Winnier et al. 1999).

#### *Urogenital expression of Foxc1*

Expression of *Foxc1* is also seen in the presumptive intermediate mesoderm that will give rise to the urogenital system (Kume et al. 2000). At 9.5 dpc there is urogenital expression in the mesonephric mesenchyme alongside the Wolffian duct (Kume et al. 2000). *Foxc1* is expressed weakly in the Wolffian duct itself, although by 11.5-12.5 dpc no expression of *Foxc1* in the Wolffian duct can be seen. As development of the urogenital system proceeds, *Foxc1* becomes expressed in the metanephric mesenchyme.

#### *Ocular expression of Foxc1*

Expression of *Foxc1* is also seen in the cells that will give rise to the ocular tissues. From 10.5-11.5 dpc, *Foxc1* is highly expressed in the head mesenchyme and by 11.5-12.5 dpc, the specific ocular tissues expressing *Foxc1*

can be identified. *Foxc1* is expressed in the mesenchyme cells of the optic cup between the lens and the retina, the periocular mesenchyme, the cornea, the prospective trabecular meshwork, the sclera, the ectoderm of the future inner eyelids, and the future conjunctival epithelium (Kidson et al. 1999). *Foxc1* expression persists in the prospective trabecular meshwork, the sclera, and the conjunctival epithelium at 16.5 dpc (Kidson et al. 1999).

The prevalent ocular expression of *Foxc1* is consistent with the idea that *Foxc1* is a major eye development locus. Similarly, the prominent expression profiles of *Foxc1* in the early nephrogenic tissues, developing cardiac tissues, and during the processes of chondrogenesis and somitogenesis, indicates *Foxc1* is an important regulator of organogenesis.

### **Clinical Description**

Axenfeld-Rieger (AR) malformations are a group of genetically and phenotypically heterogeneous disorders. Axenfeld-Rieger malformations have been mapped to three chromosomal loci: 4q25, 6p25, and 13q14. While the gene at 13q14 has yet to be identified, it is known that mutations in *PITX2* cause Axenfeld-Rieger malformations mapping to 4q25 (Alward et al. 1998; Kulak et al. 1998; Semina et al. 1996). Mutations in *FOXC1* underlie Axenfeld-Rieger malformations mapping to 6p25 (Mears et al. 1998; Nishimura et al. 1998). Axenfeld-Rieger malformations are transmitted in an autosomal dominant manner and are highly penetrant but vary greatly in expressivity. Patients with

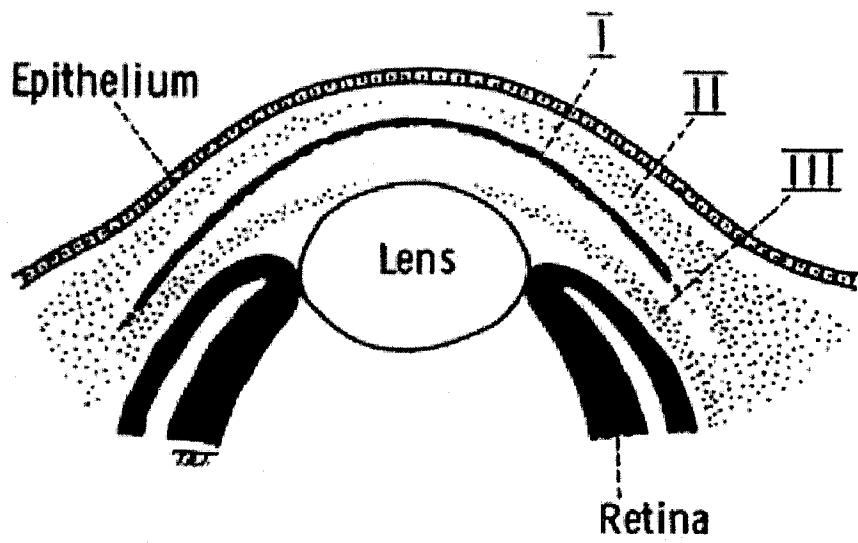
Axenfeld-Rieger malformations typically have a 50% higher incidence of glaucoma, the dire consequence of AR ocular malformations.

*Affected ocular tissues in AR malformation share a neural crest lineage.*

Both the ocular and non-ocular findings seen in patients with AR malformations are thought to arise from the aberrant migration and differentiation of neural crest derived cells (Kume et al. 1998; Shields 1983). Since there are no mesodermal somites in the head region, the majority of the mesenchyme is of neural crest origin. Cells from the neural crest migrate into the developing ocular areas in successive waves (Figure 4) (Jakobiec 1982; Johnston et al. 1979). In the first wave, neural crest cells invade the presumptive eye and form an endothelial layer on the anterior chamber. This layer will develop into connective tissue between the lens and the corneal endothelium. The second wave of neural crest cells form the corneal stroma, uveal meshwork and pupillary membrane, while the third wave forms the iris stroma. The normal differentiation and development of the corneal endothelium is entwined with the normal development and maturation of the aqueous outflow structures of the eye (Johnston et al. 1979; Kaiser-Kupfer 1989; Shields 1983). These structures include the trabecular meshwork, Schlemms canal, and juxtacanicular tissues, which all function in maintaining normal ranges of interocular pressure within the eye by regulating the outflow of aqueous tissue. A prevailing theory in the field of glaucoma research is that blockage or functional disruption of these drainage tissues leads to an increase in

**Figure 4. Three waves of neural crest derived mesenchyme invade the developing eye.**

Wave I forms the corneal endothelium. Wave II forms the corneal stroma, uveal meshwork and pupillary membrane. Wave III forms the iris stroma. Taken from (Jakobiec 1982).



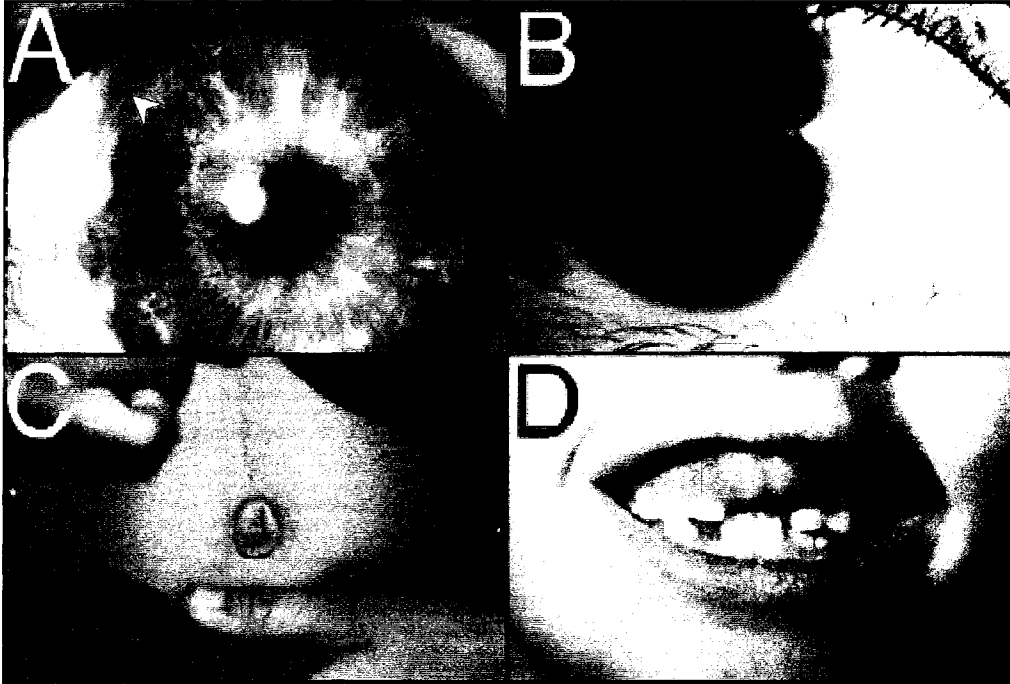
interocular pressure, eventually leading to the optic nerve damage and loss of vision characterizing glaucoma.

### *Axenfeld-Rieger Malformation*

Historically Axenfeld-Rieger malformations have been classified as Axenfeld anomaly, Rieger anomaly, or Rieger syndrome, a group of related conditions. Patients were considered to have Axenfeld anomaly when they presented with iris strands connecting the iridocorneal angle to the trabecular meshwork, and a prominent, anteriorly displaced Schwalbe's line (Figure 5a and b). If patients presented with iris hypoplasia, corectopia, or polycoria, they were considered to have Rieger anomaly. When these findings were concurrent with systemic defects, patients were considered to have Rieger syndrome. Systemic findings in Axenfeld-Rieger patients with *FOXC1* mutations include maxillary hypoplasia, telecanthus, hypertelorism, a broad, flat nasal bridge, hypodontia, hypospadias, and a protruding umbilicus (Figure 5c and d). Cardiac anomalies such as atrial septae defects, mitral valve defects, and tricuspid valve defects have been detected within patients with *FOXC1* mutations, although evidence of *FOXC1* mutations underlying cardiac defects in human is still anecdotal (Kawase et al. 2001; Mears et al. 1998; Swiderski et al. 1999; Winnier et al. 1999). Cardiac defects may simply be cosegregating with AR malformations, but given the high degree of involvement of *Foxc1* in the developing murine heart it is quite possible that *FOXC1* mutations underlie these cardiac defects.

**Figure 5. Clinical features of Axenfeld–Rieger malformations.**

A. Slate-gray, hypoplastic iris revealing the underlying pupillary sphincter muscle. Note sclerocornea (9 o'clock), prominent line of Schwalbe (5, 11 o'clock; white arrowhead at 11 o'clock) and elliptical pupil. B. Nasally displaced pupil and chocolate-colored, strongly hypoplastic iris with full-thickness iris stromal tears. Some sclerocornea is visible. C. Excessive periumbilical skin. D. Small, misshapen and absent teeth in an AR malformation patient. Taken from (Lines et al. 2002).



The overlap of ocular and nonocular defects in patients with Axenfeld anomaly, Rieger anomaly, and Rieger syndrome makes this classification scheme somewhat arbitrary, leading to the proposal that these defects be classified as Axenfeld-Rieger anomaly, for patients presenting with ocular defects only, and Axenfeld-Rieger syndrome, for patients presenting with ocular and systemic defects (Shields 1983). In light of recent molecular data, showing that mutations to a single gene can cause both the anomalous and syndromic forms of Axenfeld-Rieger, the term Axenfeld-Rieger malformations is useful as an encompassing term to describe these defects.

#### *Management and Counselling*

The most severe consequence of Axenfeld-Rieger malformations is the increased risk of developing glaucoma. The glaucoma that Axenfeld-Rieger patients develop is managed with a variety of medicinal and surgical treatments. In adult cases of Axenfeld-Rieger glaucoma, doctors initially recommend a medicinal course of treatment. These treatments include the use of beta-blocking agents and carbonic anhydrase inhibitors to reduce the production of aqueous humor, although the use of pilocarpin and other miotics may be ineffective in the treatment of AR-associated glaucoma (McDonald, I. personal communication). Surgery is recommended in cases where medical treatment does not help, and is also recommended in infantile cases. Surgical treatments include goniotomy, trabeculotomy, and trabeculectomy. The last surgical procedure is often the treatment given to patients with AR-associated glaucoma.

## Identification of the gene and mutational spectrum

The distal end of chromosome 6 was known to be important for ocular development from clinical and cytogenetic analysis of patients with distal deletions of 6p or ring chromosome 6 (Palmer et al. 1991; Plaja et al. 1994; Zurcher et al. 1990). Patients with 6p terminal deletions present with various ocular defects, such as iris hypoplasia and glaucoma, as well as non-ocular defects, including facial and dental anomalies, and cardiac defects. Linkage analysis in two families presenting with iris hypoplasia, goniodysgenesis, and a high frequency of juvenile glaucoma demonstrated the presence of an important ocular development locus at 6p25, and identified *FOXC1* as a candidate gene (Mears et al. 1996). Subsequent linkage analysis in a family diagnosed with Axenfeld-Rieger anomaly demonstrated that this disease phenotype also mapped to a critical region located at 6p25 (Gould et al. 1997). The identification of this important ocular locus led to direct analysis of candidate genes within the 6p25 critical region. These analyses allowed two groups to independently identify mutations in *FOXC1* within families diagnosed with Axenfeld-Rieger malformations (Mears et al. 1998; Nishimura et al. 1998). Concurrent with the findings in humans, *Foxc1* was identified as the gene underlying the mouse *congenital hydrocephalus* phenotype (Hong et al. 1999; Kume et al. 1998). Interestingly, some patients with deletions of 6p25 also present with hydrocephalus (Kume et al. 1998).

Mutations reported thus far in *FOXC1* have been either frameshift mutations upstream of the forkhead domain resulting in truncated proteins or

missense mutations within the forkhead domain (Table 1). One single base pair deletion was found downstream of the forkhead domain that removes only the last 49 amino acids of FOXC1 (Nishimura et al. 2001). All of the AR malformation-causing missense mutations identified to date in *FOXC1* occur within the FHD (Figure 6). Mutations at P79 have occurred twice, to 79L in one pedigree and to 79T in another (Table 1). Two different mutations have also occurred at I91 to an S and T, respectively (Table 1). The S131L and M161K mutations have each been identified in two different pedigrees and are thus likely recurring mutations (Table 1). Interestingly, the *FOXC1* F112S mutation corresponds to the same position as a F98S mutation in *Foxe3* found in the mouse mutant *dysgenic lens* (Blixt et al. 2000). There is also a R127H mutation in FOXC1 corresponding to a R553H mutation in FOXP2, a gene involved in speech capacity (Lai et al. 2001), and a R121H mutation in FOXC2. Similarly, the S131L mutation in FOXC1 corresponds to a S125L mutation in FOXC2. The occurrence of the same mutations in different FOX family genes is likely indicative of a low tolerance for change among highly conserved key residues within the forkhead domain.

### **FOXC1 Animal Model Studies**

#### *The Congenital Hydrocephalus mouse*

The spontaneous mouse mutation, *congenital hydrocephalus (ch)*, was described by Gruneberg in 1943. In 1998 a point mutation generating a truncated protein lacking the forkhead domain, was identified in *Foxc1* as the *ch* mutation

**Table 1.** Summary of Human Mutations Reported in FOXC1.

<b>Mutation</b>	<b>Position</b>	<b>Clinical Features</b>	<b>Diagnosis</b>	<b>Reference</b>
P79L	236	NL	Rieger Anomaly	(Nishimura et al. 2001)
P79T	235	Early onset glaucoma, posterior embryotoxon, iris hypoplasia, iris strands, scrotum defects, persistence of pupillary membrane, atrial septal defects.	Axenveld-Rieger syndrome	(Suzuki et al. 2001)
S82T	245	Glaucoma, corectopia, goniodysgenesis, iris hypoplasia, iris strands, posterior embryotoxon, atrial septal defects, hearing loss.	Axenveld-Rieger Anomaly	(Mears et al. 1998)
L86F	255,256	Glaucoma, posterior embryotoxon, iris hypoplasia, iridocorneal adhesions, corectopia, short stature, obesity, myocardial infarction, dental anomalies.	Axenveld-Rieger Malformation	(Saleem et al., submitted)
I87M	261	Glaucoma, iris strands, goniodysgenesis, posterior embryotoxon.	Axenveld-Rieger Anomaly	(Mears et al. 1998)
I91S	272	Parents: posterior embryotoxon, Children; iris hypoplasia and severe early onset glaucoma	Axenveld-Rieger Anomaly	(Kawase et al. 2001)
I91T	272	NL	Axenveld-Rieger Malformation	(Raymond et al. 2001)
F112S	335	A spectrum of anterior segment defects including corectopia, posterior embryotoxon, iris hypoplasia. Glaucoma from 5 months of age in one patient. Cardiac defects including mitral valve defects, mitral and tricuspid valve defects. Hypodontia, facial anomalies.	Rieger syndrome, Peter's Anomaly	(Honkanen et al. 2003; Nishimura et al. 1998; Swiderski et al. 1999)
I126M	378	Glaucoma, severe Axenveld anomalies	Axenveld Anomaly	(Nishimura et al. 1998)
R127H	380	Parents: posterior embryotoxon, Children; iris hypoplasia and severe early onset glaucoma	Axenveld-Rieger Anomaly	(Kawase et al. 2001)
S131L*	392	Glaucoma, classic Rieger anomalies, Axenveld anomalies	Rieger Anomaly, Axenveld Anomaly	(Nishimura et al. 2001; Nishimura et al. 1998)
M161K*	482	Severe early onset glaucoma, iris hypoplasia	Axenveld-Rieger Anomaly	(Komatireddy et al. 2003; Panicker et al. 2002)

Q2Stop	4	Glaucoma	Axenveld-Rieger Anomaly	(Komatireddy et al. 2003)
Q23Stop	67	Iris hypoplasia, corectopia, posterior embryotoxon, iris strands, flat midface, microdontia, umbilical anomalies, cardiac defects, hearing loss	Axenveld-Rieger Syndrome	(Mirzayans et al. 2000)
Q123Stop	367	Glaucoma, phthisis bulbi, high intraocular pressure.	Axenveld-Rieger Anomaly	(Komatireddy et al. 2003)
10-bp deletion	93-102	Glaucoma, iris hypoplasia, goniodysgenesis.	Axenveld-Rieger Anomaly	(Mears et al. 1998)
11-bp deletion	153-162	Glaucoma, Rieger anomalies, iris hypoplasia	Axenveld Anomaly	(Nishimura et al. 1998)
22-bp insertion	26-47	Parents: posterior embryotoxon, Children; iris hypoplasia and severe early onset glaucoma	Axenveld Anomaly	(Kawase et al. 2001)
10-bp deletion	99-108	NL	Axenveld Anomaly	(Nishimura et al. 2001)
8-bp deletion	116-123	NL	Rieger Anomaly	(Nishimura et al. 2001)
1-bp deletion	210	Ocular findings not listed, atrial septal defects.	Axenveld-Rieger Anomaly	(Swiderski et al. 1999)
1-bp insertion	262-265	NL	Axenveld-Rieger Anomaly	(Nishimura et al. 2001)
1-bp insertion	286	Iris hypoplasia, posterior embryotoxon, mild increased ocular pressure.	Axenveld Anomaly	(Kawase et al. 2001)
1-bp deletion	1512	NL	Axenveld Anomaly	(Nishimura et al. 2001)
6p25 duplication	NA	Glaucoma, iris hypoplasia, iris strands, goniodysgenesis.	Likely Rieger Anomaly	(Lehmann et al. 2000)
6p25 duplication	NA	Iris hypoplasia.	Likely Rieger Anomaly	(Nishimura et al. 2001)
6p25 duplication	NA	NL	Peter 's Anomaly	(Nishimura et al. 2001)
6p25 deletion	NA	Rieger syndrome phenotypes	Rieger syndrome	(Lehmann et al. 2002)

NA: Not Applicable. NL: Not Listed. **Axenveld anomaly**: iris strands connecting the iridocorneal angle to the trabecular meshwork and posterior embryotoxon.

**Rieger anomaly:** iris hypoplasia, corectopia, or polycoria. **Rieger syndrome:** Rieger anomaly plus systemic findings. **Axenfeld-Rieger anomaly:** Axenfeld anomaly plus Rieger anomaly. **Axenfeld-Rieger Syndrome:** Axenfeld-Rieger anomaly plus systemic findings. The \* indicates recurring mutations, reported in more than one pedigree.

**Figure 6. A schematic showing the position of disease-causing missense mutations within the FOXC1 forkhead domain.**

Amino acids positions at which mutations have been identified are shown in blue, the missense mutation identified at these positions is shown above. Recurrent missense mutations are shown in orange.



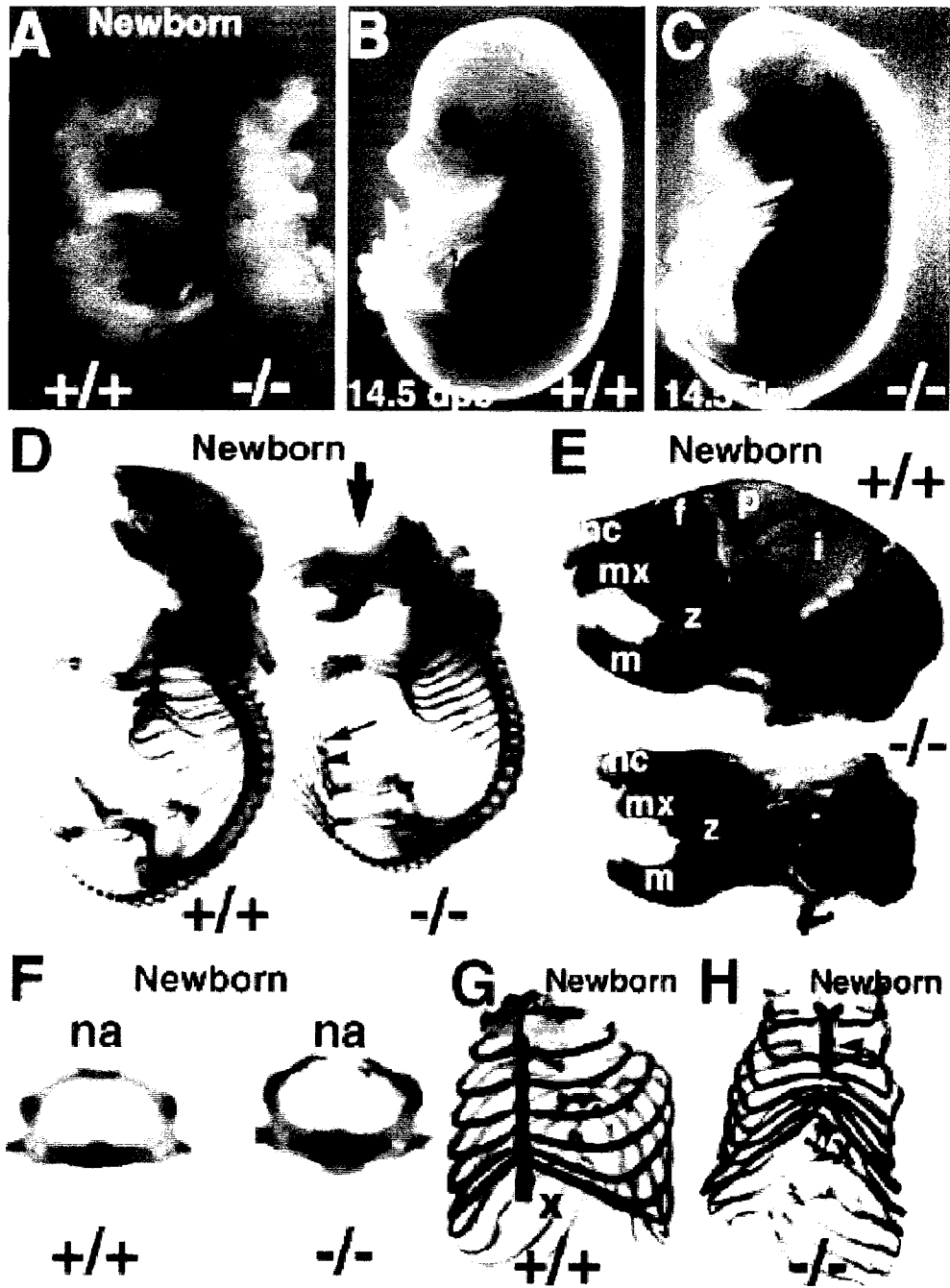
(Gruneberg 1943; Hong et al. 1999; Kume et al. 1998). The phenotype of homozygous *Foxc1<sup>lacZ</sup>* null mutants is identical to the *ch* phenotype (Kume et al. 1998).

*Foxc1<sup>lacZ</sup> and ch homozygous nulls have severe developmental defects*

*ch (Foxc1<sup>lacZ</sup>)* homozygous null mice have massively enlarged cerebral hemispheres that are hemorrhagic, with a dark purplish-blue colour. All *ch* homozygous mice die pre- or perinatally as the result of respiratory failure, showing an absence of expanded alveoli (Hong et al. 1999; Winnier et al. 1999). Embryonically, at 14.5 dpc the *ch (Foxc1<sup>lacZ</sup>)* homozygous mutant embryos can be clearly distinguished from their wild type littermates by frontal bulging of the head and a striking lack of the cranial vault, due to an absence of the calvarial bones, giving the top of the head a flat appearance (Figure 7). The *ch (Foxc1<sup>lacZ</sup>)* homozygous null embryos show a reduction of the basiooccipital, exoccipital, and hyoid bones. The superoccipital bone is severely malformed while the mandible, squamosal, and zygomatic bones are misshapen and massively ossified. Additionally the nasal septum is reduced, leading to the characteristic short snout appearance. In the axial skeleton the dorsal neural arches of the vertebrae, including the axis and atlas, fail to fuse along the whole vertebral column, with a reduction of the lateral arches and vertebral bodies (Hong et al. 1999; Kume et al. 1998). The rib cage and ribs in the *ch (Foxc1<sup>lacZ</sup>)* homozygous null embryos are reduced and fragile, showing an absence of the sternum ossification centers, except in the manubrium, weak attachment of the right and

**Figure 7. Analysis of Mice Homozygous for *Foxc1 lacZ*.**

A. Newborn mice. The *Foxc1 ch* pup has enlarged and hemorrhagic cerebral hemispheres (hydrocephalus) and open eyelids. (B and C) Embryos at 14.5 dpc showing the enlarged cerebral hemispheres of the homozygous mutant (arrow). (D–H) Skeletal defects in newborn *Foxc1 ch* mice. D. Note the absence of calvarial bones in the mutant (large arrow). All of the major skeletal abnormalities described by Grunberg for *ch* mutants were present as well as minor ones such as thinner digits (small arrow) and smaller ossification centers (arrowhead). E Lateral view of newborn skulls. The frontal (f), parietal (p), and interparietal (i) bones are absent in the homozygous mutant, and the zygomatic process (z) is enlarged and fused with the mandible (m). F. Groups of three cervical vertebrae were photographed from the posterior. Neural arches (na) are not closed dorsally in the *Foxc1 ch* mutant, and the centra are reduced in size compared with wild type. (G and H) Ventral view of rib cages. The sternbrae are completely absent in the mutant, except for the manubrium (arrowhead), and the xiphoid process (x) is also malformed. Abbreviations: f, frontal bone; i, interparietal bone; m, mandible; mx, maxilla; na, neural arches; nc, nasal cartilage; p, parietal bone; z, zygomatic process. Taken from (Kume et al. 1998).



left costal cartilage, and a misshapen and fragmented xiphoid process (Hong et al. 1999; Kume et al. 1998). The severe skeletal defects in the homozygotes, particularly with respect to facial bone development, are reminiscent of some of the syndromic features in patients with Axenfeld-Rieger malformations.

The development of other systems is also affected in *ch* (*Foxc1<sup>lacZ</sup>*) homozygous null embryos. Sections of fixed 16.5 dpc embryos show disruptions to some blood vessels in the brain (Kume et al. 1998). Ocular findings include open eyelids, a failure of the anterior chamber to form, iris hypoplasia, attachment of the lens to the cornea, a thickening of the corneal epithelium, an absence of the corneal endothelium, and a disorganized corneal stroma (Kidson et al. 1999; Kume et al. 1998). Interestingly, the thickened corneal epithelium shows an expansion of *Foxc1* expression raising the possibility of a self regulating *Foxc1* mechanism (Kidson et al. 1999). In addition to the other corneal anomalies, there is an absence of organized zonular occludens junctions in *ch* (*Foxc1<sup>lacZ</sup>*) homozygous null corneal mesenchyme cells, indicating that *Foxc1* may play a role in regulating extra cellular matrix components (Kidson et al. 1999). Evidence from mouse expression data, the ocular defects in the *ch* mouse, and the ocular defects found in humans with *FOXCI* mutations demonstrate the importance of *FOXCI* in ocular development.

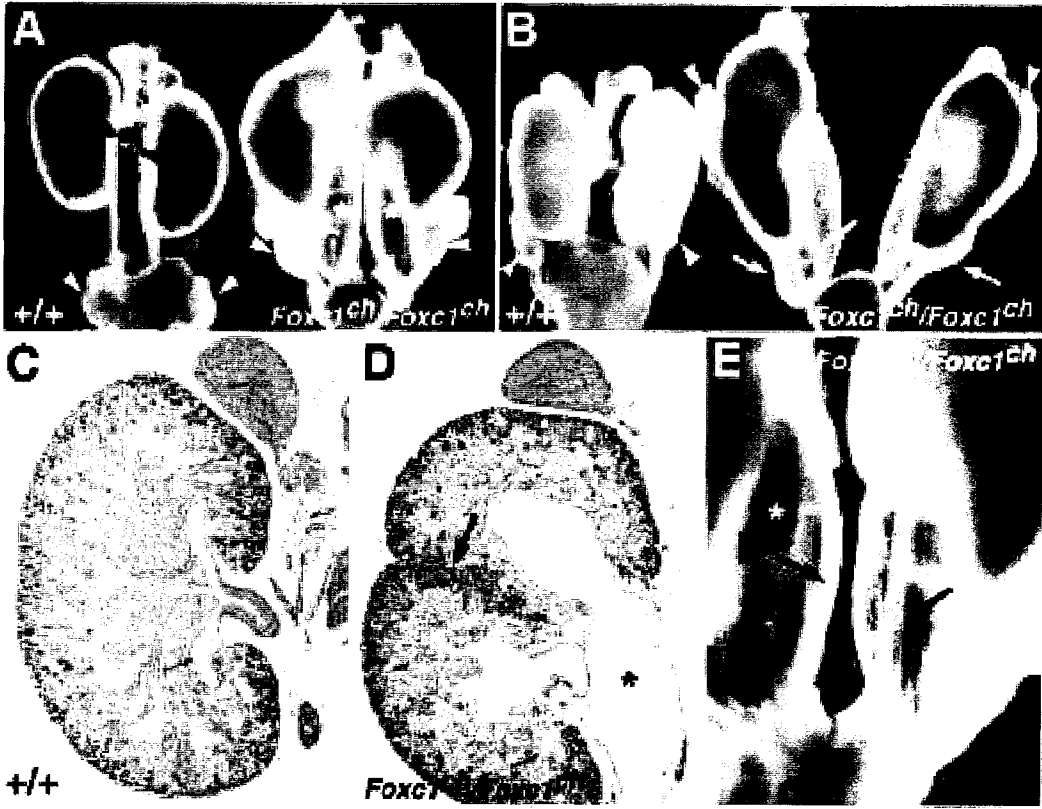
*ch* (*Foxc1<sup>lacZ</sup>*) homozygous null embryos also show disruptions to the cardiovascular and urogenital systems. Cardiovascular defects include Type B interruptions (an interrupted left aorta, where the interruption occurs distal to the origin of the left common carotid artery), a clear coarctation, or a narrowing of

the aortic arch (Winnier et al. 1999). Additional cardiac defects of *ch* (*Foxc1<sup>lacZ</sup>*) homozygous nulls include infundibular hypertrophy, ventricular septae defects, and aortic and pulmonary valve dysplasia. The pulmonary and aortic valve leaflets of the homozygous mutant mice are thickened and partially fused at the commissures. Urogenital defects in the *ch* (*Foxc1<sup>lacZ</sup>*) homozygous mice include duplex kidneys connecting to double ureters, and fluid filled enlargement of the kidney and ureter (Figure 8) (Green 1970; Kume et al. 2000). Only one of the ureters is fluid filled and dilated, the other ureter is normal (Kume et al. 2000). An ectopic uretic bud forms in *ch* (*Foxc1<sup>lacZ</sup>*) homozygous mutants by 11 dpc anteriorly to the normal uretic bud, the Wolffian duct is kinked and displaced medially, and the normal uretic bud is much broader than in wild type mice. It is thought that reciprocal interactions between the ectopic bud and the nephrogenic mesenchyme induce formation of an ectopic kidney that fuses with the normal kidney (Green 1970; Kume et al. 2000). Both sexes (males 75% and females 100%) of *ch* (*Foxc1<sup>lacZ</sup>*) homozygous mutants show anteriorly displaced gonads when compared to wild type mice (Green 1970; Kume et al. 2000). The range of defects found in *ch* (*Foxc1<sup>lacZ</sup>*) homozygous mutants demonstrates that *Foxc1* is an important regulator of skeletal, ocular, cardiac and urogenital development.

The penetrance of many of these developmental anomalies can vary depending on the genetic background of the *ch* (*Foxc1<sup>lacZ</sup>*) homozygous mutant (Hong et al. 1999; Kume et al. 2000; Smith et al. 2000; Winnier et al. 1999). *Foxc1* deficiencies tend to show greater penetrance in one mouse strain (CHMU/Le × C57/6) in comparison to other backgrounds (129 × Black Swiss or

**Figure 8. Kidney and ureter abnormalities in newborn mice homozygous for *Foxc1ch*.**

(A, B) Wild type and mutant newborn kidneys. (A) Male mutant kidneys have hydroureters (asterisks). Mutant testes (arrowheads) are located more anteriorly compared to wild-type testes (arrowheads). (B) Female mutant kidneys have hydroureters (asterisks) and normal ureter (white arrow) behind it. Yellow arrows indicate the oviducts of mutant. Mutant ovaries are located more anteriorly (arrowheads) compared to the wild type. (C, D) Sections of newborn wild type (C) and mutant (D) kidneys. Mutant has a duplex kidney showing a clear boundary of the peripheral metanephrogenic mesenchyme (arrow). Note that the upper part of the kidney connects to the hydroureter (asterisk). (E) Dorsal view of newborn mutant kidneys with double ureters. Normal ureters (arrows) and ectopic hydroureters (asterisks). Scale bar: C,D, 800  $\mu$ m. Adapted from (Kume et al. 2000).



CAST). The differential effects of background on penetrance are likely the effect of modifier genes that are able to modulate the effect of *Foxc1* deficiencies. The gene encoding Tyrosinase has recently been implicated as a possible modifier of *Foxc1* developmental anomalies arising from *Foxc1* mutations (Libby et al. 2003).

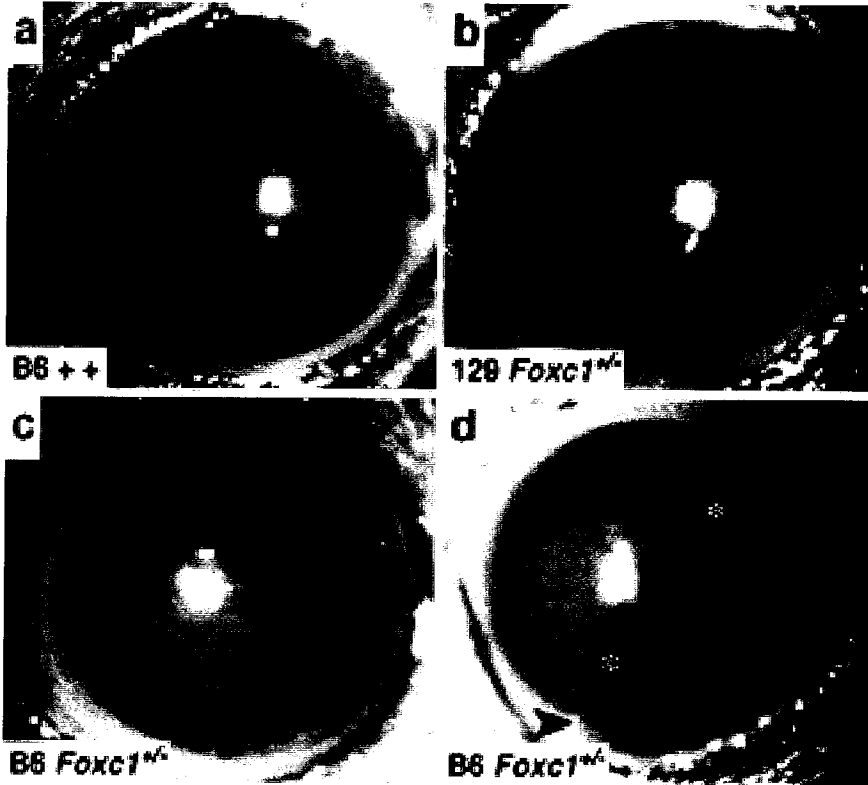
*Foxc1<sup>lacZ</sup> and ch heterozygotes have ocular defects similar to Axenfeld-Rieger malformations*

Heterozygous *ch* (*Foxc1<sup>lacZ</sup>*) mice have numerous ocular anterior segment malformations, although there is a range in expressivity (Hong et al. 1999; Smith et al. 2000). Slit-lamp analysis revealed anterior segment malformations of heterozygous *ch* (*Foxc1<sup>lacZ</sup>*) that include progressive corectopia, irregularly shaped pupils, iridocorneal adhesions and iris tears, a progressively thinning iris, posterior embryotoxon, scleralization of the peripheral cornea, and corneal opacities. Older heterozygous *ch* mice have a high incidence of corneal opacification, neo-vascularization, and cataracts.

Interestingly, histological analysis determined that anterior segment defects occur in *Foxc1<sup>lacZ</sup>* heterozygotes regardless of the background (Smith et al. 2000). The severity of the specific defect varies greatly between eyes and within individual eyes. The majority of eyes analyzed have varying degrees of abnormality in the iridocorneal angles (Figure 9). Abnormalities of the

**Figure 9. Axenfeld Rieger-like malformations seen in *Foxc1* mutant mice.**

There is a wide range of expression of the malformation phenotype, depending on the genetic background of the mice. In A and B the eyes are normal even with the *Foxc1* mutation. On the B6 genetic background the effect of the mutation is more pronounced (C and D). In C the eye shows corectopia and posterior embryotoxon, while in D the pupil is misshapen and elongated, the iris pigment epithelium is displaced (asterisks), and iridocorneal attachments can be seen (arrowhead). Adapted from (Smith et al. 2000).



iridocorneal angle include a reduced or absent Schelmm's canal, enlarged blood vessels, iris strands, and a hypoplastic, compressed, or absent trabecular meshwork (TM). Cells resembling TM mesenchymal precursor cells sometimes occupy areas lacking a TM. Interestingly, some *ch* heterozygotes in one mouse genetic background (CHUM/Le ) present with hypoplastic ciliary bodies and short thin ciliary processes while no ciliary body defects were found in *Foxc1<sup>lacZ</sup>* heterozygotes in any of the backgrounds tested (Smith et al. 2000).

The TM is normally composed of spaced trabecular beams, and organized collagen and elastic tissue, allowing drainage of the aqueous humor from the eye. Electron microscopy of the TM in *Foxc1<sup>lacZ</sup>* mice shows regional affected areas with disruptions of the extracellular matrix (Smith et al. 2000). Affected regions sometimes contain cells that resemble TM precursor cells or, in other areas, the TM cells have a normal appearance but are densely packed and continuous. Schelmm's canal contains giant vacuoles or is absent in some areas with abnormal TM cells. That the developmental ocular defects, such as iris hypoplasia and iridocorneal anomalies, in mouse *Foxc1* heterozygotes recapitulate the ocular phenotypes of *FOXC1* insufficiencies in human, indicates a high degree of conservation of FOXC1 function between mouse and human.

*Foxc1 and Foxc2 are important regulators of somitogenesis and cardiovascular development*

The closest orthologue of Foxc1 is Foxc2. At the amino acid level both proteins share 60% identity at the N-terminus, 21 % identity at the C-terminus,

99% identity in the forkhead domain, and similar expression profiles in the developing ocular, skeletal, urogenital, and cardiac systems (Hiemisch et al. 1998; Kume et al. 2000; Kume et al. 2001; Winnier et al. 1999).

Interestingly, *Foxc1*<sup>-/+</sup>/*Foxc2*<sup>-/+</sup> compound heterozygotes show non-allelic non-complementation in cardiovascular, urogenital, and ocular development. While there are no gross anomalies in the skeletal system (non-allelic complementation), the compound heterozygotes die prenatally, likely from cardiac defects (Winnier et al. 1999). Interruptions or coarctation of the aortic arch, ventricular septal defects, and valve defects are the primary cardiac anomalies found (Winnier et al. 1999). *Foxc1*<sup>-/+</sup>/*Foxc2*<sup>-/+</sup> compound heterozygotes also show abnormal development of the intermediate mesoderm, developing hydronephrosis and renal hypoplasia (Kume et al. 2000). *Foxc1*<sup>-/+</sup>/*Foxc2*<sup>-/+</sup> compound heterozygotes also have ocular findings that are comparable to *Foxc1*<sup>-/+</sup> single heterozygotes (Smith et al. 2000) (see above). However, congenital corneal vascularization and open eyelids at birth are phenotypes that are specific to the *Foxc1*<sup>-/+</sup>/*Foxc2*<sup>-/+</sup> compound heterozygotes. These findings show an interesting relationship between *Foxc1* and *Foxc2*, demonstrating that both genes are involved to some extent in the development of the ocular, cardiac, and urogenital system. The fact that the skeletal system is not affected in the compound heterozygotes but is severely affected in *Foxc1* null homozygotes, may be indicative of *Foxc1* and *Foxc2* complementation or may reflect a lack of involvement of *Foxc2* in the development of the skeletal system.

Compound *Foxc1*<sup>-/-</sup>/*Foxc2*<sup>-/-</sup> homozygotes have severe defects in somitogenesis (Kume et al. 2001). By the stage at which their wild-type littermates have 8 somites, compound *Foxc1*<sup>-/-</sup>/*Foxc2*<sup>-/-</sup> homozygotes show an absence of somites, no segmentation of the presomitic mesoderm, and a kinked neural tube. Expression of the zebrafish homologue *foxc1a* is required for somitogenesis in zebrafish (Topczewska et al. 2001; Topczewska et al. 2001). *Foxc1*, in conjunction with *Foxc2*, therefore has a critical function in vertebral somitogenesis.

Development of the cardiovascular system appears to be more aberrant in the compound homozygous mice. *Foxc1*<sup>-/-</sup>/*Foxc2*<sup>-/-</sup> homozygotes die around 9.0-9.5 dpc, earlier than either single homozygote, with severe cardiac defects. The heart is still able to beat weakly even though the myocardium is underdeveloped. The compound homozygotes show a reduction in heart size, a reduction in the size of the first branchial arch, and an absence of the second branchial arch (Kume et al. 2001). At 9.5 dpc the compound homozygotes are smaller in size, and have an open neural tube anteriorly. Histological examination shows severe disorganization and underdevelopment of the blood vessels and mesenchyme in the head. The severity of these defects in the compound heterozygous mice shows that *Foxc1* and *Foxc2* have critical functions in the development of the somites, cardiovascular system, and the organization of the head mesenchyme with respect to ocular development.

## Developmental Pathogenesis

To date the *Tbx1* gene is the only *in vivo* target of FOXC1 identified. Human *TBX1* maps to the center of the DiGeorge syndrome (MIM #188400) chromosomal region on 22q11.2. In *Tbx1* heterozygous mice the aortic arch is often malformed (Jerome and Papaioannou 2001; Lindsay et al. 2001; Merscher et al. 2001), similar to what is seen in homozygous *Foxc1*<sup>-/-</sup> mice (Kume et al. 2001; Winnier et al. 1999). *Foxc1*, along with *Foxc2* and *Foxa2*, is involved in the expression of *Tbx1* in the head mesenchyme and pharyngeal endoderm (Yamagishi et al. 2003). A novel FOX binding site was identified in the 5' untranslated region of *Tbx1* that, when deleted in transgenic mice, abolished *Tbx1* expression in the head mesenchyme and pharyngeal endoderm. This result is the first direct evidence for an *in vivo* target of *Foxc1*. In a *Foxc1*<sup>-/-</sup> null background, *Tbx1* expression is reduced but only in areas where *Foxc1* and *Tbx1* are co-expressed, consistent with *Foxc1* regulation of *Tbx1*. *Tbx1* expression is induced by *Shh*, mediated by *Foxc1* and *Foxc2* proteins. In homozygous *Shh* null mutants, *Foxc1* expression is down regulated in comparison to *Foxc1* expression in wild type mice, accompanied by a down regulation in *Tbx1* expression.

During normal development, the neural crest cells from the top of the mesencephalon at the first pharyngeal arch will delaminate from the surface ectoderm and migrate laterally and ventrally, going on to form the maxillary and mandibular processes. These neural crest cells also become positioned in between the optic primordia and the surface ectoderm (Johnston et al. 1979; Kaiser-Kupfer 1989). While *Tbx1* is excluded from the mesenchyme of the pharyngeal

arches, it is thought to mediate the fate of these cells via Fgf8 dependent cell communication (Vitelli et al. 2002). It is interesting that patients with AR malformations can show hypoplastic development of the maxillary and mandibular processes (for example patients carrying P79T mutations, see Table 1), providing circumstantial evidence of a developmental link between FOXC1, Tbx1, and Fgf8.

While the upstream elements and downstream targets of FOXC1 remain largely unknown, there is a significant amount of data revealing genes that show altered expression on *Foxc1*<sup>-/-</sup> single homozygous and *Foxc1*<sup>-/-</sup>/*Foxc2*<sup>-/-</sup> compound homozygous backgrounds (Table 2b). In the *Foxc1*<sup>-/-</sup> single homozygotes, *Gdnf* (*glial cell line-derived neurotrophic factor*) and *Eya1* (human homologue of the *Drosophila eyes absent* gene) expressions are anteriorly expanded (Table 2a) (Kume et al. 2000). *Gdnf* is expressed in the mesenchyme of the developing urogenital system and both *Gdnf* and *Eya1* are required for uretic bud formation (Abdelhak et al. 1997; Moore et al. 1996). Homozygous nulls of either *Gdnf* or *Eya1* do not form uretic buds. *Eya1* homozygous nulls do not express *Gdnf* in the nephrogenic mesenchyme, suggesting that *Eya1* acts upstream of *Gdnf* to regulate *Gdnf* expression.

Experiments using micromass cultures of the sternum primordium from *Foxc1*<sup>-/-</sup> homozygotes indicate that Foxc1 mediates BMP2 and TGFβ1 signalling (Kume et al. 1998). Wild type cultures will show enhanced chondrogenesis in response to BMP2 or TGFβ1, but this response is drastically reduced in the *Foxc1*<sup>-/-</sup> homozygote micromass cultures, indicating that *Foxc1* is required for

**Table 2.** Summary of Genes affected by Foxc1 (Foxc2) deletions.A) *Foxc1*<sup>-/-</sup> homozygotes

Gene	Function/Expression	Defect	Reference
<i>Foxc1</i>	Downregulated in the corneal endothelium as the presumptive corneal mesenchyme differentiates.	Endothelial cells do not differentiate and Foxc1 expression persists.	(Kidson et al. 1999)
<i>Gdnf</i>	Essential for uretic bud formation.	Anterior and medial expansion of Gdnf expression.	(Kume et al. 2000)
<i>Eya1</i>	Expression overlaps with Gdnf. Essential for uretic bud formation. Likely upstream of Gdnf.	Anterior expansion of Eya1 expression.	(Kume et al. 2000)
<i>BMP2</i>	Wild-type micromass cultures of sternal primordium undergo enhanced chondrogenesis in the presence of BMP2.	Micromass cultures of sternal primordium from Foxc1 <sup>-/-</sup> cells have a significantly reduced response to BMP2.	(Kume et al. 1998)
<i>Tbx1</i>	Downstream target of FOXC1.	Foxc1 <sup>-/-</sup> mice show lack of Tbx1 expression in the head mesenchyme and pharyngeal endoderm.	(Yamagishi et al. 2003)
<i>TGFβ1</i>	1) Wild-type micromass cultures of sternal primordium undergo enhanced chondrogenesis in the presence of TGFβ1. 2) TGFβ1 treatment leads to FOXC1 mediated growth arrest of HeLa cells.	Micromass cultures of sternal primordium from Foxc1 <sup>-/-</sup> cells have a significantly reduced response to TGFβ1.	(Kidson et al. 1999; Zhou et al. 2002)
<i>zol</i>	Major component of the bands of the occluding junctions between wild-type endothelial cells.	Absent in mutant Foxc1 <sup>-/-</sup> cells. Punctate expression is seen in mesenchyme adjacent to lens of eye.	(Kidson et al. 1999)

B) *Foxc1*<sup>-/-</sup>/*Foxc2*<sup>-/-</sup> compound homozygotes

Gene	Function/Expression	Defect	Reference
<i>Paraxis</i>	Normally expressed in somites, anterior PSM.	No expression. Very low levels anteriorly near neural tube	(Kume et al. 2001)
<i>Tbx18</i>	Normally expressed in anterior portion of somite.	No expression. Expression normal in single <i>Foxc1</i> <sup>-/-</sup> and <i>Foxc2</i> <sup>-/-</sup> homozygotes.	
<i>Uncx4.1</i>	Normally expressed in posterior portion of somite.	No expression. Expression normal in single <i>Foxc1</i> <sup>-/-</sup> and <i>Foxc2</i> <sup>-/-</sup> homozygotes.	
<i>Pax1</i>	Normally expressed in somites.	No expression in somites.	
<i>MyoD</i>	Normally expressed in somites.	No expression in somites.	
<i>EphrinB2</i>	ephrin/Eph pathway involved in formation of boundary between S0 and S1 somites.	<i>ephrinB2</i> is expressed but expression is downregulated and diffuse.	
<i>Notch1</i>	Expressed in anterior PSM with highest levels in S2 somite.	Strongly downregulated. Only very faint bands in the presumptive S1 and S2 somites.	
<i>Mesp2</i>	A bHLH transcription factor expressed in anterior portion of S2 somite. May function to specify anterior cell fate.	Strongly downregulated.	
<i>Mesp1</i>	Closely related to <i>Mesp2</i> .	Strongly downregulated.	
<i>Lunatic Fringe</i>	Encodes a modulator of Notch receptor activity.	Reduced expression with diffuse expression pattern.	
<i>Dll1</i>	Encodes a Notch ligand. Expressed throughout PSM, and posterior half of S1 somite.	Anterior boundary diffuse, expression in somite region diffuse.	
<i>Hes5</i>	A target of the Notch signaling pathway. Expressed in two stripes of the anterior PSM.	Pattern of expression is diffuse and down regulated. Expression is normal in the neural tube.	

C) Zebrafish *foxc1a* knock downs.

Gene	Function/Expression	Defect	Reference
<i>Paraxis</i>	Normally expressed in somites, anterior PSM.	No expression.	(Topczewska et al. 2001)
<i>Mesp-b</i>	A bHLH transcription factor expressed in anterior portion of S2 somite. May function to specify anterior cell fate.	No expression.	
<i>EphrinB2</i>	ephrin/Eph pathway involved in formation of boundary between S0 and S1 somites.	Strongly downregulated.	
<i>Notch5</i>	Highly expressed in the developing somites.	Strongly downregulated.	
<i>Notch6</i>	Highly expressed in the developing somites.	Strongly downregulated. Boundaries are expanded	
<i>EphA4</i>	ephrin/Eph pathway involved in formation of boundary between S0 and S1 somites.	Strongly downregulated.	

cartilage development. Work in HeLa cells has shown that TGF- $\beta$  is able to induce a FOXC1 mediated arrest in cell cycle (Zhou et al. 2002).

Recent work has shown that *Tyrosinase* (*Tyr*) is a modifier of the ocular defects caused by *Foxc1* mutations (Libby et al. 2003). Tyrosinase is involved in the conversion of tyrosine to L-dihydroxyphenylalanine (L-dopa) and L-dopa to dopaquinone. L-dopa is known to affect development and is involved in the production of catecholamines, which are also developmentally important. *Tyr*<sup>-/-</sup> homozygous mice have a pigment deficiency and are albinos, with mild ocular defects. Interestingly, the ocular defects seen in heterozygote *Foxc1*<sup>+/-</sup> mice are much more severe on a *Tyr*<sup>-/-</sup> background than what could be accounted for by additive effects of *Foxc1*<sup>+/-</sup> and *Tyr*<sup>-/-</sup> defects.

*Foxc1* may be involved in the regulation of its own expression. As mentioned above, within *Foxc1*<sup>lacZ</sup> homozygous mutants, *Foxc1* expression persists in the presumptive corneal mesenchyme, whereas in normal embryos *Foxc1* is down regulated as the endothelial cells differentiate (Kidson et al. 1999).

Many genetic and systemic defects are only seen on compound *Foxc1*<sup>-/-</sup>/*Foxc2*<sup>-/-</sup> homozygous backgrounds (see above), demonstrating that to some extent, *Foxc1* and *Foxc2* can complement each other. The compound homozygotes do not express *paraxis* in the somites and anterior presomitic mesoderm, the normal sites of *paraxis* expression, while *Foxc1*<sup>-/-</sup> and *Foxc2*<sup>-/-</sup> single homozygotes show no *paraxis* defect (Burgess et al. 1995; Kume et al. 2001). Interestingly, the mesodermal cells are correctly specified as paraxial

mesoderm, as indicated by *Mox1* and *pMesogenin1* expression, but show a significant differentiation defect, as indicated by an absence of *Pax1* and *MyoD* expression (Kume et al. 2001) (Table 2b). In zebrafish, *foxc1a* has been shown to regulate the expression of *paraxis* (Table 2c) (Topczewska et al. 2001).

*Foxc1<sup>-/-</sup>/Foxc2<sup>-/-</sup>* compound homozygotes also have defects in Notch signalling in the anterior presomitic mesoderm (Kume et al. 2001). Notch signalling, in conjunction with *Mesp2* down regulation of *Dll1* in the anterior somite, is thought to be required for the establishment of anterior and posterior cell fates in the anterior presomitic mesoderm (Takahashi et al. 2000). Compound null homozygotes of *Notch1* and *Notch4* (*Notch1<sup>-/-</sup>/Notch4<sup>-/-</sup>*) or the Notch signalling genes *presenilin1* and *presenilin2* (*presenilin1<sup>-/-</sup>/presenilin2<sup>-/-</sup>*) have cardiovascular and somite formation defects similar to *Foxc1<sup>-/-</sup>/Foxc2<sup>-/-</sup>* compound homozygous nulls (Donoviel et al. 1999; Krebs et al. 2000). *Notch1*, normally expressed in the anterior presomitic mesoderm with highest expression in somite S2, is strongly down regulated in the *Foxc1<sup>-/-</sup>/Foxc2<sup>-/-</sup>* compound homozygous nulls, as are other genes in Notch signalling pathways (*Mesp2*, *Mesp1*, *Lunatic fringe*, *Dll1*, *Hes5*; Table 2b). There is thought to be a regulatory loop between *Mesp2*, *Notch1*, and *Dll1* in the anterior presomitic mesoderm (Takahashi et al. 2000). In *Dll1* homozygous mutants, *Foxc1* is expressed at lower levels in the somites and presomitic mesoderm, when compared to wild type embryos (Kume et al. 2001). Additionally, ectopic expression of *Foxc1* is seen throughout the neural tube of the *Dll1* homozygous null embryo. While *Foxc1* is expressed at lower levels in the *Dll1* null mouse, *Foxc1* is not thought to

be an obligatory component of the *Mesp2*-Notch1-Dll1 regulatory loop (Kume et al. 2001).

Zebrafish appear to recapitulate to some extent, the function of *foxc1a* in the genetic regulation of somitogenesis. Expression of *mesp-b* is absent, while *notch6* and *notch5* are strongly down regulated in *foxc1a* “knocked down” fish (Table 2c) (Topczewska et al. 2001). Similar to the *Foxc1*<sup>-/-</sup>/*Foxc2*<sup>-/-</sup> compound homozygous mice, *foxc1a* “knock down” zebrafish show a strong down regulation of *ephrinB3* and *ephA4*, genes required to establish intersomitic boundaries (see Table 2b and 2c).

Clearly FOXC1 is important for the normal development of ocular, skeletal, cardiovascular, and urogenital systems. As described above, defects such as AR malformations are thought to arise from a defect in migration and differentiation of neural crest mesenchyme involved in the formation of the eye. FOXC1 is likely to play a role in signalling cascades that lead to differentiation of the neural crest mesenchyme or in regulating the cell fates of the developing ocular tissues. Evidence that the extra cellular matrix component *zol* is not expressed properly raises the possibility that FOXC1 acts to regulate the expression or function of proteins involved in cell-cell adhesion (Kidson et al. 1999). Smith et al. (Smith et al. 2000) also find deficiencies in the ocular extra cellular matrix of *Foxc1* heterozygotes. Similarly, the failure of *Foxc1*<sup>-/-</sup> sternum primordium cells to condense and differentiate into cartilage in response to BMP2 and TGFβ1 may be indicative of abnormal cell-cell adhesion (Kidson et al. 1999; Kume et al. 1998).

Foxc1 may interact with factors in the Notch signalling pathway to regulate gene expression, and may also interact with other *Fox* genes that are expressed in the axial, non-axial, and lateral plate mesoderm (Kume et al. 2001). Both *Foxc1* and *Foxc2* expression overlap with *Foxb1* and *Foxd2* (Kume et al. 2001). Alternatively, Kume et al. proposed that Foxc1 may act to remodel chromatin structure, and thus regulate the transcription of genes involved in mesodermal development, similar to models proposed for Foxa1 (Cirillo et al. 2002; Cirillo et al. 1998; Cirillo and Zaret 1999; Kume et al. 2000; Kume et al. 1998). Given the wide expression of *FOXCI* and the involvement of the gene in a variety of developmental systems, it may be found that FOXC1 has diverse functions that change in different tissues, at specific times.

### **Forkhead Domain Structure**

The three dimensional topology of the FHD was first resolved using X-ray crystallography on Foxa3 (formerly HNF3 $\gamma$ ) bound to a DNA target (Clark et al. 1993), and has since been studied using NMR analysis of FOXC2, Foxd3, and FOXO4 (Jin et al. 1999; van Dongen et al. 2000; Weigelt et al. 2001). This DNA binding motif is a variant of the helix-turn-helix motif, consisting of three  $\alpha$ -helices, two  $\beta$ -sheets, and two large loops that form “wing-like” structures (Figure 10) (Clark et al. 1993; Jin et al. 1999; van Dongen et al. 2000; Weigelt et al. 2001). Forkhead domains are thus often referred to as winged-helix domains. As mentioned previously, all the disease-causing missense mutations identified to date are located in the FHD (Figure 11). The FHD is highly conserved, and

**Figure 10. Structure of the forkhead domain.**

A. A schematic of the FOXA3 forkhead domain bound to DNA.  $\alpha$ -helices are shown as coils while  $\beta$ -strands are represented as arrows.  $\alpha$ -Helix 3, the recognition helix, lies across the major groove of the DNA. Adapted from (Clark et al. 1993) B. Topology of the forkhead domain. The recognition helix (H3),  $\alpha$ -helix3, is shown in red. The remaining  $\alpha$ -helices (H1 and H2),  $\beta$ -sheets (S1, S2, and S3) and wings (W1 and W2) are shown in white. N and C indicate the N and C terminal portions, respectively. Taken from (Gajiwala and Burley 2000).

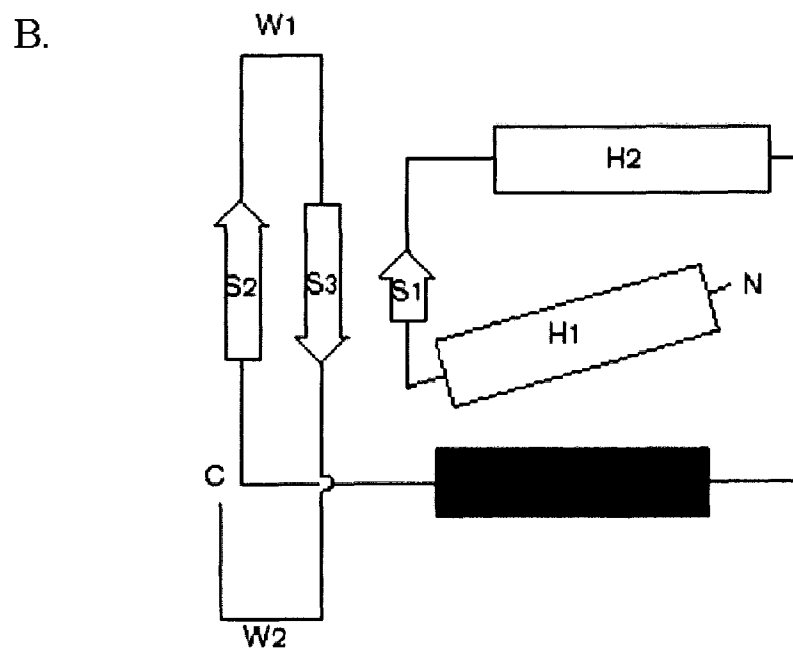
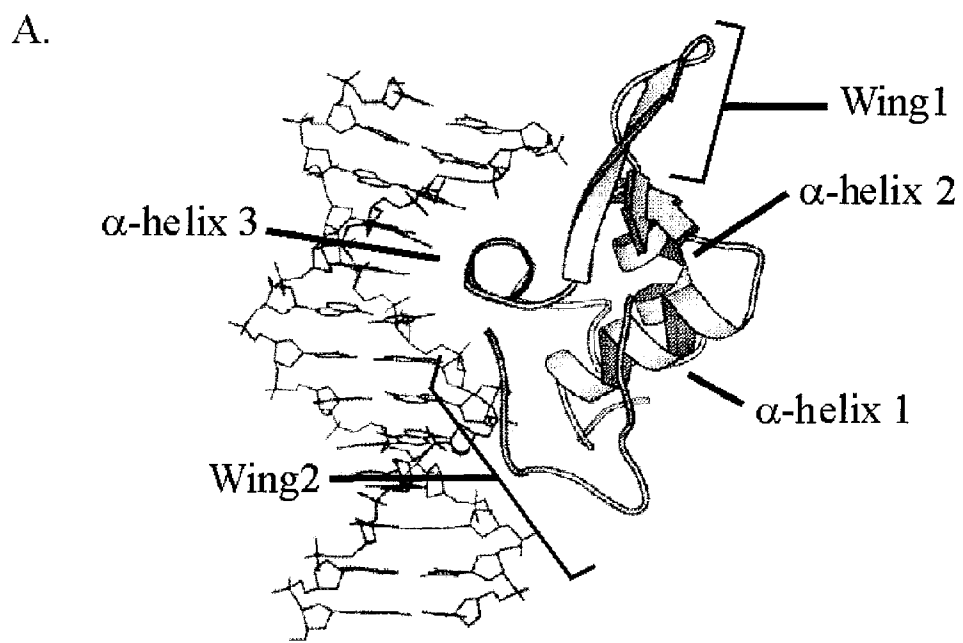


**Figure 11. Position of FOXC1 disease-causing missense mutations studied herein, relative to FHD secondary structures.** Amino acid residues at which mutations have occurred are indicated in blue. The missense mutations are indicated above the FHD primary structure, the secondary structures of the FHD are shown below the FHD primary structure.



structural studies have shown limited three-dimensional variation between different FOX FHDs; this implies limited variation in modes of DNA recognition. The structural basis of differences in DNA sequence recognition remains undetermined; however, there is evidence that the third helix, which is positioned in the major groove of DNA (Overdier et al. 1994), and the second wing (Pierrou et al. 1995) guide protein-DNA interactions. Rather than alterations in the gross topology of the FHD being the basis of DNA recognition, it is thought that differences in charge along the interface between the FHD and DNA provide the basis for sequence specificity (Weigelt et al. 2001).

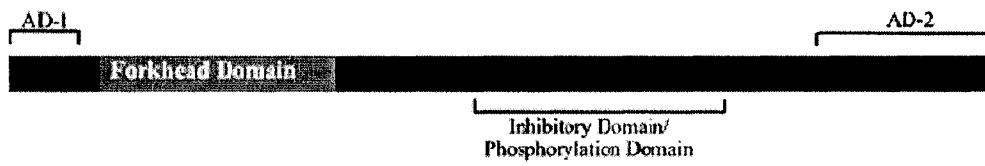
Analysis of the FOXC1 FHD determined that indeed this motif is able to bind DNA, with *in vitro* site selection experiments determining FOXC1 bound a nine base pair core sequence 5'-GTAAATAAA-3' with high affinity (Pierrou et al. 1994). These experiments also found that when the FOXC1 FHD binds, it bends the DNA approximately 94°. Recent experiments analyzing FOX binding sites upstream of the *Tbx1* gene found FOXC1 is also able to bind the DNA sequence 5'-AAAACAAACAGGC-3' in electrophoretic mobility shift assays (Yamagishi et al. 2003).

### **The Transactivation Domains**

After my initial work on FOXC1, described later in this thesis, further characterization of FOXC1 was done by Dr Fred Berry to define the transactivation domains of FOXC1. FOXC1 transactivation activity is mediated

**Figure 12. FOXC1 transactivation domains.**

Transcriptional activation domains are located at residues 1–51 (AD-1) and 435–553 (AD-2). A transcriptional inhibitory domain/phosphorylation domain is located in the central region of the FOXC1 protein at residues 215–366. Adapted from (Berry et al. 2002).



by N- and C-terminal activation domains (Figure 12) (Berry et al. 2002). The N-terminal activation domain is located within amino acid residues 1-51 while the C-terminal activation domain is located within amino acid residues 435-553. FOXC1 constructs lacking both these domains have reduced ability to transactivate gene expression, while the fusion of these activation domains to a GAL4 DNA-binding domain increases transcriptional activation of a GAL4 reporter gene. Interestingly, the C-terminal activation domain-GAL4 DNA-binding domain fusion protein is able to transactivate gene expression at levels 10 times that of full-length FOXC1-GAL4 DNA-binding domain chimeric proteins. The comparatively lower transactivation ability of full-length FOXC1 may be due to the presence of an inhibitory domain located within amino acid residues 215-365 (Figure 12) (Berry et al. 2002). The FOXC1 inhibitory domain is not able to independently repress transcription but instead functions to inhibit the transcriptional potential of activation domains. Additionally, amino acid residues 215 and 366 are phosphorylated, altering the protein conformation of FOXC1 (Berry et al. 2002).

### **Rationale for Project**

Clearly FOXC1 is an important transcription factor in numerous developmental programs; however, its molecular function as a transcription factor remained largely undefined. Specifically, I was interested in the relationship between amino acid conservation within the FHD and the function of FOXC1 as a transcription factor. The presence of naturally occurring, disease

causing, missense mutations within the FHD, provided an opportunity to probe the FHD in a biologically relevant manner. In addition to my biochemical studies of the FHD, a collaboration was established utilizing computational analyses to study conformational energy differences between wild type and mutant FOXC1 FHDs. This combination of biochemical and computational analyses was utilized to understand the roles different regions of the FHD play in organizing the FOXC1 molecule.

These analyses have shown FOXC1 to be a transcriptional activator, driving expression of a reporter construct. I have demonstrated that FOXC1 is a nuclear protein, and delineated the sequences required for the exclusive localization of FOXC1 to the nucleus. I have also demonstrated that FHD missense mutations can have a variety of effects on FOXC1 function. FOXC1 missense mutations were found to reduce FOXC1 protein levels, cause the mislocalization of FOXC1 within the cell, impair the DNA binding activity of FOXC1, alter the DNA binding specificity of FOXC1, and/or reduce the function of FOXC1 as a transcriptional activator.

To complement my studies of naturally occurring, disease causing missense mutations within the FHD, I initiated a second line of study into the effect of amino acid side chain charge on FHD function. Key amino acids, selected on the basis both of having a large predicted effect on the conformational energies of FOXC1 and being at positions where missense mutations had occurred, were converted individually to alanine (neutral charge), glutamate (-ve charge), or lysine residues (+ve charge). Through these studies, amino acid

residues within the FHD having a role in organizing the FOXC1 molecule so that it is competent for nuclear translocation, to bind DNA, and is competent to activate gene expression were studied further, extending our understanding of the roles of both primary and secondary amino acid sequences within the FHD on FOXC1 function. Amino acids able to alter the DNA binding specificity of FOXC1 were also identified. Because of the high conservation of amino acids within the FHD, and the limited three-dimensional topological variation between FHDs of different FOX proteins, it is likely that this information will be applicable to other members of the FOX family of transcriptional activators.

## Results

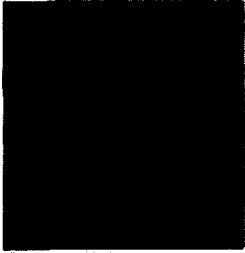
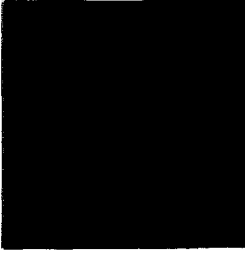
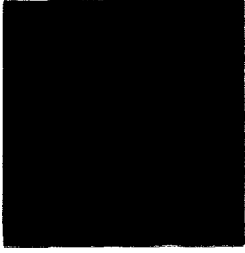
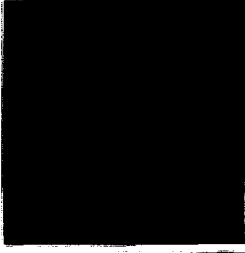
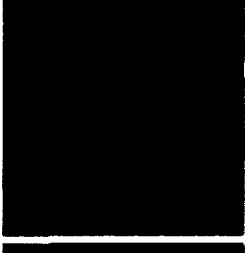
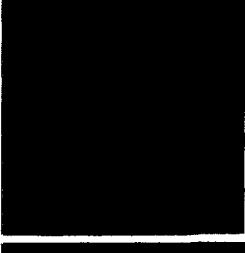
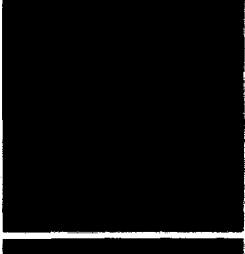
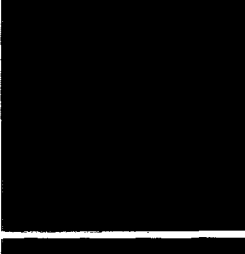
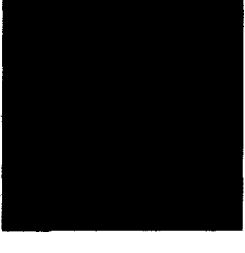
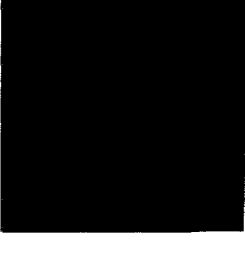
### FOXC1 localization and delineation of Nuclear Localization Signals

FOXC1 is a DNA-binding protein (Pierrou et al. 1994) and as such, should localize to the nucleus. In order to determine the sequences within the FHD that allow for the translocation of FOXC1 into the nucleus, a series of deletion constructs was made. Previous work has indicated that the nuclear localization signals (NLSs) in FOXA2 and FOXF2 FHDs are bipartite signals (Hellqvist et al. 1998; Qian and Costa 1995), comprised of a region at the N-terminus of the FHD and a second region rich in basic amino acids at the C-terminal end of the FHD. Deletions of FOXC1 were constructed in which amino acids 78-93 (the putative N-terminal NLS) and 168-176 (the putative C-terminal NLS) were deleted, both individually and in combination. As a negative control, the entire FHD was removed ( $\Delta 69-176$ ), herein referred to as  $\Delta$ Box.

Utilizing an antibody against the vector encoded Xpress epitope, FOXC1 was found to localize exclusively to the nucleus (Figure 13). FOXC1  $\Delta 69-178$  showed no exclusive nuclear localization (0% of the cell population), demonstrating that the FHD contains information required for nuclear translocation or retention of FOXC1. Deletion of residues 168-176 reduced the exclusive nuclear localization of FOXC1 from 91% to 0%, while FOXC1  $\Delta 78-93$  gave a mixture of nuclear and cytoplasmic staining. The FOXC1  $\Delta 78-93$  molecule still shows prominent nuclear localization of FOXC1, however this localization is not exclusive. Deletion of both putative NLSs ( $\Delta 78-93$  and  $\Delta 168-176$ ) results in predominantly mixed cytoplasmic and nuclear localization (72%)

**Figure 13. The FOXC1 NLS resides in the FHD.**

Indirect immunofluorescence of Xpress epitope tagged FOXC1 proteins in COS-7 cells visualized by Cy3 fluorescence are presented in the left panels. Nuclei stained with 4, 6-diamidino-2-phenyl-indole (DAPI) are presented in the right panels. Positions of the amino acids deleted in the FOXC1 FHD are indicated. To quantitate the extent of recombinant FOXC1 protein localization, at least 100 cells were randomly selected, and the percentage of cells exhibiting Cy3 fluorescence in the nucleus only (N), in both the nucleus and cytoplasm (N+C), and in the cytoplasm only (C) was determined. Taken from (Berry et al. 2002).

	CY3	DAPI	N	N+C	C
FOXC1			91	0	9
$\Delta 69-178$			0	75	25
$\Delta 168-176$			0	96	4
$\Delta 78-93$			6	93	1
$\Delta 78-93+$ $\Delta 168-176$			0	72	28

similar to what is seen when the entire FHD is removed (75%). Therefore regions 78-93 and 168-176 are required for proper nuclear localization of FOXC1.

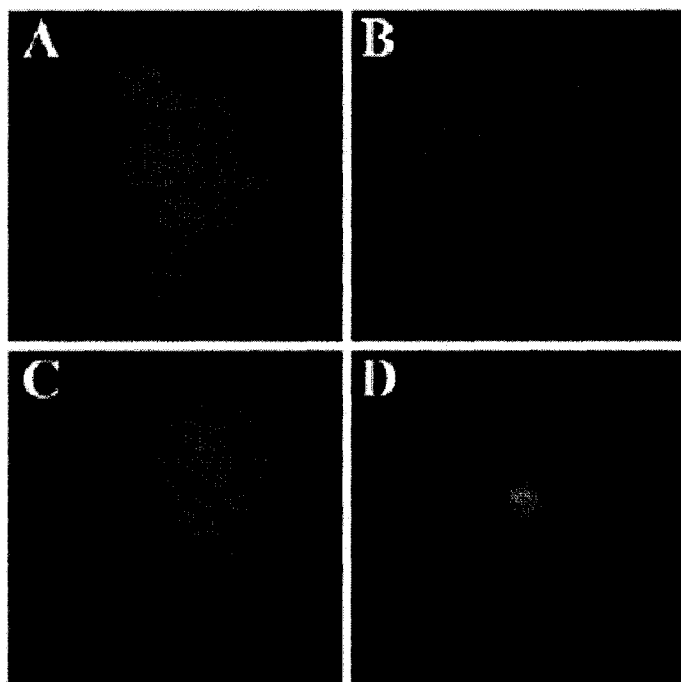
The two putative NLSs were fused to green fluorescent protein (GFP) in order to determine if these signals are sufficient for nuclear translocation. When FOXC1 amino acids 77-93 were fused to GFP, localization of the GFP molecule was seen throughout the cell, similar to what is seen for GFP alone (Figure 14). This portion of the FHD therefore is not sufficient for the nuclear localization and thus does not represent a *bona fide* NLS. This region may represent a putative nuclear localization accessory domain, necessary but insufficient for nuclear localization. Conversely, fusion of the C-terminal putative NLS to GFP resulted in the localization of GFP exclusively to the nucleus. Specifically, the chimeric GFP molecule appeared to accumulate in a subnuclear region resembling the nucleolus. These data indicate that residues 168-176 are sufficient to localize GFP to the nucleus and thus represent a *bona fide* NLS domain.

### **Analysis of FOXC1 Missense Mutations**

#### *Expression and mutagenesis of FOXC1*

To study the effects of missense mutations on FOXC1 function, the *FOXC1* cDNA was cloned into the pcDNA4 His/Max expression plasmid. Site directed mutagenesis was attempted using the entire cDNA of *FOXC1*, but the high G-C content of FOXC1 precluded mutagenesis. A smaller, *Apa* I – *Rsr* II fragment, spanning the FOXC1 forkhead domain, was mutagenized by PCR-based site-directed mutagenesis. The mutagenized fragment was then subcloned

**Figure 14.** Residues in the FOXC1 FHD are sufficient for nuclear localization. GFP fluorescence was visualized in HeLa cells transfected with (A) GFP alone, (B) GFP FOXC1, (C) GFP 78–93, or (D) GFP 168–176. Taken from (Berry et al. 2002).



back into the FOXC1 pcDNA4 His/ Max expression plasmid. Whole cell extracts of COS-7 cells transfected with the FOXC1 recombinant constructs were resolved by SDS-PAGE and Western analysis. Detection of the N-terminal, vector-encoded, Xpress epitope demonstrated a stable product, approximately 80 kDa in size for wild type FOXC1, and FOXC1 containing nine of the ten missense mutations (Figure 15). The predicted molecular weight for recombinant FOXC1 is 65 kDa, 4 kDa for the Xpress epitope and 61 kDa for FOXC1. Recombinant FOXC1 proteins were equalized using band intensities of western blots.

*The FOXC1 I87M mutation results in reduced protein levels.*

When cell extracts were made from COS-7 cells transfected with the FOXC1 constructs, less than 5% of wild type amounts of the FOXC1 I87M mutant could be isolated. To confirm that the FOXC1 I87M missense mutation reduced the stability of FOXC1, LacZ pcDNA4 HIS/Max was co-transfected in COS-7 cells with I87M FOXC1 or the wild type FOXC1 construct, and protein extracted. Both transfected COS-7 plates produced LacZ, indicating that the cells were able to produce protein. However, the I87M FOXC1 variant was only present in small amounts as compared to wild type FOXC1 (Figure 16b). Northern analysis was then done to test that the FOXC1 cDNA containing the I87M mutation was able to produce mRNA. As seen in Figure 16a, when mRNA is extracted from COS-7 cells transfected with equivalent amounts of

**Figure 15. Western blot analysis of both recombinant FOXC1 and FOXC1 containing missense mutations.**

Transfected COS-7 whole-cell extracts were resolved by SDS-PAGE and by the N-terminal Xpress epitope detected by immunoblotting with a mouse anti-Xpress monoclonal antibody. Western experiments were done at three separate times.

The first analysis studied S82T, F112S, I126M, and S131L (A). The second analysis was of P79L, P79T, I91S, I91T, and R127H (B). The third analysis was of L86F (C).

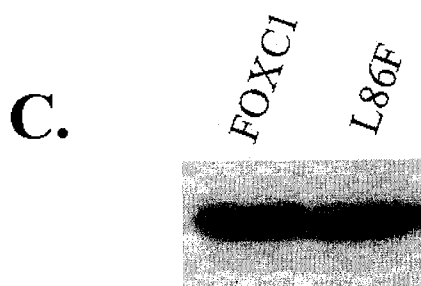
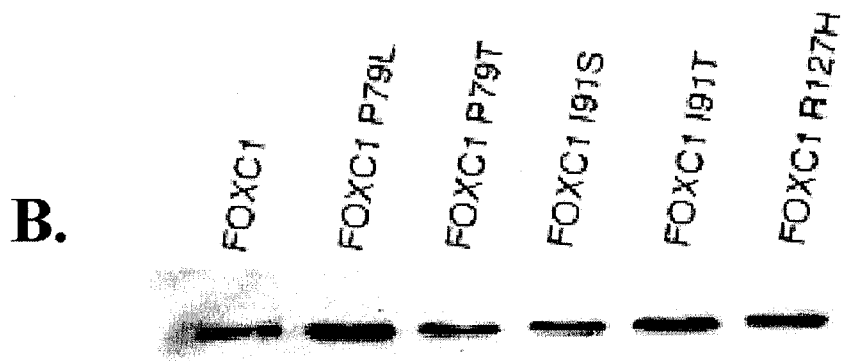
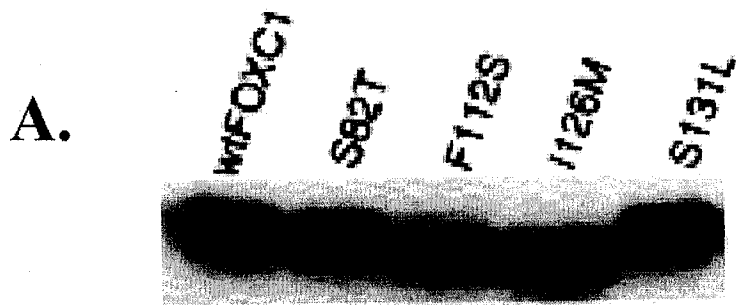
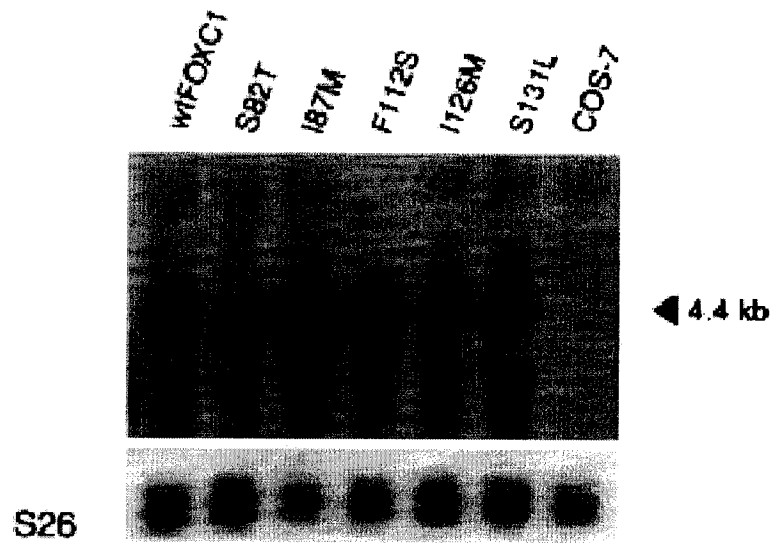


**Figure 16. The I87M mutation leads to a reduction in FOXC1 protein levels.**

A. Northern analysis of COS-7 extracts transfected with FOXC1 pcDNA4 His/Max wild type and missense mutation constructs. A [<sup>32</sup>P]-labeled N-terminal fragment of FOXC1 was used to probe the blot, detecting an appropriately sized product at 4.4 kb. S26 cDNA was used as a loading control. B. FOXC1 I87M reduces FOXC1 levels. COS-7 cells were transiently cotransfected with LacZ pcDNA4 His/Max and either FOXC1 pcDNA4 His/Max or FOXC1 I87M pcDNA4 His/Max. Transfected COS-7 whole-cell extracts were resolved by SDS-PAGE and by the N-terminal Xpress epitope detected by immunoblotting. Only small amounts of the FOXC1 I87M mutant protein were detected.

**A.**



**B.**



recombinant plasmid DNA, the amount of mRNA between the FOXC1 variants appears to be equal. It would appear therefore, that although the I87M FOXC1 variant is being introduced into cells, mRNA is being produced, and the protein machinery of the cell is competent to synthesize new proteins, FOXC1 containing the I87M mutation shows reduced stability.

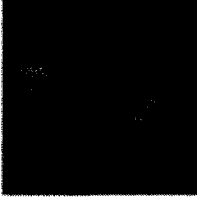
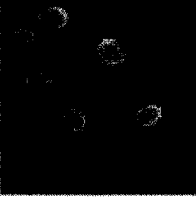
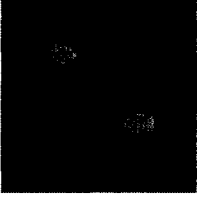
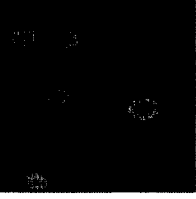
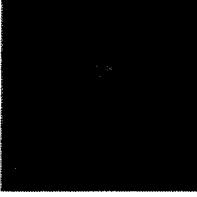
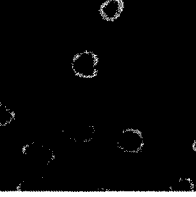
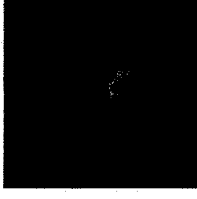
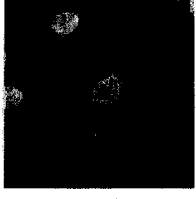
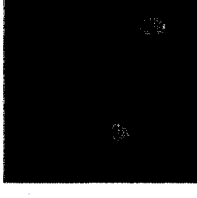
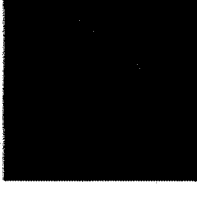
### *Subcellular Localization*

The effects of the missense mutations on FOXC1 localization were tested in COS-7 cells transiently transfected with the pcDNA4 His/Max FOXC1 missense mutation vectors. FOXC1 P79L and FOXC1 P79T show a mild nuclear localization defect. Sixty-three percent of cells expressing FOXC1 P79L and 64% of cells expressing FOXC1 P79T show exclusive nuclear localization of FOXC1, compared with 95% for wild type FOXC1 (Figure 17b). FOXC1 S82T showed wild type levels of exclusive nuclear localization in 90% of the cell population (Figure 17a), as did FOXC1 L86F, also with wild type FOXC1 levels of exclusive nuclear localization (Figure 17c). A reduction in nuclear localization was also seen with FOXC1 I91T, with only 52% of the cells showing localization of FOXC1 to the nucleus (Figure 17b). Interestingly, disruption to nuclear localization was much more drastic with FOXC1 I91S, in which nuclear localization is reduced to only 15% of the cell population (Figure 17b). The FOXC1 F112S mutation, located between helices 2 and 3, again displays wild type levels of exclusive nuclear localization at 94% of the cell population (Figure 17a). Nuclear localization of FOXC1 also appears to be severely disrupted when

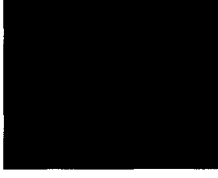
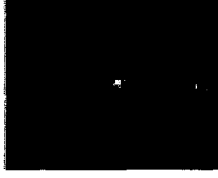
**Figure 17. Missense mutations can perturb the nuclear localization of FOXC1.**

Indirect immunofluorescence of Xpress epitope tagged FOXC1 proteins in COS-7 cells visualized by Cy3 fluorescence. Nuclei are stained with DAPI. The tables to the right indicate the percentage of cells with the indicated subcellular localization. To quantitate the extent of recombinant FOXC1 protein localization, at least 100 cells were randomly selected, and the percentage of cells exhibiting Cy3 fluorescence in the nucleus only, in both the nucleus and cytoplasm, and in the cytoplasm only was determined. A. Localization of S82T, I87M, F112S, I126M, and S131L FOXC1 mutant proteins. ND indicates that the percentage of exclusive nuclear localization was not determined for this FOXC1 mutation. B. Subcellular distribution of P79L, P79T, I91S, I91T, and R127H FOXC1 mutations. C. L86F.

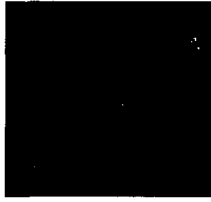
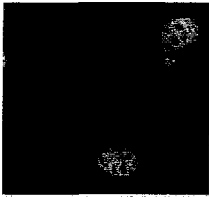
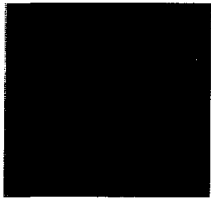
**A.**

	Cy3	DAPI	Nuclear	Nuclear + Cytoplasmic	Cytoplasmic
<b>FOXC1</b>			95%	4.5%	0.5%
<b>S82T</b>			90%	8.5%	1.5%
<b>I87M</b>			ND	ND	ND
<b>F112S</b>			94%	5%	1%
<b>I126M</b>			84%	13%	3%
<b>S131L</b>			72%	28%	0%

**B.**

	Cy3	DAPI	Nuc	Nuc/Cyto	Cyto
FOXC1			95%	4.5%	0.5%
P79L			63%	5%	33%
P79T			64%	6%	30%
I91S			15%	30%	56%
I91T			52%	14%	34%
R127H			17%	0%	83%

C.

	Cy3	DAPI	Nuclear	Nuclear + Cytoplasmic	Cytoplasmic
FOXCI			84%	15%	1%
FOXCI L86F			80%	10%	10%

the R127H mutation is present; only 17% of the cells show exclusive nuclear localization of FOXC1 (Figure 17b). Nuclear localization of FOXC1 S131L showed some reduction to 72% compared to 95% for wild type FOXC1 (Figure 17a). A schematic of the FHD with NLSs and positions of the disease causing missense mutations is shown in Figure 18.

Interestingly, FOXC1 containing the I87M mutation could still be localized to the cell nucleus by immunofluorescence. The immunofluorescent signal was weaker and present in a smaller percentage of cells (less than 1%) within the visual field compared to the other missense mutations and wild type FOXC1 (Figure 17a). This weak immunofluorescence is likely due to the reduced stability of the FOXC1 I87M mutant protein. As a result of the instability of this protein, the FOXC1 I87M mutation was not tested further.

#### *Electrophoretic Mobility Shift Assays (EMSAs)*

EMSAs demonstrated that the FOXC1 forkhead domain preferentially forms DNA-protein complexes with an *in vitro* derived oligonucleotide, the FOXC1 binding site (Pierrou et al. 1994) (Table 3). This oligonucleotide was used in EMSA experiments to investigate how FOXC1 missense mutations affect FOXC1 binding of the FOXC1 binding site (Figure 19). FOXC1 carrying a P79T, P79L, S82T, L86F, I91S, or I91T missense mutation was found to retain reduced but readily detectable DNA binding function. This function is reduced in comparison to wild type FOXC1 by 2 to 5-fold in all cases, when equal amounts of wild type and mutant FOXC1 protein were tested.

**Figure 18. Nuclear localization signals and the positions of the missense mutations relative to the FHD secondary structures.** The C-terminal NLS and N-terminal putative nuclear accessory signal are indicated with grey boxes. The residues at which missense mutation occur are shown in blue while the missense mutations are shown above. Missense mutations that cause a severe impairment of FOXC1 localization are shown in red, while missense which disrupt FOXC1 nuclear localization to a lesser extent are indicated in orange.

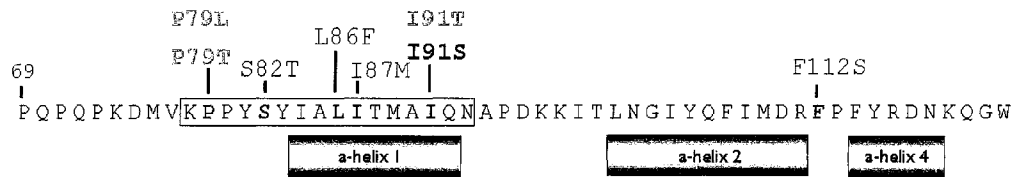


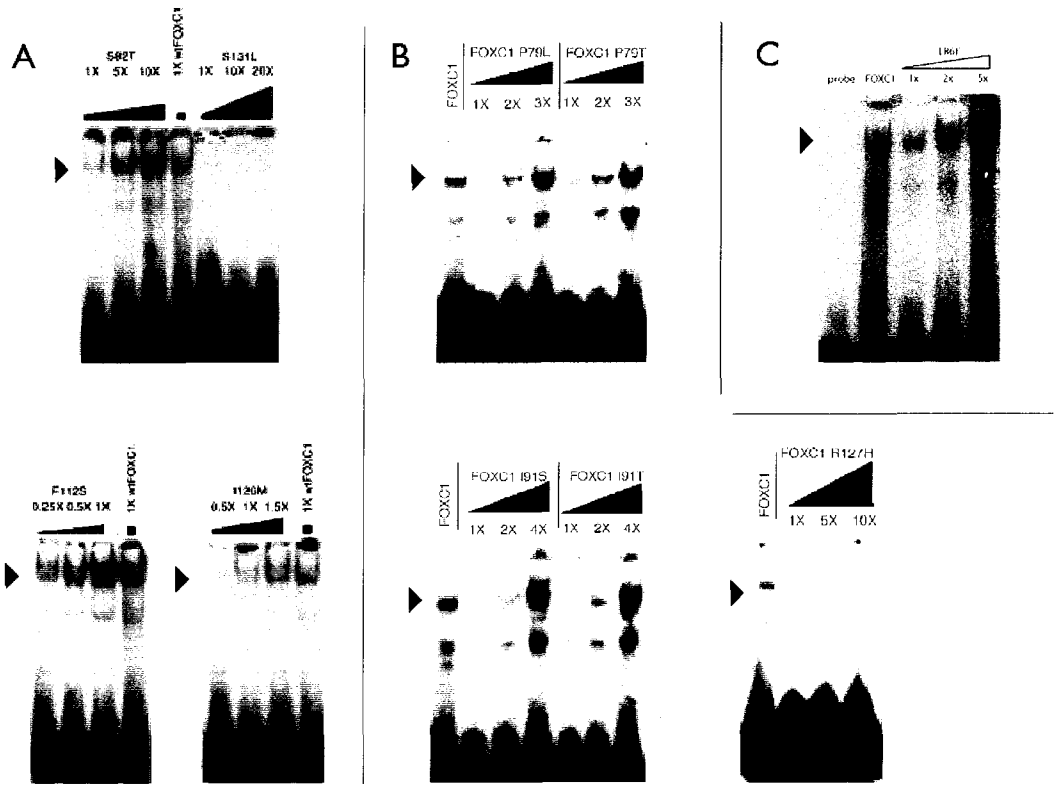
**Table 3.** The FOXC1 binding site and variant oligonucleotides.

Oligonucleotide	Forward	Reverse
<b>FOXC1 binding site</b>	gatccaaag <u>taataa</u> acaacaga	gatctctgtt <u>gtttatt</u> actttg
1	gatccaaa <u>ctaataa</u> acaacaga	gatctctgtt <u>gtttatt</u> agttg
2	gatccaaag <u>aaaataa</u> acaacaga	gatctctgtt <u>gtttattt</u> ctttg
3	gatccaaag <u>gtaataa</u> acaacaga	gatctctgtt <u>gtttatta</u> actttg
4	gatccaaag <u>tataata</u> acaacaga	gatctctgtt <u>gtttatata</u> ctttg
5	gatccaaag <u>taatta</u> acaacaga	gatctctgtt <u>gtttaatt</u> actttg
6	gatccaaag <u>taaaaa</u> acaacaga	gatctctgtt <u>gtttttt</u> actttg
7	gatccaaag <u>taaatta</u> acaacaga	gatctctgtt <u>gttaatt</u> actttg
8	gatccaaag <u>taataata</u> acaacaga	gatctctgtt <u>gtatatt</u> actttg
9	gatccaaag <u>taataat</u> acaacaga	gatctctgtt <u>gattatt</u> actttg

The 9-bp core sequence of the *in vitro* derived FOXC1 binding site is underlined. Each of the variants has a converted nucleotide, shown in boldface. Purines were converted to pyrimidines and pyrimidines to purines with an equivalent number of hydrogen bonds. These conversions are thought to cause sequence dependent variations in the width of the major and minor grooves (Ulyanov et al. 2002). Modeling of these mutations also predicts that these alterations will cause localized variation in the width of the minor and major grooves of the DNA.

**Figure 19. FOXC1 missense mutations can disrupt the DNA-binding capacity of FOXC1.**

Equalized recombinant FOXC1 containing cell extracts were incubated with [<sup>32</sup>P]-labelled FOXC1 binding site (see Table 3) and resolved by native PAGE. Filled black arrowheads indicate the position of the FOXC1-DNA complex. FOXC1 S82T (A), P79L, P79T, I91S, I91T (B), and L86F (C) show reduced DNA binding capacity. FOXC1 F112S and I126M (A) appear to bind the FOXC1 binding site at or near wild type levels. FOXC1 S131L (A) or R127H (B) binding of the FOXC1 binding site could not be detected.



Two of the mutations tested did not appear to perturb FOXC1 binding. FOXC1 carrying the F112S or I126M missense mutation binds the FOXC1 binding site at or near wild type FOXC1 protein levels. In contrast, the R127H and S131L missense mutations appear to disrupt FOXC1 DNA binding entirely. Even at 10 and 20X the amount of protein respectively, DNA binding of FOXC1 R127H and S131L mutants was not detected.

*The binding specificity of the FOXC1 I126M mutation is altered*

To test if the FOXC1 missense mutations altered the DNA binding affinity of FOXC1, variant oligonucleotides of the FOXC1 binding site were constructed (Table 3) and EMSA reactions were done using the variant FOXC1 binding sites. All of the missense mutations, except one, showed affinities for the variant oligonucleotides that were equivalent to wild type FOXC1 relative affinity for the same oligonucleotides. The one exception was the FOXC1 I126M mutant; this protein did show altered specificity compared to wild type FOXC1 protein (Figure 20a,b). The affinity of FOXC1 I126M for the variant FOXC1 binding site oligonucleotides 2 (alteration to core binding site shown in bold and underlined; GAAAAATAAA), 3 (GTTAATAAA), 8 (GTAAATATA), and 9 (GTAAATAATT) was higher than the affinity of wild type FOXC1 protein for these variant binding sites. The affinity of FOXC1 I126M for variant FOXC1 binding sites 2 and 9 was also higher than its affinity for the FOXC1 site.

**Figure 20. Effect of FOXC1 missense mutations on DNA-binding specificity.**

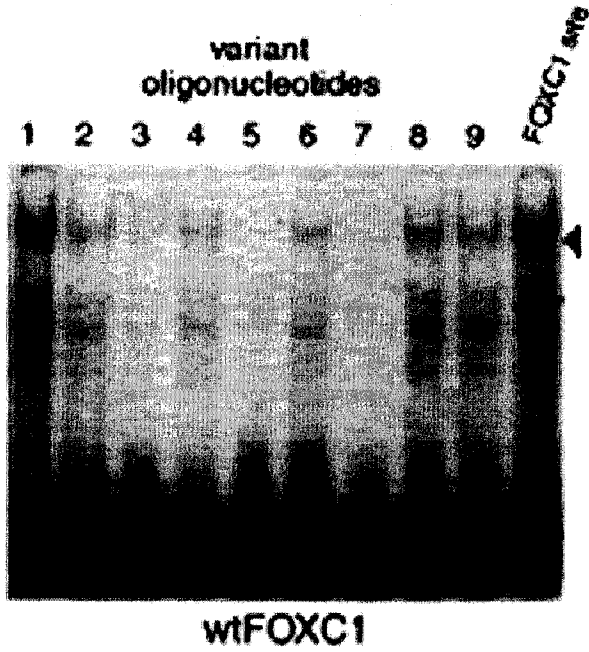
EMSAs were performed with [<sup>32</sup>P]-labelled variant sites (see Table 3) incubated with COS-7 protein extracts containing either wild type or mutant FOXC1.

Recombinant proteins were equalized to wild type FOXC1 by western blotting.

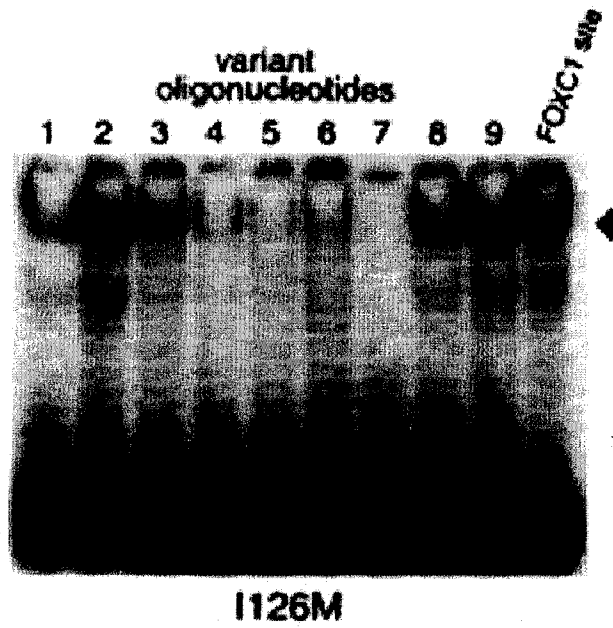
The blackened arrowheads indicate the position of the FOXC1-DNA complex.

The FOXC1 I126M protein (B) shows an increased affinity for variant oligonucleotides 2, 3, 8, and 9, compared with wild-type FOXC1's affinity for these oligonucleotides (A). Also, compared with its affinity for the FOXC1 site, I126M shows an increased affinity for variant oligonucleotides 2 and 9.

A.



B.



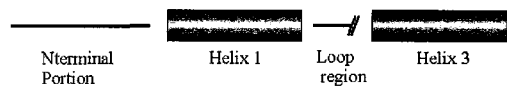
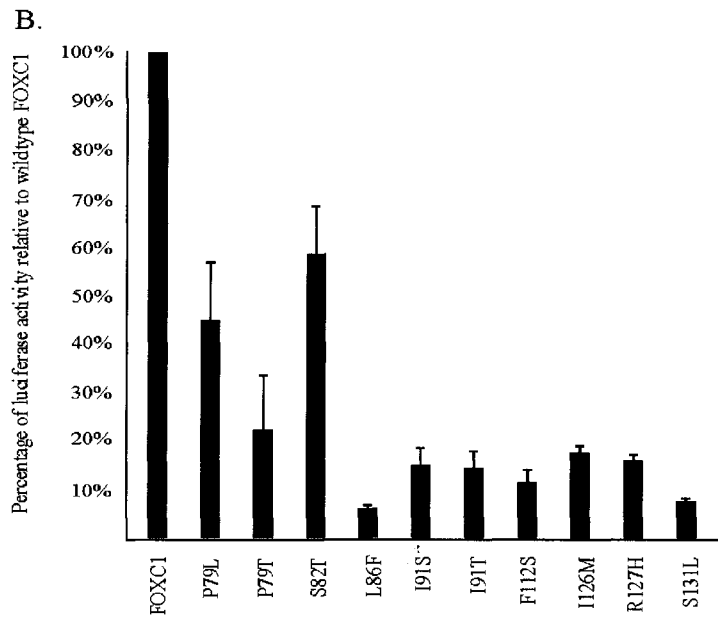
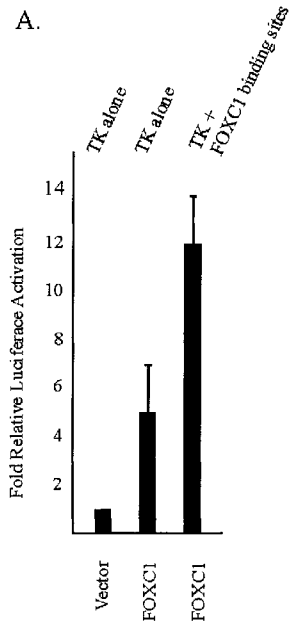
### *Transactivation assays*

FOXC1 is thought to act as a transcription factor; therefore the ability of FOXC1 to regulate expression of a reporter gene was tested. The Herpes Simplex virus Thymidine Kinase (TK) promoter was positioned upstream of a luciferase reporter. HeLa cells were co-transfected with the TK-luciferase reporter construct and pcDNA4 His/Max or FOXC1 pcDNA4 His/Max. FOXC1 was found to stimulate transcription from the TK promoter alone, showing a 5-fold increase in luciferase activity over an empty vector control (Figure 21a). The effect of the FOXC1 binding site on FOXC1 transactivation ability was then tested. Six copies of the FOXC1 binding site were positioned upstream of the Herpes Simplex virus TK promoter, and again the ability of FOXC1 to activate transcription of a luciferase reporter was tested. When the FOXC1 binding sites were inserted upstream of the TK promoter, activation of the luciferase gene by FOXC1 was approximately 12.5 times more than the basal levels of the TK promoter alone (Figure 21b).

The effect of the missense mutations on FOXC1 function was then tested. FOXC1 carrying the P79L mutation retained 45% of wild type FOXC1 transactivation activity, while FOXC1 P79T only retained 22% of wild type FOXC1 activity. The FOXC1 S82T mutant transactivated the luciferase reporter at 57% of wild type levels. FOXC1 L86F shows severe disruption of FOXC1 transactivation with only 6% of wild type transactivation of the luciferase reporter detected. Similarly the I91 mutations both appear to severely reduce the transactivation of FOXC1 (I91S is 15% and I91T is 14%) when compared to wild

**Figure 21. FOXC1 is an activator of transcription, a function disrupted by missense mutations.**

A. A comparison of FOXC1 activation of a luciferase reporter construct either without or with FOXC1 binding sites positioned upstream of the thymidine kinase (TK) promoter. The thick bars represent the mean of the values while the Y error bars indicate the standard deviation of the values. A schematic of the reporter construct with the FOXC1 binding sites is shown above. B. Missense mutations in the forkhead domain of FOXC1 disrupt the ability of FOXC1 to activate transcription from a luciferase reporter. Below the graph is a schematic of the regions in the FHD where these missense mutations are located.



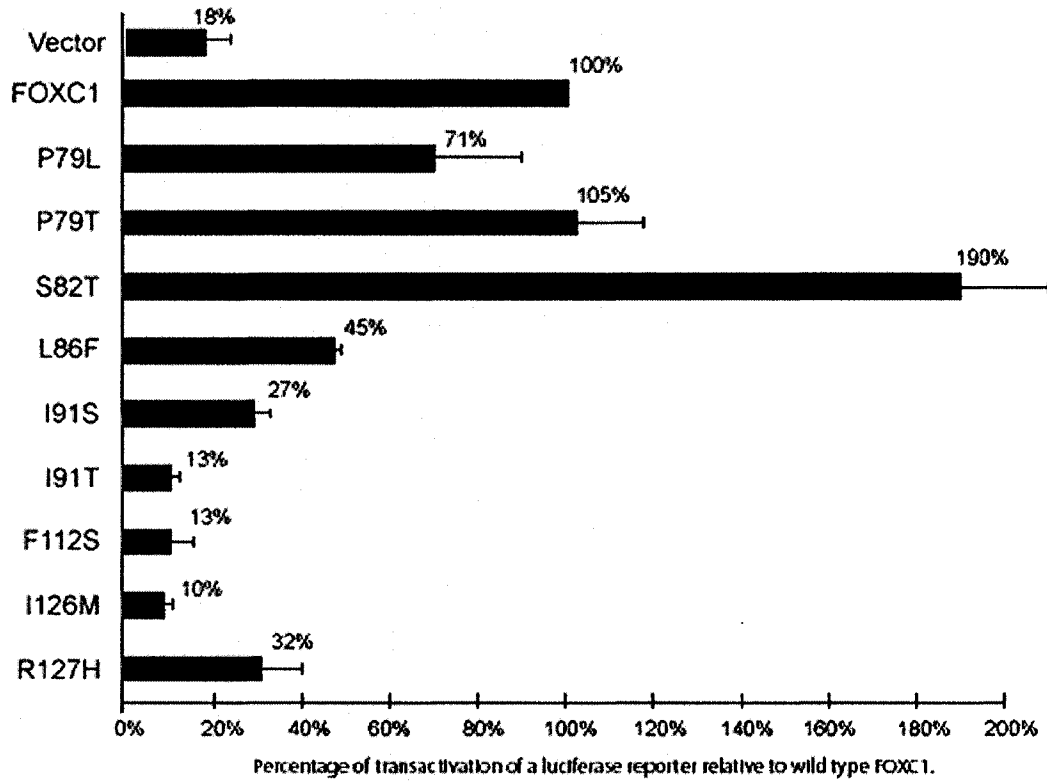
type FOXC1 transactivation levels. The FOXC1 F112S mutant was able to transactivate expression of luciferase by only 12% of the level of wild type activation. Mutations in  $\alpha$ -helix 3 also severely perturbed FOXC1 transactivation. FOXC1 I126M missense mutant was able to transactivate expression of luciferase at only 17% of wild type FOXC1 levels. Similarly, the level of FOXC1 transactivation was reduced to 16% of wild type activity by the presence of the R127H mutation. The FOXC1 S131L mutant showed no transactivation of the luciferase reporter (7% of wild type levels compared to 8% for the empty vector alone; Figure 21b).

*Some FOXC1 missense mutation transactivation defects can be restored by addition of an exogenous DNA binding domain*

In order to investigate if the transactivation defects were caused primarily by a reduction or altered nature of the FOXC1-DNA interactions, or if the defect to transactivation was due to overall structural defects to the FOXC1 molecules, a GAL4 DNA binding domain (BD) was positioned in front of recombinant missense FOXC1 open reading frames. The ability of the exogenous GAL4 BD to rescue the FOXC1 mutant transactivation defect was then tested. In collaboration with Dr Fred Berry, it was found that the GAL4 BD was able to rescue transactivation of FOXC1 P79L/T mutants, bringing transactivation to near wild type FOXC1 levels (Figure 22). Partial rescue of transactivation was seen with FOXC1 I91S and R127H (27% and 32% respectively). No transactivation above vector was seen with the FOXC1 I91T – GAL4 BD

**Figure 22. The addition of an exogenous DNA binding domain can restore transactivation capacity in some FOXC1 missense mutations.**

The GAL4 DNA binding domain was subcloned N-terminal to the FOXC1 open reading frame as shown in the schematic. The resulting chimera was tested for the capacity to drive transactivation from a luciferase reporter with GAL4 binding sites positioned upstream of the luciferase gene. The thick bars represent the mean of the values while the X error bars indicate the standard deviation of the values. Restoration of transactivation to wild type levels of FOXC1 is seen in P79L and P79T, while S82T shows stronger transactivation compared to wild type FOXC1. Transactivation by FOXC1 L86F is partially rescued by the addition of an exogenous DNA binding domain.



construct. The ability of the GAL4 BD to rescue transactivation of four previously characterized FOXC1 mutants (S82T, L86F, F112S, and I126M) that bound the FOXC1 binding site but were unable to transactivate gene expression was also tested. When fused to the FOXC1 L86F mutant, the GAL4 BD partially rescued transactivation to 45% of wild type activity from 6% of wild type activity without the exogenous DNA binding domain. Interestingly, when the S82T FOXC1 mutant was fused to the GAL4 DB, transactivation surpassed wild type activity, giving 190% of wild type activity. Transactivation of the F112S and I126M FOXC1 mutants is not rescued by the addition of an exogenous GAL4 BD.

A summary of the effects of these disease-causing missense mutations on FOXC1 function is shown in Table 4.

**Table 4.** Summary of molecular defects caused by missense mutations in FOXC1.

Mutation & 2° structure involvement	Nuclear	DNA binding capacity	Molecular Defect		GAL4 TA
			TA	Altered binding specificity	
<b>P79L</b> N-terminal region	++	+	+		++
<b>P79T</b> N-terminal region	++	+	+/-		+++
<b>S82T</b> N-terminal region	+++	+	+		++++++
<b>L86F</b> α-helix1	+++	++	-		+
<b>I87M</b> α-helix1			Reduces protein stability		
<b>I91S</b> α-helix1	-	+	-		+/-
<b>I91T</b> α-helix1	+	+	-		-
<b>F112S</b> T-loop	+++	+++	-		-
<b>I126M</b> α-helix3	+++	+++	-	Yes	-
<b>R127H</b> α-helix3	-	-	-		+/-
<b>S131L</b> α-helix3	++	-	-		ND

Listed are missense mutations of FOXC1 studied herein and the molecular effects of the mutation. TA: transactivation, ND: not determined, GAL4 TA: GAL4 transactivation. Nuclear localization and transactivation scoring: 81-100% (+++), 61-80% (++), 41-60% (+), 21-40% (+/-), 0-20% (-). DNA binding scoring: 1X (+++), 2X-4X (++), 5X-9X (+), 10X (+/-), <10X (-).



### **Charge conversion studies at key forkhead domain residues**

FOXC1 was mutated independently to an alanine (A), a glutamate (E), or a lysine (K) residue at each of positions P79, L86, I87, I91, I126, and R127, by site directed mutagenesis. The rationale for choosing these positions was two fold. Firstly, using molecular modeling and threading analyses, alterations predicted to significantly alter the structure of the FHD were identified. These analyses were done by Drs Banerjee-Basu and Baxevanis, and predicted that I126E and I126K would significantly alter FHD structure. Secondly, these residues were known to be critical to FOXC1 function from my analysis of naturally occurring missense mutations at these positions.

#### *FOXC1 expression is impaired by mutations at I87*

Expression and Western analysis of the recombinant proteins revealed that all the plasmid constructs expressed recombinant FOXC1 with the exception of FOXC1 mutated at position 87. When I87 was converted to an A, E, or K amino acid residue, FOXC1 protein could not be detected by Western analysis (Figure 23b). Northern blot analysis indicated that mRNA was being expressed from the transfected recombinant FOXC1 plasmid (Figure 23a). FOXC1 87A/E/K mRNA was detected by Northern analysis, but respective proteins could not be detected by Western analysis. This finding is consistent with the notion that these alterations at I87 drastically reduce the levels of these recombinant proteins, as is also seen with the I87M mutation.

**Figure 23. Conversion of I87 to an alanine, glutamate, or lysine residue reduces protein levels of FOXC1.**

A. Northern blot analysis showing expression of FOXC1 and FOXC1 87 A/E/K mRNA. The northern blot was probed with an N-terminal portion of the FOXC1 gene (see Experimental Procedures). Loading amounts were equalized on a 1 times 3-(N-morpholino) propane sulfonic acid, pH 7.0, 0.66M formaldehyde agarose gel (see Experimental Procedures). B. Western blot analysis showing detection of only wild type FOXC1 protein. FOXC1 I87A, E, or K protein is not detected with the anti-Xpress antibody.



### *Subcellular localization of charge conversion mutants*

Disease-causing missense mutations within the FHD are able to disrupt the normal nuclear localization of FOXC1 in COS-7 cells; therefore the subcellular localization of these conversion constructs was determined. By immunofluorescence, the subcellular localization of the FOXC1 mutant proteins was found to be highly variable and dependent upon both the position of the amino acid change and the charge of the amino acid change (Figure 24 and Table 5). With the exception of amino acid residue R127, conversion of the amino acid to the neutral alanine amino acid had the least severe disruption on nuclear localization of FOXC1. Nuclear localization was the least perturbed by the presence of the neutral charged P79A (91% nuclear). The charged amino acids, P79E and P79K, were more disruptive to FOXC1 localization, at 80% and 75% nuclear respectively. At position L86 the change to the uncharged alanine disrupts the nuclear localization of FOXC1 to a similar level as what is seen with P79K. Again when charged amino acids are substituted for leucine at position 86, subcellular localization becomes more perturbed (L86E at 51% nuclear, L86K at 64% nuclear) than what is seen with the alanine substitution (72% nuclear). The localization of FOXC1 seen with mutations at amino acid positions 79 and 86 is predominantly nuclear but is not confined as strictly to the nucleus when compared to cells expressing wild type FOXC1. When charged amino acids are substituted for I91, the disruption becomes severe with 25% of the population showing nuclear localization for I91E and only 5% of the cellular population showing nuclear staining when FOXC1 carries the I91K mutation. I91A shows

**Figure 24. A, E, and K conversions in the FOXC1 FHD differentially disrupt the nuclear localization of FOXC1.**

COS-7 cells were transiently transfected with recombinant Xpress<sup>TM</sup> epitope-tagged constructs. Cy3 fluorescence indicates the position of the Xpress epitope-tagged FOXC1 proteins within the cell. DAPI staining indicates the position of the nuclei. Quantification of subcellular distribution of FOXC1 is given in Table 5.

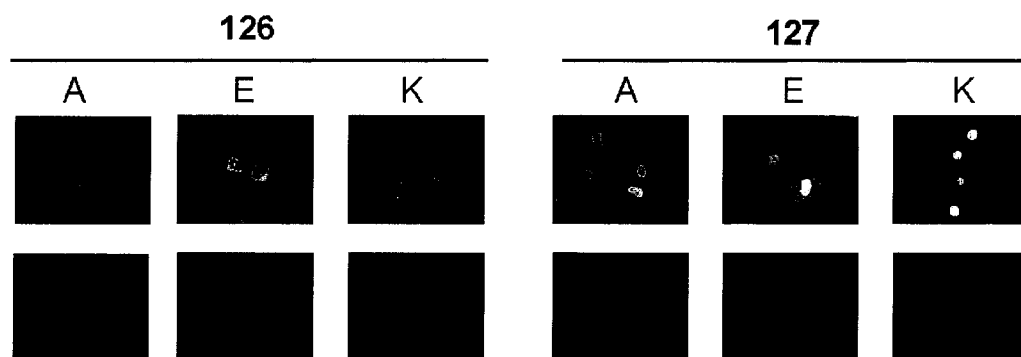
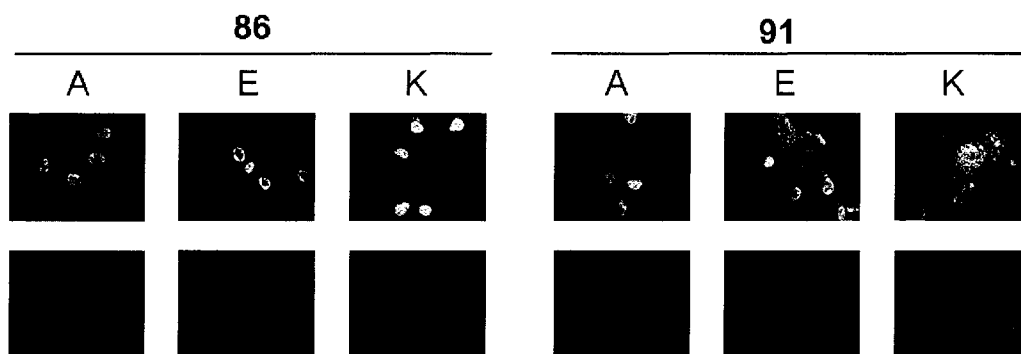
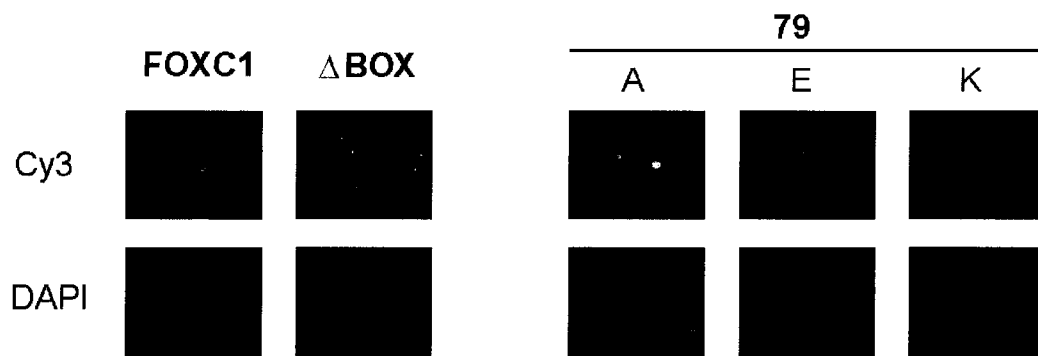


**Table 5.** Summary of subcellular localization of wild type and converted FOXC1 molecules.

	Nuclear	Mixed	Cytoplasmic
FOXC1	99%	1%	0%
$\Delta$ BOX	0%	77%	23%
P79A	91%	8%	1%
P79E	80%	19%	1%
P79K	75%	25%	0%
L86A	72%	28%	0%
L86E	51%	49%	0%
L86K	64%	36%	0%
I91A	55%	18%	27%
I91E	24%	76%	0%
I91K	5%	95%	0%
I126A	77%	23%	0%
I126E	0%	69%	31%
I126K	0%	55%	47%
R127A	56%	44%	0%
R127E	0%	100%	0%
R127K	88%	12%	0%

Nuclear indicates that FOXC1 was detected exclusively in the nucleus while cytoplasmic indicates that FOXC1 was detected exclusively in the cytoplasm. Mixed indicates that FOXC1 was found in both the nucleus and cytoplasm. A minimum of 100 cells was scored for each mutant.

levels of nuclear localization that are similar to levels seen with L86E. The differences to nuclear localization upon substitution of differently charged amino acids is most pronounced in residues I126 and R127, both of which are located in  $\alpha$ -helix 3 of the FHD. The substitution of charged residues at I126 prevents the strict nuclear localization of FOXC1 in any cells in the population, leading instead to both mixed nuclear and cytoplasmic staining, as well as cytoplasmic staining only.

The mislocalization of FOXC1 I126E and I126K appears to be different from the mislocalization when the other amino acids are altered. As can be seen in Figure 24, the majority of the immunofluorescent signal given by these mutations localizes to a perinuclear space, within what may be the endoplasmic reticulum. Conversely, FOXC1 carrying the I126A alteration shows much stronger nuclear localization, where levels are similar to what is seen with P79K or L86A. Finally, FOXC1 R127A, at 56% nuclear, does have a nuclear localization defect but this is much less severe than the disruption seen for FOXC1 R127E, in which mislocalization is complete. Nuclear localization of FOXC1 R127K approaches wild type levels (88%) with little defect in localization seen.

*Charge conversion mutations differentially perturb the DNA binding capacity of FOXC1*

As the FHD is the domain through which FOXC1 – DNA interactions are mediated, it was of interest to test how altering the amino acid and charge at

different positions affects the ability of FOXC1 to bind an *in vitro* derived FOXC1 binding site (BS) (Table 3). As seen in Figure 25, FOXC1 with alterations to amino acids P79, L86, or I91 is still able to bind DNA, although in some cases this binding capacity is reduced. The binding capacity of FOXC1 P79A and P79K is at or near wild type levels, while P79E appears to bind with a 3 to 4-fold reduction in affinity for the FOXC1 binding site. The binding capacity of FOXC1 L86A, E, or K is at or near wild type FOXC1 levels. Binding capacity of FOXC1 with alterations at I91 is reduced in the cases of I91A, and K with 3 to 4-fold reductions in affinity for the FOXC1 binding site. FOXC1 I91E binds the FOXC1 binding site with wild type FOXC1 affinity.

The deficiencies in FOXC1 binding are more pronounced when I126 or R127 are exchanged for A, E, or K (Figure 25). Binding capacity of FOXC1 is completely disrupted by the presence of an alanine or glutamic acid at 126. When a lysine is present binding capacity is retained; however, there is an approximate 10-fold increase in the amount of FOXC1 I126K protein required for wild type levels of DNA binding. Two of the R127 changes, R127A and R127K, show residual binding capacity but the levels of this capacity are reduced to well below 10X wild type FOXC1 levels. The R127E mutation shows no capacity for DNA binding by this assay.

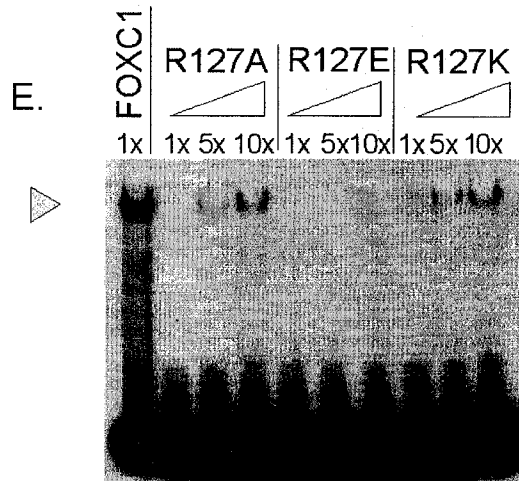
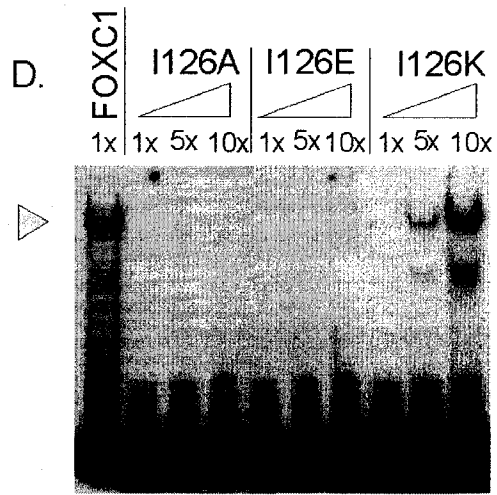
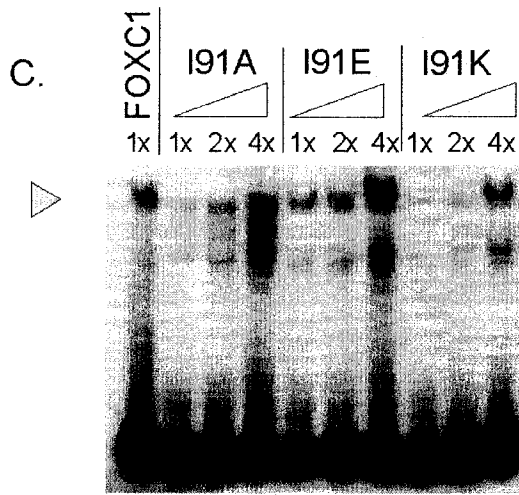
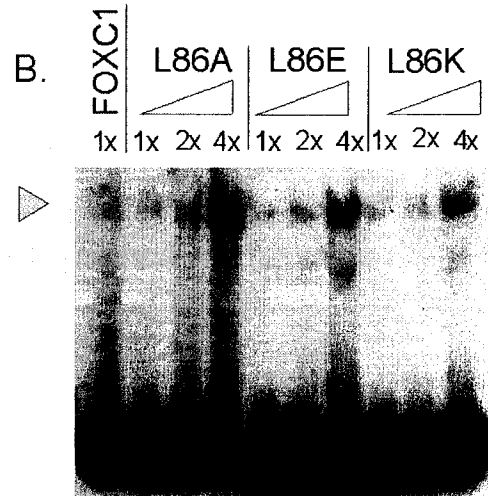
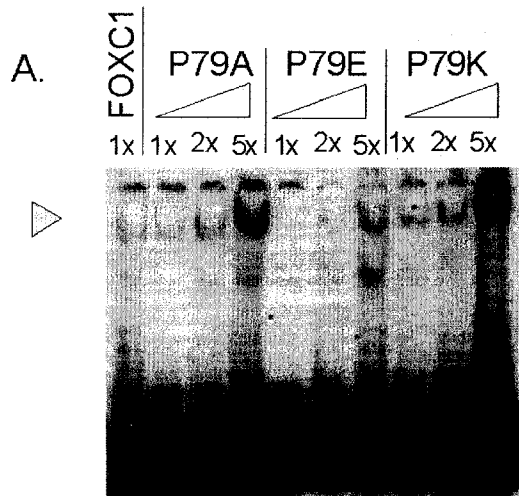
*Amino acids in  $\alpha$ -helix 3 of the FHD regulate FOXC1 DNA binding specificity.*

Data from the analysis of the I126M missense mutation shows that mutations within  $\alpha$ -helix 3 are able to alter the binding site specificity of FOXC1.

**Figure 25. FOXC1 A, E, and K mutations disrupt the DNA-binding capacity of FOXC1 to different extents depending on position and charge.**

Equalized recombinant FOXC1 containing cell extracts were incubated with [<sup>32</sup>P]-labelled FOXC1 binding site (see Table 3) and resolved by native PAGE.

Position of the predominant FOXC1-DNA complex is indicated with the filled grey arrowhead.



It is also known that the specificity of many protein-DNA interactions is reliant upon the interactions of charged amino acid side chains such as arginines, lysines, and glutamic acids, and the charges inherent in the DNA. We therefore utilized the series of FOXC1 binding site variants (Table 3) to test if in fact any of the charge mutations were able to alter the binding site specificity of FOXC1. Only FOXC1 R127A and R127K (Figure 26) display altered binding site specificity in comparison to wild type FOXC1. Compared to wild type FOXC1 affinity, R127A has a reduced binding affinity for variant oligonucleotides 1 and 2 and an increased affinity for variant oligonucleotide 7 (Figure 26a and b). In a manner that is strikingly different from wild type FOXC1 or any of the other mutant FOXC1 proteins tested in this study, R127K shows an affinity for variant oligonucleotide 7 that is stronger than the affinity of FOXC1 R127K for the FOXC1 binding site (Figure 26a and c). These data indicate that  $\alpha$ -helix 3 of the FHD in FOXC1 may play a strong role in regulating the specificity of FOXC1 – DNA interactions.

#### *Transactivation Assays*

FOXC1 is able to potently drive expression of a reporter construct when the FOXC1 binding site is present in front of the construct promoter (see Figure 27 inset). The effect of the different charges at the different positions on the ability of FOXC1 to drive transactivation was tested. The majority of constructs tested had severely reduced transactivation activity, including those FOXC1 mutations that retained DNA binding activity (FOXC1 79A/E, 86A/E/K,

**Figure 26. Conversion of R127 to an alanine or lysine residue alters the binding specificity of FOXC1.**

FOXC1 containing cell extracts were incubated with [<sup>32</sup>P] - labelled FOXC1 binding site or variant oligonucleotides (see Table 3) and resolved by native PAGE. Position of the predominant FOXC1-DNA complex is indicated with the filled grey arrowhead, an asterisk indicates oligonucleotides that the FOXC1 proteins bind with altered affinity. A. Wild type FOXC1. B. FOXC1 127A no longer binds oligonucleotides 1 and 2 while binding oligonucleotide 7. C. FOXC1 127K binds oligonucleotide 7 with a greater affinity than its affinity for the FOXC1 binding site.

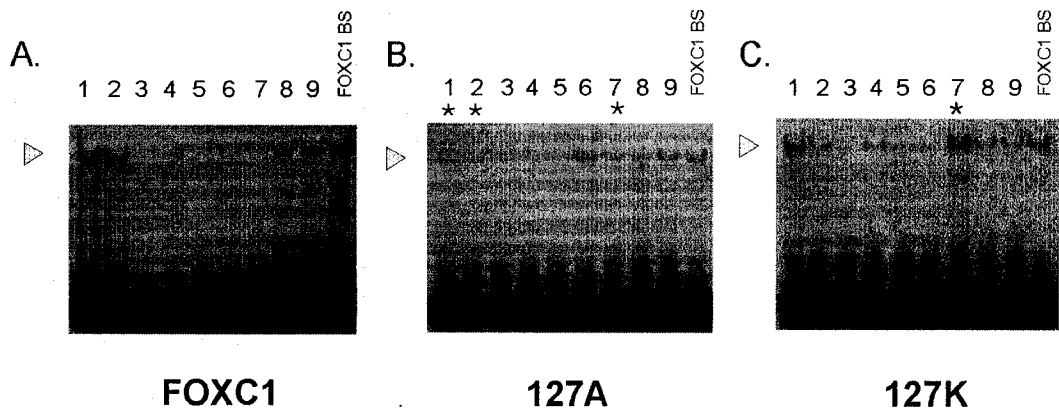
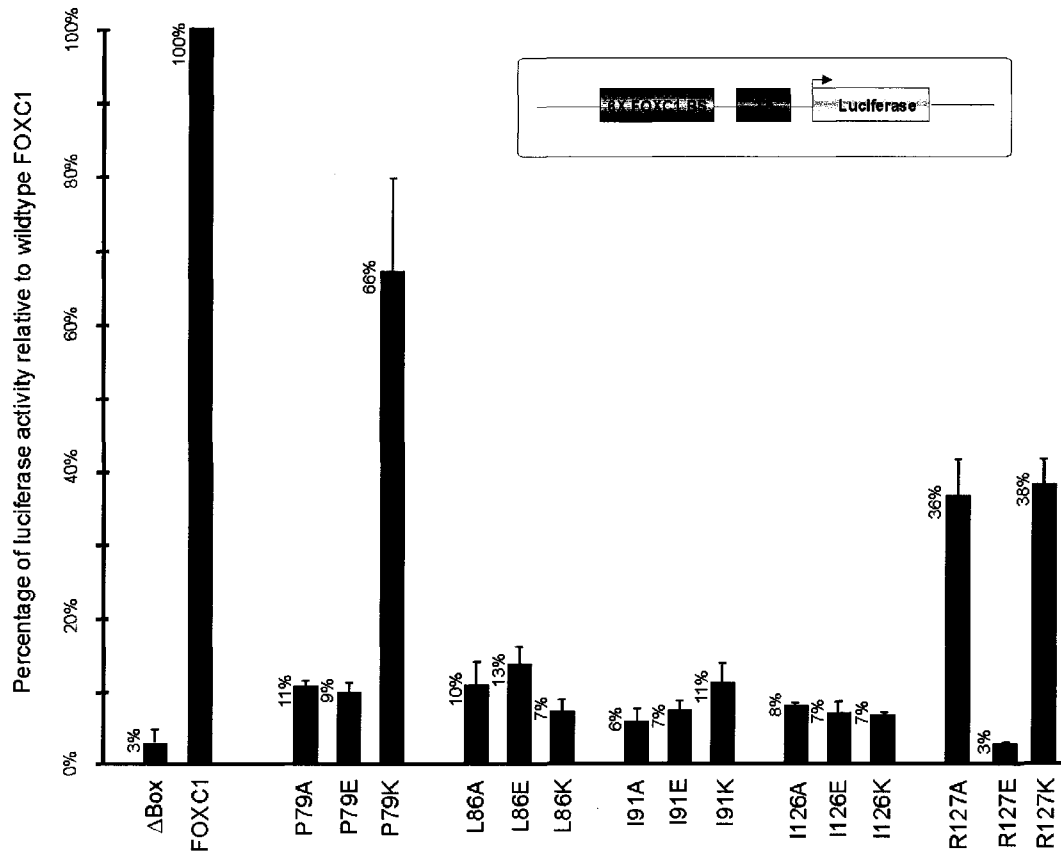


**Figure 27. Disruption of transactivation of a luciferase reporter construct by FOXC1 A/E/K proteins.**

The thick black bars represent the mean of the values; the Y error bar indicates the standard deviation of the values. The inset shows a schematic of the FOXC1 binding site – thymidine kinase promoter - luciferase gene reporter construct.



91A/E/K, 126K). Notable exceptions were FOXC1 P79K, R127A, and R127K. FOXC1 P79K retained an average transactivation capacity of 66% of wild type activity, while FOXC1 R127A and R127K had transactivation capacities of 36% and 38% of wild type FOXC1 activity, respectively.

A summary of the molecular effects of these charge conversion mutations on FOXC1 function is shown in Table 6.

#### **Helix 4 Alanine Mutagenesis Studies**

Analyses of the DNA binding site specificity of FOXA2, showed that a 20 amino acid stretch, adjacent to the N terminus of helix 3, was able to influence the DNA binding specificity of this protein (Overdier et al. 1994). This region encompasses the putative helix 4 that lies between helices 2 and 3. In order to test the functional significance of helix 4, amino acids 114 through 118 were independently converted to alanine residues and the consequences to FOXC1 function tested (Figure 28).

FOXC1 was mutagenized as described above, and expressed in COS-7 cells. Proteins were equalized and EMSA reactions performed (Figure 29). As can be seen in Figure 29, conversion of amino acids to alanines in this region does not impair FOXC1 affinity for the FOXC1 binding site. In order to test if the binding site specificity was altered, EMSAs were done using the panel of variant oligonucleotides (Table 3). As seen in Figure 30, the binding site specificity of the FOXC1 helix 4 constructs does not differ significantly from wild type FOXC1.

**Table 6.** Summary of the molecular consequences of conversion of these critical amino acid positions to an alanine, glutamic acid, or lysine residue.

Change	Structure	Molecular Defect			
		Exclusive nuclear	DNA binding	Altered specificity	Trans-activation
<b>P 79 A</b>		91%	+++	No	10.5%
<b>P 79 E</b>		80%	++	No	9.0%
<b>P 79 K</b>		75%	+++	No	66.3%
<b>L 86 A</b>	$\alpha$ -helix 1	72%	++	No	9.7%
<b>L 86 E</b>	$\alpha$ -helix 1	51%	+++	No	12.8%
<b>L 86 K</b>	$\alpha$ -helix 1	64%	++	No	7.3%
<b>I 87 A</b>	$\alpha$ -helix 1	Reduced Protein Levels			
<b>I 87 E</b>	$\alpha$ -helix 1	Reduced Protein Levels			
<b>I 87 K</b>	$\alpha$ -helix 1	Reduced Protein Levels			
<b>I 91 A</b>	$\alpha$ -helix 1	55%	++	No	6.4%
<b>I 91 E</b>	$\alpha$ -helix 1	24%	++	No	7.0%
<b>I 91 K</b>	$\alpha$ -helix 1	5%	++	No	11.4%
<b>I 126 A</b>	$\alpha$ -helix 3	77%	-	No	8.3%
<b>I 126 E</b>	$\alpha$ -helix 3	0%	-	No	6.8%
<b>I 126 K</b>	$\alpha$ -helix 3	0%	+	No	6.6%
<b>R 127 A</b>	$\alpha$ -helix 3	56%	+	Yes	36.3%
<b>R 127 E</b>	$\alpha$ -helix 3	0%	-	No	2.7%
<b>R 127 K</b>	$\alpha$ -helix 3	88%	+	Yes	38.0%

Listed are the amino acid conversions studied in this paper, the secondary amino acid structures involved and the molecular defect. Exclusive nuclear indicates the percentage of cells showing FOXC1 localization exclusively to the nucleus. DNA binding is compared to wild type FOXC1 with +++ indicating wild type or near wild type levels, ++ showing a 3-5 fold reduction, and + indicating a greater than

ten fold reduction. Transactivation refers to the percentage of luciferase activity relative to wild type FOXC1.

**Figure 28. A schematic of the FHD, indicating the position of the amino acids converted in the  $\alpha$ -helix 4 studies.**

Amino acids converted individually to alanines are shown in blue and underlined.

Primary amino acid sequence is shown above while the secondary structures formed are illustrated below.

69

**P**Q**Q**P**Q**PKDMVKPPYSYIALITMAIQNAPDKKITLNGIYQFIMDRFP**FYRDNKQGW**

**α-helix 1**

**α-helix 2**

**α-helix 4**

178

QNSIRHNLSLNECFVKVPRDDKKPGKGSYWTLPDPSYNMFENGSLRRRRR**F**KKKD

**α-helix 3**

**Beta 2**

**Wing 1**

**Beta 3**

**Wing 2**

**Figure 29. Conversion of amino acids in Helix 4 of the FHD does not perturb FOXC1 DNA binding.**

A. Western blot showing expression and equalization of FOXC1 wild type and recombinant proteins. Protein was detected using the anti-Xpress antibody against the vector encoded N-terminal express tag. B. EMSA showing that all the helix 4 alanine mutations retain DNA binding capacity that is at or near wild type FOXC1 levels. The filled grey arrowheads indicate the position of the FOXC1 DNA complex.

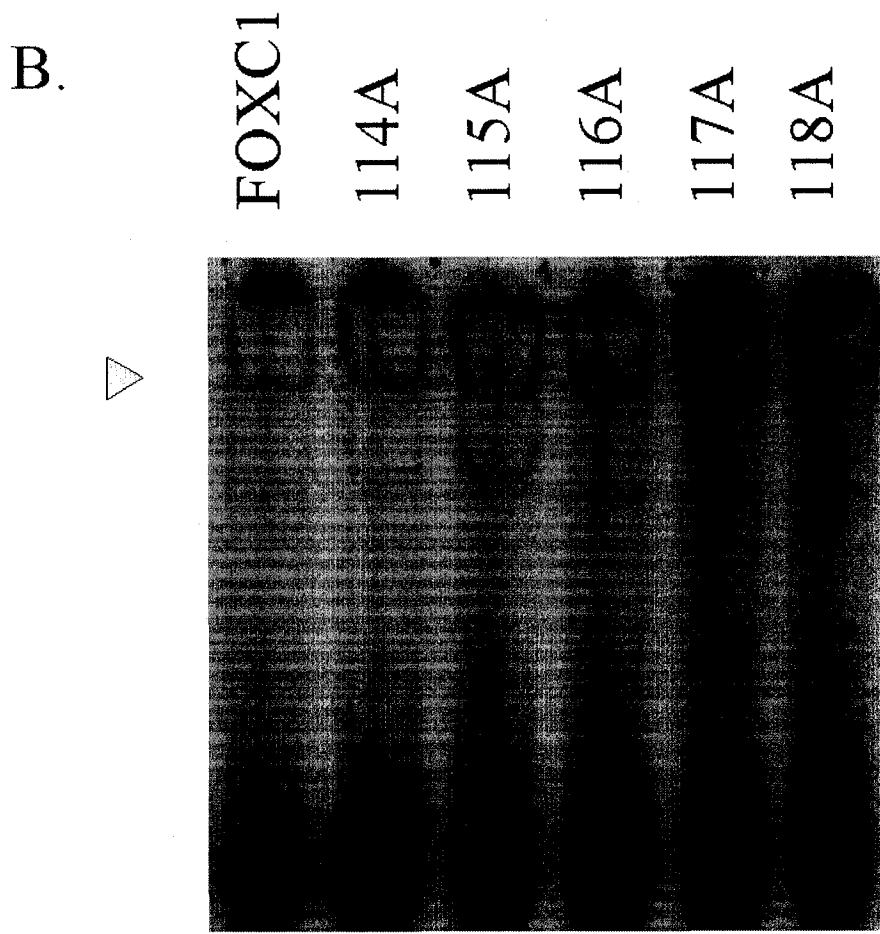
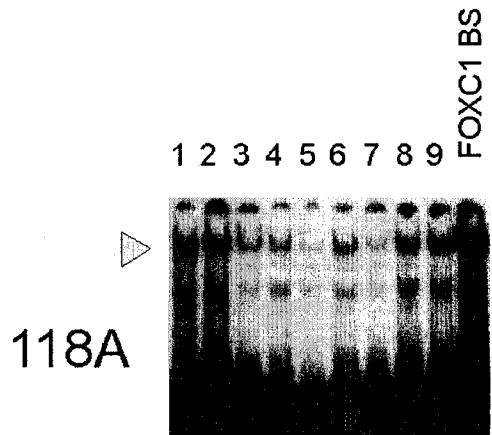
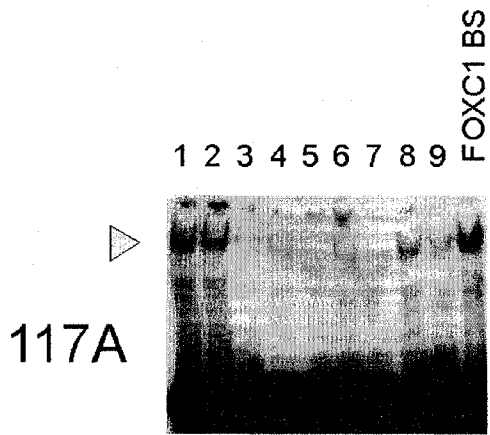
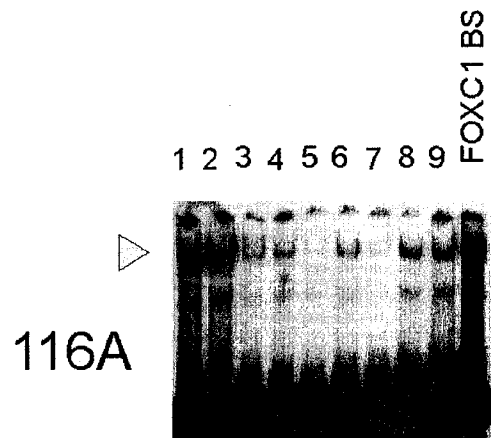
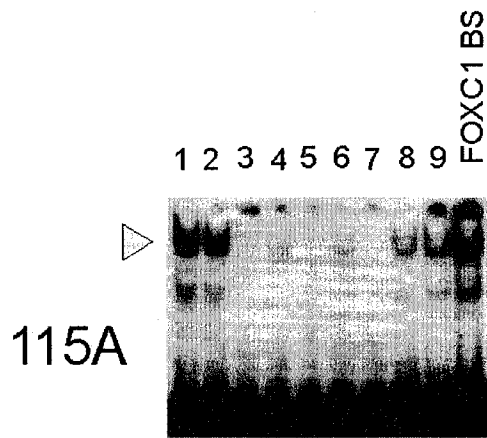
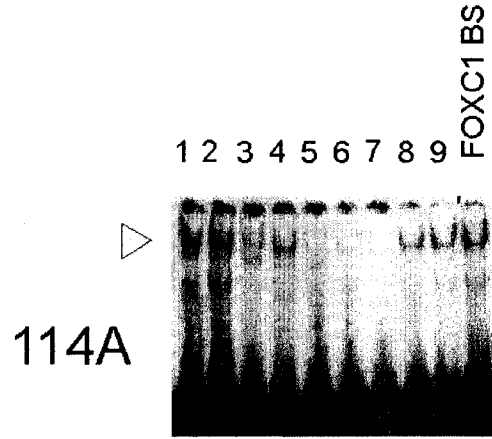
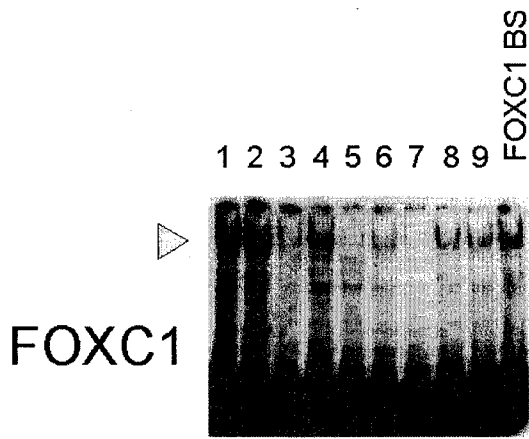


**Figure 30. Conversion of amino acids in helix 4 of the FHD does not alter the DNA binding specificity of FOXC1.**

EMSA was performed with [<sup>32</sup>P]-labelled variant sites (see Table 3) incubated with COS-7 protein extracts containing either wild type or alanine mutant FOXC1. Recombinant proteins were equalized to wild type FOXC1 by western blotting. The filled grey arrowheads indicate the position of the FOXC1 DNA complex.



Finally, transactivation assays were done to test if any of these alanine conversions were able to alter the transactivation capacity of FOXC1. These experiments were problematic in that there were large experiment-to-experiment differences in the levels of transactivation. FOXC1 F114A and Y115A both show a reduction in transactivation in comparison to wild type FOXC1 but the amount of reduction was variable ranging from 50% to 126% for F114A and 6% to 86% for Y115A. Similarly, FOXC1 R116A, D117A, and N118A all showed highly variable rates of transactivation even from experiment to experiment. When results were averaged, R116A appears to show a transactivation reduction of FOXC1; however, in some assays FOXC1 R116A transactivated at wild type levels. Similarly, transactivation assays with FOXC1 D117A and N118A showed highly variable rates of transactivation from experiment to experiment, sometimes displaying a transactivation defect, and at other times transactivating better than wild type FOXC1. The highly variability of the results makes interpretation of the transactivation studies quite difficult.

### **Helix 1 Disruption Studies**

In order to study the function of helix 1 as whole, a proline was exchanged for the leucine at position 86, the site of the naturally occurring L86F mutations described earlier. Prolines are known to break  $\alpha$ -helices, thus the role of  $\alpha$ -helix 1 in organizing the FHD for proper FOXC1 function could be assessed.

FOXC1 L86P drastically reduces the nuclear localization of FOXC1 protein with only 20% of the cell population showing exclusive nuclear localization of FOXC1 L86P (Figure 31a). The FOXC1 L86P molecules localize either within the cytoplasm or to aggregates in what appears to be the endoplasmic reticulum.

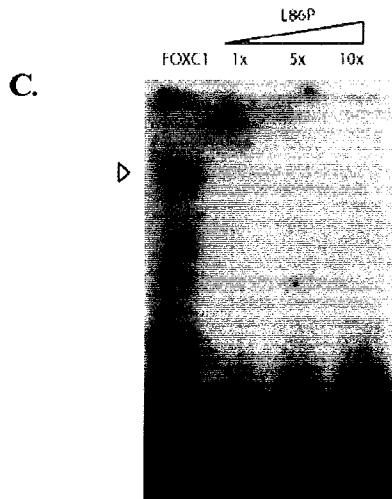
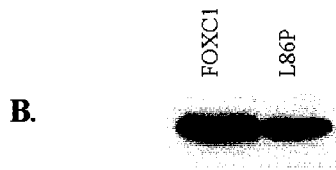
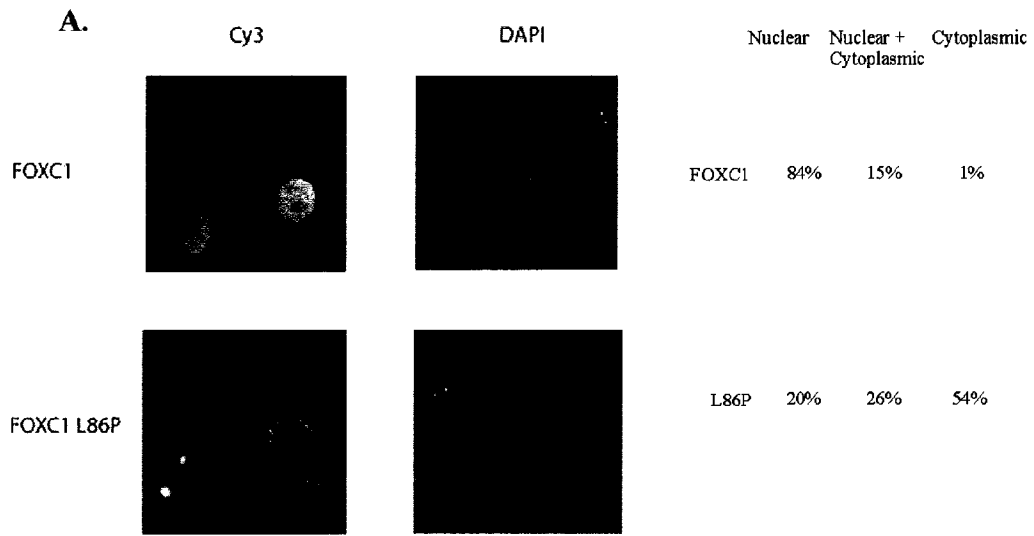
This mutation did not affect the overall stability of FOXC1 as recombinant protein of the correct molecular weight was detected by western analysis (Figure 31b). COS-7 cell extracts containing L86P recombinant FOXC1 were used in EMSA assays to determine if this mutation has an effect upon the ability of FOXC1 to bind the FOXC1 binding site. The FOXC1 L86P mutation completely abolished DNA binding in FOXC1 (Figure 31c).

The effect of the L86P mutation upon the transactivation potential of FOXC1 was then investigated. Using the luciferase reporter construct with FOXC1 binding sites, the transactivation ability of FOXC1 is severely perturbed by the L86P mutation (Figure 32a). FOXC1 in which the forkhead domain was deleted, ? Box, activated luciferase expression at only 4% of wild-type FOXC1. The presence of FOXC1 L86P resulted in 16% luciferase transactivation compared to wild type FOXC1.

In order to test the ability of L86P to act in a dominant negative manner, wild type FOXC1 was co-transfected with L86P and the effect on transactivation measured. The presence of the mutant FOXC1 protein did not alter the levels of activation of the reporter construct by wild type FOXC1 (Figure 32).

**Figure 31. The conversion of L86 to a proline severely disrupts FOXC1 localization and DNA binding capacity.**

A. FOXC1 L86P mislocalizes within COS-7 cells. On the right is indicated the percentage of cells with exclusive nuclear localization, mixed nuclear and cytoplasmic localization, and exclusive cytoplasmic localization. B. Western analysis showing that FOXC1 L86P can be expressed and is stable. C. FOXC1 L86P DNA binding cannot be detected. EMSAs showing that even at 10X the levels of wild type FOXC1, DNA binding is not seen. The filled grey arrowhead indicates that position of the predominant FOXC1-DNA complex.



**D.**

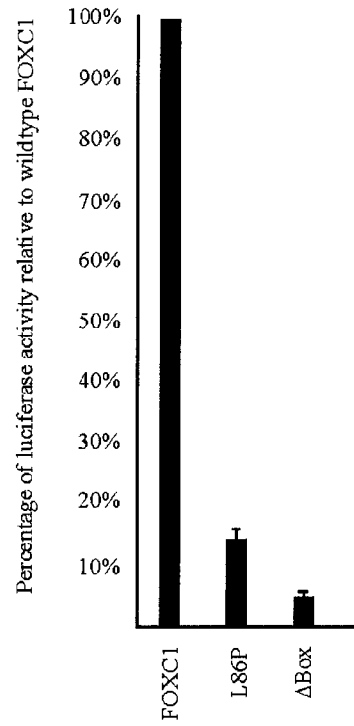
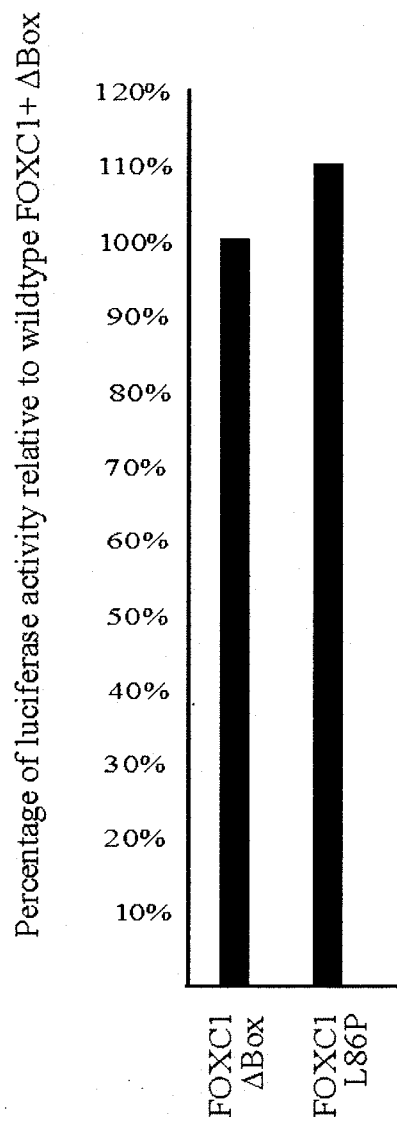


**Figure 32. Transactivation studies with FOXC1 L86P.**

FOXC1 L86P does not act in a dominant negative manner, with no reduction in transactivation when co-transfected with wild type FOXC1.



## Discussion

### Identification of Nuclear Localization Signals within the FOXC1 FHD

At the N and C terminal boundaries of the FHD are two regions required for the exclusive nuclear localization of FOXC1. Previous work on nuclear localization signals (NLSs) in FOXA2 and FOXF2 FHDs demonstrated that the NLS in these forkhead domains is bipartite (Hellqvist et al. 1998; Qian and Costa 1995). The first NLS region in FOXC1 is located within residues 77 to 93 (<sup>77</sup>VKPPYSYTIALITMAIQN<sup>93</sup>); deletion of these amino acids leads to both cytoplasmic and nuclear staining (Figure 13). While the nuclear localization of this protein is not exclusively nuclear, a strong nuclear signal remains. This region is not a NLS because when it is fused to GFP, the fusion protein was localized throughout the cell (Figure 14). This region is highly conserved between FHDs but it does not resemble other known NLSs. This sequence may function as an NLS accessory domain, required but insufficient for nuclear translocation. The second domain is found within residues 168 and 176, consisting of a highly basic stretch of amino acids <sup>169</sup>RRRRRFKK<sup>176</sup> that resembles the highly basic SV40 large T antigen NLS (PKKRKV). When fused to GFP, the fusion protein localized to a subcellular compartment within the nucleus that resembled the nucleolus. This region likely represents a real NLS, necessary for FOXC1 nuclear localization and sufficient to target GFP to, and within, the nucleus.

### **Analysis of the Region Preceding $\alpha$ -Helix 1**

Of the positions tested herein, mutations at positions located N-terminal to  $\alpha$ -helix 1 cause the mildest disruptions to the nuclear localization of FOXC1. Maintaining a neutral charge by conversion to an alanine residue does not perturb localization to the same extent as conversions to charged residues. These data would indicate that position P79 of FOXC1 is not directly involved in nuclear transport or retention, as altering the residue to an alanine does not significantly perturb the subcellular distribution of FOXC1. FOXC1 P79L and P79T mutations both show exclusive nuclear localization levels of 63% and 64% respectively, a more severe defect to nuclear localization than what is seen with substitutions to A, E, or K residues at this position. The decrease seen in nuclear localization when 79 is converted to L, T, E, or K suggests that these amino acids are able to interfere, to an extent, with the ability of FOXC1 to organize into a three-dimensional conformation that facilitates the exclusive nuclear translocation or retention of FOXC1. These data would indicate that P79 is therefore involved to some extent in the proper folding or organization of the FHD.

The S82T FOXC1 mutation does not appear to impair the nuclear localization of FOXC1. Although the serine at amino acid 82 of the FHD is highly conserved throughout the forkhead family, the presence of a threonine at this position does occur naturally, albeit rarely, within the forkhead family. FOXH1 (FAST1) and Foxh2 (Fast2) both have a threonine instead of a serine at positions equivalent to FOXC1 amino acid 82, and both proteins function in a manner consistent with nuclear localization (Labbe et al. 1998; Yeo et al. 1999;

Zhou et al. 1998). In this light, it is not surprising that the S82T change does not disrupt the NLS and the FOXC1 S82T protein correctly localizes to the cell nucleus.

The fact that all of the 79 mutant proteins and FOXC1 S82T still retain DNA binding capacity indicates that the FHD itself must be largely intact and the native structure preserved. Although a reduction in DNA binding is seen with P79L and T, P79A, E, and K bind at wild type levels, suggesting that P79 is not a critical amino acid in the formation of FOXC1-DNA complexes. The reduction in DNA binding seen with P79L and T indicates that P79 has some role in the proper organization of the FHD in such a manner that FOXC1 can bind DNA with high affinity. Similarly, a reduction in DNA binding is seen with FOXC1 S82T. To produce wild type levels of DNA binding, 5X the amount of FOXC1 S82T protein is required. The fact that FOXC1 S82T is still able to bind the FOXC1 binding site is again consistent with the idea that the three dimensional conformation of the FHD is grossly intact and FOXC1 as a whole, is competent to bind DNA at appreciable levels.

Changes from a proline at amino acid 79 and a serine at amino acid 82 do appear to change the overall structure of FOXC1 enough that problems with transactivation occur. It is interesting that while FOXC1 P79K shows the most significant defect in FOXC1 subcellular localization of P79A, E, or K, it is the only one of the three that retains transactivation capacity, at 66% of wild type levels (Figure 27). The addition of the exogenous GAL4 DNA binding domain appears to allow recovery of transactivation of the P79L and P79T to levels of

transactivation that are comparable to wild type FOXC1 levels. These data would indicate that mutations at position P79 do not exert a large intramolecular influence, thus when the obligation to bind DNA via the FHD is relieved by the presence of the GAL4 binding domain, the transactivation domains located within FOXC1 are able to exert their influence and activate transcription of a reporter.

FOXC1 S82T, while showing deficiencies in DNA binding, is still able to drive expression of the luciferase reporter at 57% of wild type levels. Clearly, while the conformations of both FOXC1 P79K and S82T are altered enough that FOXC1 S82T DNA binding efficiency is reduced and FOXC1 P79K interactions with the nuclear transport machinery are altered, both molecules retain enough native structure to bind the FOXC1 binding site and participate in transcription from a reporter construct, to some extent.

Interestingly, when FOXC1 S82T is fused with a GAL4 DNA binding domain, the GAL4-BD - S82T chimera is able to transactivate at 190% of GAL4-BD - FOXC1 chimera levels. This increased transactivation potency of GAL4-FOXC1 S82T perhaps indicates that S82T may exert an influence both within the FHD and within the adjacent inhibitory domain or the transactivation domains (Berry et al. 2002). The S82T FOXC1 protein binds the FOXC1 binding site at 25-33% of wild type FOXC1 levels, yet is able to transactivate at 57% of wild type FOXC1 levels. Thus while the S82T mutation impairs DNA binding to some extent, it may have a second effect and act to relieve inhibition of transactivation by the inhibitory domain. When the defect to DNA binding is bypassed by the

addition of the exogenous GAL4 DNA binding domain, the enhancement to transactivation becomes more apparent.

The data from the GAL4 experiments would indicate that the missense mutations are of three general types. The first class of mutation (P79L and P79T) has an effect on the FHD only, and when the requirement to bind via the FHD is relieved, the FOXC1 molecule is able to function as a transcriptional activator. The second class of mutation (I91T, F112S, and I126M) has effects that extend beyond the FHD. When the requirement to bind via the FHD is relieved, FOXC1 is altered enough that the transactivation domains do not function. The third class of mutations (S82T, L86F, I91S, and R127H) has effects that are both intra- and intermolecular. These are the mutations that could only be partially rescued by the addition of the exogenous DNA binding domain, or showed relief of inhibition when the endogenous DNA binding domain was bypassed (S82T-GAL4 showed 190% of wild type activity).

### **Analysis of Altered Amino Acids within $\alpha$ -Helix 1**

#### *I87 is a key residue in the stability of the FOXC1 molecule*

The isoleucine residue at position 87 is located in the first helix and is one of the main participants involved in the formation of the hydrophobic core. Threading analyses done by Drs Banerjee-Basu and Baxevanis have shown I87 is involved in favourable hydrophobic interactions with I99, I104, and I108 in helix 2; and with I126, L130, and L132 in helix 3. None of these favourable hydrophobic interactions are disrupted by the substitution of a methionine (a

hydrophobic amino acid) at position 87 in place of the isoleucine.

Experimentally however, the FOXC1 I87M mutation results in a protein with reduced stability (Figure 16) possibly reflecting extrinsic cellular mechanisms that underlie the reduced stability of this protein. Protein instability may thus represent the mechanism by which the I87M mutation of FOXC1 causes disease within patients. Similarly, when FOXC1 was converted at I87 to A, E, or K, no FOXC1 protein could be detected by Western blot analysis using the anti-Xpress antibody. FOXC1 therefore, appears to be intolerant of changes at position 87 with respect to the expression of the protein. Transcription of the FOXC1 87M/A/E/K mRNA is robust (Figure 23) so possible defects lie in translation of the mRNA, or in the inherent stability of the protein product. These data imply that I87 is critical in formation of a stable FHD and FOXC1 molecule.

*L86 functions to organize the FHD in such a manner that FOXC1 is transcriptionally competent*

Since mutations at position 87 lead to a drastic reduction in the levels of protein of FOXC1, presumably by destabilizing the protein, it is interesting that mutations at amino acid 86, including the relatively severe proline mutation, do not affect FOXC1 protein stability. While the L86F and L86P mutations result in stable protein products, mutations at this position are still able to disrupt FOXC1 function. FOXC1 L86F is localized to cell nuclei and retains the ability to bind the FOXC1 binding site in EMSA experiments. The binding of L86F FOXC1 to

the FOXC1 binding site is impaired in comparison to wild type, but clearly the FHD retains enough of its overall structure to bind DNA.

The analysis of charge conversion mutations L86 A/E/K reveals that disruptions in  $\alpha$ -helix 1 can impair exclusive localization of FOXC1 to the nucleus. As is the case with other normally neutrally charged positions, when converted to a charged amino acid (86 E/K), the defect to nuclear localization is more pronounced than when the conversion is a neutral alanine residue. With respect to DNA binding, conversion of L86 to A/E/K does not appear to inhibit or alter DNA binding affinity or specificity.

The L86P synthetic mutation severely perturbs the nuclear localization of FOXC1. Given that FOXC1 L86F localizes to the nucleus at wild type levels, it seems likely the inclusion of a proline within helix 1 disrupts the helical structure, perturbing the overall structure of the FHD enough that the transport machinery is no longer able to accumulate FOXC1 in the nucleus. The L86P alteration is also severe enough to abolish FOXC1 DNA binding.

FOXC1 L86F/P/A/E/K mutations all severely impair the transactivation ability of FOXC1. In the case of L86F/A/E/K, although the mutations still have appreciable DNA binding capacity, the ability of FOXC1 to drive transcription of the luciferase reporter is severely perturbed, possibly due to failed interactions with the transcriptional machinery. These data indicate that position 86 has an intermolecular role, as evidenced by the diminished transcriptional activity of FOXC1 L86F/A/E/K, even though DNA-binding still occurs. As for FOXC1 L86P, this mutant shows a serious disruption in nuclear localization and does not

appear to bind the FOXC1 binding site in EMSAs. It is likely that the substitution of a proline at position 86 disrupts  $\alpha$ -helix 1 to a greater extent than the other 86 mutations, which are less likely to break the  $\alpha$ -helix structure.

While the disruption to transactivation of FOXC1 L86A/E/K and P is severe in comparison to wild type FOXC1 transactivation, there is still residual transactivation above what is seen for the  $\Delta$ Box and L86F FOXC1 proteins. It is possible that the EMSAs, which show an absence of L86P binding to the FOXC1 binding site, may not be sensitive enough to detect a small amount binding that is sufficient for transactivation above the baseline. It is also possible that some binding of FOXC1 L86P does occur when the FOXC1 binding site is presented in context of the reporter plasmid and not on the smaller FOXC1 binding site oligonucleotide used in the EMSAs. Nevertheless, the severe disruption of transactivation ability of all the FOXC1 L86 conversions, illustrates the importance of this residue to FOXC1 function.

The addition of the exogenous GAL4 DNA binding domain appears to allow partial recovery of transactivation of the L86F FOXC1 proteins supporting the idea that the L86 position does not exert a large intramolecular influence. When the obligation to bind DNA via the FHD is relieved by the presence of the GAL4 BD, the transactivation domains located within FOXC1 are able to exert their influence and activate transcription of a reporter, to some extent. Conversely,  $\alpha$ -helix 1 overall plays a strong intramolecular role, likely required for the proper formation of the FHD, as demonstrated by the severe DNA binding defects seen with FOXC1 L86P.

*I91 is a key residue in the organization of the FHD with respect to nuclear localization and transcription*

At position I91, a change in amino acid composition from isoleucine to a threonine reduces the nuclear localization to almost half of wild type levels at 52%, similar to levels seen with I91A (55%). Conversion of I91 to E and K causes a more severe disruption (24% and 5% exclusive nuclear localization respectively) than what is seen with the neutral threonine and alanine residues. Interestingly FOXC1 I91S, which is also a neutrally charged amino acid residue, shows a severe impairment to exclusive nuclear localization at 15%. Additionally, A, E, and K mutations at position 91 appear to disrupt the nuclear localization more than what is seen with the equivalent amino acid substitutions at position 86. I91 may be a key residue in the nuclear import or retention of FOXC1, possibly interacting with the nuclear transport machinery; however this is unlikely as this residue is predicted to be oriented towards the hydrophobic core of the FHD. Clearly while the threonine and alanine residues, while reducing nuclear localization, still allow some FOXC1 interaction with the translocation machinery, while the lysine and serine residues strongly interfere with this interaction. With respect to the impairment to nuclear localization seen with FOXC1 I91S, it is possible the 91S residue becomes phosphorylated and thus interferes with key interactions with the nuclear transport machinery. *In silico* analysis however does not predict that either the 91S or 91T residues would be phosphorylated. The I91 residue is located within the region that constitutes the putative nuclear localization accessory signal, described earlier. This region

(amino acids 77-93) of the FHD is required but insufficient for nuclear localization. Mutations at position 79 appear to disrupt nuclear localization to some extent (63-64% nuclear localization) while mutations the S82T and L86F mutations do not affect the nuclear localization. Therefore while some changes are tolerated within the NLAS with respect to nuclear localization, other changes (I91S) will severely perturb nuclear localization. Taken together, these data indicate that I91 is an important residue in the organization of the FHD with respect to nuclear transport. Further testing will be required to understand how these 91 mutations alter the ability of FOXC1 to interact with the nuclear transport machinery.

All of the I91 mutations tested (91A/E/K/S/T) severely disrupted transactivation by FOXC1. These data indicate that I91 is an important residue in organizing the FHD into a conformation that facilitates not only FOXC1 nuclear translocation but also transcriptional potential.

The fact that the mutations N-terminal to helix 1 and within helix 1 (79A/E/K/L/T, 86A/E/K/F, 91A/E/K/S/T), with the exception of FOXC1 L86P and I87 mutations, are able to bind the FOXC1 binding site supports the idea that the N terminal portion of the FHD, including  $\alpha$ -helix 1, does not play a major role in the formation of the FOXC1 protein-DNA complex. While FOXC1 DNA binding in the presence of these mutations ranges from levels that are 50 - 100% of wild type FOXC1, the fact that these FOXC1 molecules still bind is indicative of preservation of the structural integrity of the FOXC1 FHD.

### **Analysis of Loop/Helix4 Region**

The region lying between helix 2 and helix 3 is referred to as the T-loop region (Carlsson and Mahlapuu 2002; Clark et al. 1993; Kaufmann and Knochel 1996) and may form a fourth helix, depending on the interpretation of data from NMR studies (Carlsson and Mahlapuu 2002; Clark et al. 1993; Jin et al. 1999; van Dongen et al. 2000; Weigelt et al. 2001). One naturally occurring mutation (F112S) has been identified in this region. To complement our studies of this region, a series of alanine mutations to probe the region that constitutes helix 4 were constructed (F114A, Y115A, R116A, D117A, and N118A). All the mutations located in these regions localized exclusively to the nucleus at wild type FOXC1 levels. The DNA binding capacity of these mutations for the FOXC1 binding site also appear to be at or near wild type levels and when tested against the variant oligonucleotide panel, these mutations did not appear to alter the binding site specificity of FOXC1. From these data it would appear that this region is not involved in guiding either the nuclear localization or the DNA binding of FOXC1. A study of FOXA3 binding specificity revealed that the twenty amino acids N-terminal to helix 3, including the T loop region, helix 4, and the C-terminal portion of helix 2, are able to direct the specificity of FOXA3-DNA interactions (Overdier et al. 1994). It is therefore possible and, based on studies of FOXA3, likely that this region does in fact play a role in guiding the specificity of FOXC1-DNA interaction. The specificity of protein-DNA interactions are speculated to be directed through a combination and distribution of charged amino acids (Weigelt et al. 2001); therefore single amino acid

conversions like those used to probe helix 4, may not be sufficient to produce a pronounced effect.

Given that none of the alanine mutations within helix 4 affected localization or DNA binding capacity of FOXC1, it seems likely that helix 4 is not involved in organization of the FHD with respect to these functions. Defects may exist in the transactivation capacity of the helix 4 mutants. However, transactivation defects of the helix 4 mutations (114-118) are difficult to evaluate. From experiment to experiment the levels of transactivation relative to wild type FOXC1 were highly variable. FOXC1 F114A, Y115A, and R116A did show a drop in transactivation on average but this drop was highly variable and in one experiment F114A was found to have increased transactivation. FOXC1 D117A and N118A both showed drastic differences in transactivation levels, sometimes enhancing reporter transcription, other times impairing FOXC1 transactivation. These experiment to experiment differences may reflect an artefact of the assay system due to problems with the particular population of HeLa cells used, problems with transfection differences, problems with detection of the luciferase signal, or perhaps subtle differences in temperature. Experiments are still ongoing to better characterize the transactivation of the FOXC1 helix 4 mutants.

FOXC1 F112S shows a severe impairment to transactivation while still binding at near wild type levels. These data indicate that F112 is an important position in organizing the FHD in such a manner that FOXC1 is able to transactivate. This is achieved either by relieving transcriptional inhibition from the inhibitory domain, or promoting transactivation from the N and C terminal

transactivation domains, likely done via protein-protein interactions. Molecular modeling, done by Drs. Banerjee-Basu and Baxevanis, shows the F112 mutation is located outside the hydrophobic core, in the loop region between helices 2 and 4. This position is not involved in hydrophobic core formation; hence, replacement at this position did not interfere with the overall pattern of intermolecular interactions. (It is important to note that this computational method only takes into account residues involved in pairwise contacts with other residues. As such, residues with their side chains pointed outwards, such as F112, are presumably not involved in such interactions, so the net effect of mutations at these positions cannot be assessed directly by these analyses.) That FOXC1 F112S binds DNA as effectively as the wild-type protein, but does not transactivate reporter constructs that contain the same DNA target sequence, can be explained by the predicted location of this mutant residue, away from the DNA-binding face of FOXC1. The F112S mutation in FOXC1 may interfere with protein-protein interactions necessary for the transactivation of downstream genes.

To date no AR malformation-causing missense mutations have been identified in helix 2 of the FOXC1 FHD. The role helix 2 plays in the organization of the FHD thus remains largely undefined. In  $\lambda$  repressor, a DNA binding protein with a helix-turn-helix structure like FOXC1, there are positive control mutations that affect the activation ability but have no effect on binding capacity (Guarente et al. 1982; Hochschild et al. 1983). The missense mutations in the  $\lambda$  repressor occur either on the exposed surface of helix 2 or in the turn

between helix 2 and 3 affecting the interaction of the  $\lambda$  repressor with RNA polymerase rather than the protein's interaction with DNA (Hawley and McClure 1983; Li et al. 1994). Similarly a positive control mutation in the pituitary transcription factor Pit1 has been shown to occur in helix 2 of its DNA binding domain (Assa-Munt et al. 1993; Pfaffle et al. 1992). It remains to be determined if helix 2 functions in a similar manner in FOXC1 and if mutations can be generated to specifically construct positive control mutants. Molecular modeling would be useful in predicting which amino acids are exposed on helix 2. An example of a positive control mutation in FOXC1 may be FOXC1 F112S, positioned in the loop region between helices 2 and 3, which only shows a transactivation defect in these studies, possibly due to a disruption of protein-protein interactions.

Interestingly, in the mouse mutant *dysgenic lens (dyl)*, *Foxe3*, the gene responsible for the *dyl* phenotype, has two missense mutations, F93L and F98S, in the FHD. These positions correspond to F107 and F112 in the FOXC1 FHD respectively. The F112S mutation identified in patients with AR malformations corresponds to the F98S mutation found in *dyl* mice (Blixt et al. 2000). The *dyl* mice show a developmental disorder whereby the lens vesicle fails to separate from the ectoderm causing a fusion between the lens and the cornea, eventually forming a dysplastic, cataractic lens. When the *dyl* mutations were introduced into the *Foxe3* FHD it was found that the combination the two mutations disrupted the DNA binding capacity (Ormestad et al. 2002). This is in contrast to what was seen with the F112S mutations alone in FOXC1; this molecule retained

DNA binding capacity. It is probable that the F93L substitution, also found in the *dyl* allele of *Foxe3*, is exerting an effect in addition to the effect of the F98S substitution. It must also be noted that only the FOXE3 FHD was tested in the absence of the remainder of the FOXE3 molecule. It is therefore possible that the effects of these mutations on DNA binding are more pronounced when the FHD is tested in isolation.

### **Analysis of Key Residues within Helix 3**

*I126 is involved in FHD organization with respect to localization, transactivation, and DNA binding specificity*

The FOXC1 I126M mutation shows wild type levels of nuclear localization and DNA binding of the FOXC1 binding site. When I126 is mutated to an A, E, or K, the effect of the charged E and K residues on localization is drastically different than the neutral A residue. Both FOXC1 I126E and I126K cell populations show only cells with mixed or cytoplasmic localization, while FOXC1 I126A localizes exclusively to the nucleus in 77% of cells (Figure 24 and Table 5). The molecular consequences of these charge differences are also strikingly different when the DNA binding capacity of the FOXC1 126 A/E/K mutants is tested. FOXC1 I126 A and E both fail to bind the FOXC1 binding site by EMSAs, while FOXC1 I126K is still able to bind, although with much reduced affinity (Figure 26). Thus the conversion to a positively charged lysine residue drastically perturbs both the subcellular distribution of FOXC1 and DNA binding capacity of FOXC1, even though the FHD domain does retain enough

wild type structure to bind the FOXC1 binding site to some extent. Conversely the conversion of I126 to an alanine is able to completely disrupt the DNA binding capacity of FOXC1 but causes only a mild disruption to FOXC1 localization to the nucleus, indicating that FOXC1 126A is still able to interact with the nuclear transport machinery. All four of the FOXC1 126 constructs (M/A/E/K) fail to transactivate gene expression (Figures 20 and 27). The failure of FOXC1 I126A and I126E to drive transcription from the FOXC1 binding site reporter construct is easily explained by the failure of these FOXC1 constructs to bind the FOXC1 binding site. The implication for FOXC1 I126K would be that the change in the structure of the FHD prevents FOXC1 transactivation domains outside the FHD from activating transcription. The isoleucine at position 126 within  $\alpha$ -helix 3 is thought to be an important residue in the formation of a hydrophobic core, based upon threading analysis done by Drs. Banerjee-Basu and Baxevanis. The reduction in transactivation by recombinant I126M is probably due to subtle changes in intermolecular interactions, predicted by molecular modeling to result in a more rigid molecule. The I126M mutation may render FOXC1 unable to alter the conformation of target DNA thus preventing transcription initiation. From these data it would appear that I126 has a role in organizing the FHD in such a way that FOXC1 can be transported to or retained within the nucleus, can bind DNA, and can activate transcription.

All of the FOXC1 missense mutants retaining DNA binding capacity were tested to determine if the binding was sequence specific. In order to test this, variants of the 9 base pair core of the FOXC1 binding site were used in

EMSA to determine if affinities for any of the variants changed relative to wild type FOXC1 affinity for the same variant. One base at a time was converted from a purine to a pyrimidine with an equivalent number of hydrogen bonds, or *vice versa* (Table 3). Interestingly, the DNA binding specificity of FOXC1 was altered by the I126M mutation. The I126M mutant protein showed an increased affinity, as compared to wild type FOXC1 protein, for variant binding sites 2, 3, 8, and 9 while still binding to the *in vitro* derived FOXC1 binding site at levels comparable to wild type FOXC1 (Table 3 and Figure 20). The affinity of FOXC1 I126M for the other variant binding sites was not increased in comparison to wild type FOXC1. These data would indicate that altering amino acids in helix 3 alters the specificity of FOXC1-DNA interaction (see below).

*R127 is a key residue of the FHD with respect to FOXC1 function*

The R127 position is an invariant position in FOX proteins. The R127H FOXC1 missense mutation showed severely impaired nuclear localization, abolished DNA binding capacity, and no transactivation ability. Additionally, fusion of the FOXC1 R127H open reading frame with GAL4 did not rescue the transactivation capability of this molecule, indicating that 127H has severe intramolecular consequences in FOXC1. While expression of FOXC1 R127H produces a stable protein in COS cells (Figure 15b), the R127H mutation may cause gross structural anomalies to FOXC1 such that the protein is completely non-functional. The R127H mutation found in AR malformation patients is an orthologous mutation to the R553H mutation found in the FHD of FOXP2, a

forkhead gene that underlies severe language deficits (Lai et al. 2001). My data indicate that the R553H mutation identified in FOXP2 would likely also severely perturb the FOXP2 forkhead domain, leading to a similar spectrum of molecular defects as those observed for FOXC1, disrupting the ability of FOXP2 to transactivate target genes required for proper language development programs.

Analysis of FOXC1 127 charge conversion proteins revealed that 127 is the only position in which the construct converted to a lysine displayed more wild type subcellular distribution than the construct converted to an alanine. Given that R127 is a positively charged amino acid, it is understandable that the R127K conversion gave the most wild type phenotype with respect to localization; the charge of the side chain is conserved. FOXC1 R127E failed to bind the FOXC1 binding site in these EMSAs while FOXC1 R127A and K were both still able to bind the FOXC1 binding site, although this binding capacity is reduced by more than 10 fold compared to wild type FOXC1 affinity for this site (Figure 25). Interestingly both FOXC1 R127A and K were found to have altered binding site specificity compared to both wild type FOXC1 and each other (Figure 26). The specificity of binding of FOXC1 R127A appears to become less stringent with binding of variant oligonucleotides 6-9 and wild type FOXC1 binding site being approximately equivalent. Conversely the binding specificity of R127K appears to be altered so that this FOXC1 molecule now has a higher affinity for variant oligonucleotide 7, than for the FOXC1 binding site (Figure 25).

Resolution of the crystal structure of FOXA2 (Clark et al. 1993) and NMR of the solution structure of FOXC2 (van Dongen et al. 2000), the latter

containing a FHD 97% identical to that of FOXC1, indicates that helix 3 lies across the DNA in the major groove, possibly functioning as a recognition helix. The I126M missense mutation is able to alter the binding specificity of FOXC1, although not to the same extent as to what is seen with 127K. The crystal and NMR resolved structures show that the R127 side chain extends away from the amphipathic helix 3 and is likely to be a contact point between FOXC1 and DNA (Clark et al. 1993; Jin et al. 1999; van Dongen et al. 2000; Weigelt et al. 2001). Thus the positively charged 127K would attract the negatively charged DNA, while 127A would neither attract nor repulse, hence both these FOXC1 constructs would still be able to bind DNA. The inability of R127E to bind DNA is consistent with the prediction that the presence of the negative charge at this contact point may create repulsion between FOXC1 R127E and the DNA.

In spite of showing a severe reduction in binding to the FOXC1 binding site, both FOXC1 R127A and R127K are able to drive expression of a reporter construct, at levels that are 36% and 38% of wild type FOXC1 levels respectively (Figure 26). It would appear that, based on the levels of transcription relative to the levels of binding, that the transactivation domains are properly organized in FOXC1 R127A/K molecules. These data indicate that the key role of R127 is to function in the proper recognition and binding of the FOXC1 binding site, as well as indicating that R127 does not function to organize the FHD in such a manner as to make FOXC1 transcriptionally competent.

### *S131 severely perturbs FOXC1 DNA binding capacity*

The serine residue at position 131, found in the third helix, is on the hydrophilic face of the FOXC1 forkhead model. Threading analysis, done by Drs Banerjee-Basu and Baxievani, predicts that S131 is not involved in hydrophobic core formation; the substitution of a serine residue by a leucine residue is not predicted to significantly perturb the FHD structure. It is possible that S131 is involved in DNA binding. In good agreement with the structural predictions, experimentally the S131L missense mutation drastically reduces the ability of FOXC1 to bind the FOXC1 binding site. This mutation shows some deficiency in nuclear localization at 72% so while the threading analysis does not predict significant alteration from wild type FHD configuration, there is some change in the FHD that causes inefficiency in nuclear translocation or retention and an obliteration of DNA binding.

### *Helix-3 Summary*

Clearly  $\alpha$ -helix 3 contains residues that not only guide FOXC1-DNA interaction, but also regulate the specificity of those interactions (I126 and R127). Residues in helix 3 also appear to function in the general organization of the FHD such that FOXC1 can be properly localized within the cell. Finally, as evidenced by the addition of an exogenous DNA binding domain, residues in helix 3 have some role in organizing the FOXC1 molecule in such a manner that the

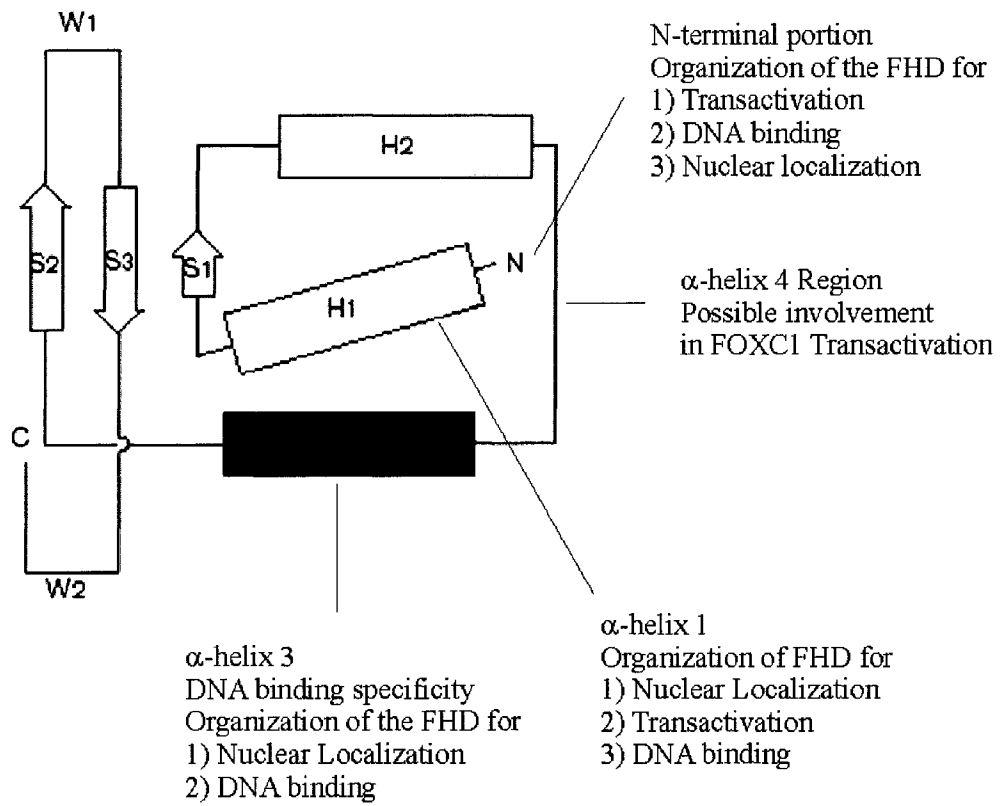
transactivation domains are functional. A summary of the functions of the secondary structures within the FHD is shown in Figure 33.

### **Architecture of other Helix-Turn-Helix DNA-binding Domains**

It was the DNA binding domains of prokaryotic proteins that were first described as helix-turn-helix (HTH) motifs. Since that time, structurally analogous variations of the HTH motif have been identified in eukaryotic DNA binding domains such as the homeodomain, the ETS-type DNA binding domains, and the forkhead DNA binding domain.

Homeodomain proteins share a conserved pattern of hydrophobic amino acids (Konig and Rhodes 1997) that form a hydrophobic core, packed between three  $\alpha$ -helices, two of which are part of the HTH motif. In contrast to prokaryotic HTH proteins, homeodomains are able to bind DNA as monomers, as are ETS and forkhead transcription factors, although some homeodomain transcription factors such as Hesx, do form dimers (Brickman et al. 2001). The ability of homeodomain proteins to function as monomers is thought to be mediated by the N-terminal arm that precedes  $\alpha$ -helix 1 (D'Elia et al. 2001). The N-terminal arm extends into the minor groove of the DNA where it contacts the bases and phosphate backbone of the DNA, thereby stabilizing homeodomain-DNA interactions. A recent review indicated that the N-terminal arm is a mutational hot spot in homeodomains, supporting the idea that this portion of the homeodomain is critical to function (D'Elia et al. 2001). For example, in the homeodomain protein MSX2, a proline to histidine mutation was identified in the

**Figure 33. The topology of the FHD with the function of specific regions indicated.**



N-terminal arm that enhanced the affinity of MSX2 for DNA (Ma et al. 1996), while mutations in the N-terminal arm of the photoreceptor homeodomain transcription factor CRX have been shown to reduce DNA binding with a concomitant reduction in transactivation capacity (Chen et al. 2002). While structurally distinct, stabilization of DNA binding by the N-terminal arm of the homeodomain is a mechanism similar to the stabilization of forkhead domain-DNA interactions by wing 2 of the forkhead domain (see Future Directions).

A common structural theme in all the HTH DNA-binding domains is the presentation of  $\alpha$ -helix 3, the recognition helix, within the major groove of the DNA. Similar to what is seen with mutations in  $\alpha$ -helix 3 of the FOXC1 FHD,  $\alpha$ -helix 3 mutations in homeodomains reduce the affinity of the homeodomain for DNA (Chen et al. 2002; D'Elia et al. 2001; Koizumi et al. 2003). Again in HTH proteins, the question of how DNA specificity is generated from grossly similar three-dimensional topologies arises. ETS transcription factors are able to generate different sequence specificities through nonconserved residues distal to  $\alpha$ -helix 3. An example of this is found in SAP-1 and Elk-1, both members of the ETS family of transcription factors (Muller 2001). The ETS binding domain is, like the forkhead domain, a winged-HTH DNA binding domain, comprised of three  $\alpha$ -helices packed against a four-stranded, anti-parallel  $\beta$ -sheet (Kodandapani et al. 1996). SAP-1 and Elk-1 are 80% identical in the ETS domain and 100% identical in  $\alpha$ -helix 3. In Elk-1, an asparagine residue (A69), C-terminal to  $\alpha$ -helix 3 forms a contact with the DNA backbone. In SAP-1, the corresponding residue is a valine and is not a DNA contact. This lack of contact by the valine

residue leads to a conformation change of the SAP-1 ETS DNA binding domain. Residues adjacent to the valine are repositioned such that an adjacent tyrosine residue is inserted into the major groove of the DNA. Thus a single amino acid residue is able to alter the conformation of the ETS domain, and as a result generate DNA binding specificity. These types of conformational changes are likely similar to what is seen in forkhead domains, where the alteration of a small number of residues is able to alter DNA binding specificity, even though  $\alpha$ -helix 3 has a high degree of sequence conservation.

The organization of nuclear localization signals (NLSs) is varied among the HTH proteins. As described in FOXC1, the NLS is part of the forkhead domain and is bipartite, with the primary basic NLS at the C-terminus, and an accessory signal at the N-terminus of the forkhead domain. In the ETS-DNA binding domain, the NLS is bipartite, comprised of a stretch of eight basic amino acids resembling the SV40 large T antigen NLS (PKKRKV), located within the ETS domain, and an accessory signal of basic amino acids located C-terminal to the ETS domain (De Haro and Janknecht 2002). In homeodomain proteins, the NLS is thought to be located primarily in  $\alpha$ -helix 3, although in some homeodomain proteins, sequences outside of helix 3 are required for the exclusive nuclear localization of the protein (Fei and Hughes 2000; Hessabi et al. 1999; Kozłowski and Walter 2000).

## Genotype and Phenotype Correlations

The clinical features of the patients carrying FOXC1 mutations provide further evidence for FOXC1 being an important regulator of mesodermal development. Experiments in murine models have shown that *Foxc1* heterozygotes have ocular findings (Hong et al. 1999; Kidson et al. 1999; Kume et al. 1998; Smith et al. 2000; Winnier et al. 1999) including iris hypoplasia and maldevelopment of the iridocorneal angle (Smith et al. 2000), while *Foxc1* homozygous null mice have severe cardiac, ocular, skeletal, and urogenital developmental defects (Hong et al. 1999; Kume et al. 2000; Kume et al. 1998; Kume et al. 2001; Swiderski et al. 1999; Winnier et al. 1999). Findings of ocular anomalies in AR patients is a strong demonstration of mouse models recapitulating human defects. Similarly murine models have also demonstrated that *Foxc1* plays important roles cardiac development (Swiderski et al. 1999; Winnier et al. 1999). While some AR malformation patients have been reported to present with cardiac defects, the cardiac anomalies in this patient may simply be co-morbid, or may reflect still poorly understood stochastic and genetic background influences on *FOXC1*-associated human disease.

Data from patients with *FOXC1* mutations (Kawase et al. 2001; Komatireddy et al. 2003; Lehmann et al. 2002; Lehmann et al. 2000; Mears et al. 1998; Mirzayans et al. 2000; Nishimura et al. 2001; Nishimura et al. 1998; Panicker et al. 2002; Suzuki et al. 2001) in addition to work done in mice (Kidson et al. 1999; Kume et al. 2000; Kume et al. 1998; Kume et al. 2001; Mears et al. 1998; Smith et al. 2000) show strong evidence for a haploinsufficiency model for

*FOXC1*. In humans, missense mutations that still produce full-length FOXC1 with reduced activity cannot be distinguished at a phenotypic level from patients with null or nonsense mutations. The S82T FOXC1 missense mutation helps define the range of FOXC1 activities that lead to a disease state. The S82T missense mutation has almost 60% of wild type transactivation activity, yet the phenotypic consequences in patients with FOXC1 S82T mutations are the same as in those patients with the I87M mutation, which produces less than 5% of wild type FOXC1 protein amounts. In fact, the ocular phenotypic differences between patients with any of the missense mutations were the same as the differences in ocular phenotypes between patients with the same missense mutations (Honkanen et al. 2003; Mears et al. 1998; Suzuki et al. 2001). Within a family with a given missense mutation of *FOXC1* there is often a spectrum of phenotypic consequences.

Although the penetrance of *FOXC1* defects within the eye is high (Kawase et al. 2001; Komatireddy et al. 2003; Lehmann et al. 2002; Lehmann et al. 2000; Mears et al. 1998; Mirzayans et al. 2000; Nishimura et al. 2001; Nishimura et al. 1998; Panicker et al. 2002; Suzuki et al. 2001), there are likely environmental factors and/or modifier genes that result in variable expressivity. For example it would appear tyrosinase may function to modify AR-like malformation phenotypes in *Foxc1*<sup>-/+</sup> heterozygous mice (Libby et al. 2003). It is also possible that other components of the L-DOPA pathway may act as FOXC1 modifiers.

Much of the phenotypic variability likely reflects developmental events related to the timing, location, and level of expression of developmentally important downstream targets of FOXC1. From individual to individual there may be differences in which developmentally important regulators are activated at the right time, in the proper location, and at the correct levels. Alternatively, in some groups of cells the proper developmental regulators are insufficiently or incorrectly activated.

Regulation of FOXC1 levels is therefore critical for proper development. Reports from other groups indicate that individuals with three copies of FOXC1 show anterior eye segment defects (Lehmann et al. 2002; Lehmann et al. 2000). Combined with data presented here on partial activity of one of the FOXC1 missense mutations, we can conclude that the regulation of FOXC1 levels is extremely stringent with more than 78% of wild type (normal allele activity plus FOXC1 S82T activity) but less than 150% of wild type levels (activity of three alleles) of FOXC1 being required for correct FOXC1 function.

Mutations in FOXC1 and PITX2 result in similar ocular phenotypes. While genotype-phenotype correlations have been established for defects in PITX2 (Kozlowski and Walter 2000; Priston et al. 2001), it appears that no such relationship can be established for FOXC1. Mutant PITX2 proteins that retain partial function result in milder anterior eye segment defects than in patients with no PITX2 function, but this clearly is not the case for FOXC1. Aberrant ocular development arising from PITX2 mutations may follow a different mechanism or pathway than ocular defects arising from FOXC1 mutations.

## **Future Directions**

While a significant amount of work has been done to understand FOXC1 function, both developmentally and biochemically, there is still much more work to do. With respect to the FHD, the question of DNA binding specificity remains unresolved. We know that residues within helix 3, the recognition helix, are able to regulate the DNA binding specificity. These residues (in particular R127) are not likely to underlie differential site recognition between different FOX proteins, because they are highly conserved between members of the FOX family.

Previous work shows that within FOXA3-FOXQ1 chimeric proteins, the 20 amino acids preceding helix 3 are able to regulate the DNA binding specificity of FOXA3 (Overdier et al. 1994). While both FOXA3 and FOXQ1 possess an identical pentapeptide (Phe-Pro-Tyr-Tyr-Arg) in this 20 amino acid region, the three residues preceding and five residues following this segment are protein specific and it may be through these sequences that binding specificity is regulated. FOXC1 shares a highly similar pentapeptide motif (Phe-Pro-Phe-Tyr-Arg); however, the amino acids outside this region are common to both FOXC1 and other FOX proteins. Results from the analysis of mutations in helix 3 presented in this thesis also indicate that amino acids I126 and R127 can regulate DNA binding specificity. It is likely that a combination of charged and non-charged molecules in both  $\alpha$ -helix 3 and the 20 amino acids preceding helix 3 create a specific surface charge, and thus DNA binding specificity, for each FOX molecule. Experiments are now underway by Ms T. Murphy to convert FOXC1 to a FOXC1-FOXH1 chimeric protein that preferentially binds a FOXH1 binding

site. At present, the twenty amino acids preceding helix 3 are being converted to FOXH1 amino acid sequence; it remains to be seen if amino acids elsewhere in the FHD will need to be converted, in order to facilitate FOXC1 binding of a FOXH1 binding site.

Portions of the wing 2 region are also thought to play a role in regulating specificity of the protein-DNA interactions (Pierrou et al. 1995). The generation of temperature-sensitive mutations in wing 2 of FOXA1 has demonstrated that mutations in wing 2 can impair transcriptional activity of winged helix proteins (Stevens et al. 2000). Wing 2 associates with the three-helix bundle, in particular helix 1, perhaps stabilizing and enhancing DNA binding. It has been proposed that the evolution of wing 2 coincided with the ability of FOX proteins to function as monomers (Stevens et al. 2000). Interestingly two mutations within the wing 2 region of FOXC1 (M161K and G165R; see Figure 6) have recently been identified in patients with AR malformations (Panicker et al. 2002). Studies of these wing mutations may provide insight into the function of this region with respect to DNA binding specificity.

The nature of FOXC1 interactions with the basic transcriptional machinery also needs to be investigated. EMSAs using COS-7 cell extracts containing recombinant FOXC1 show three species of the FOXC1-DNA complex (Figure 16), raising the possibility that other proteins are associating with the FOXC1-DNA complex, although these complexes may represent either differentially phosphorylated FOXC1 or alternatively, degradation products of FOXC1. Preliminary work done by Dr Fred Berry and myself also indicates that

FOXC1 may physically interact with TFIID, however this work has yet to be confirmed. Nonetheless, FOXC1 interactions with general transcription factors remain a distinct probability.

Another intriguing line of investigation of FOXC1 function comes from studies of FOXA proteins. With the resolution of FOXA3 structure, it was found that the FHD of the FOXA proteins bore a striking resemblance to the unrelated globular domain of histone H5 (Clark et al. 1993). The globular domain of histone H5 is a winged-helix-turn-helix motif but has only wing 1, lacking wing 2. After the core histone proteins and 146 bp of DNA assemble into the nucleosome core particle, histone H5 interacts with DNA to form a higher order chromatin structure, the 30 nm filament. This structural similarity raised the possibility of FOXA function at the nucleosome. By studying developmental regulation of the transcription of the serum albumin gene, FOXA1 has been shown to open chromatin, relaxing the chromatin from the 30 nm fibre state to a locally decondensed, nucleosome state, with FOXA binding the linker regions between nucleosomes (Cirillo et al. 2002; Cirillo et al. 1998; Cirillo and Zaret 1999). This ability to interact with compacted chromatin is conferred by the C-terminal portion of FOXA, which functions as a transcription activation domain, like the C-terminal portion of the FOXC1 protein. The amino acid sequences within this region are quite divergent between FOXA1 and FOXC1, however the possibility of FOXC1 assembly on nucleosomes remains tantalizing.

## Conclusions

These experiments were undertaken in order to understand firstly, how these disease-causing missense mutations disrupt the function of FOXC1, and secondly, in order to better understand the function of the FHD at a molecular, biologically relevant level. To these ends, it was found that the missense mutations tested were able to perturb FOXC1 function as a transcription factor in a variety of manners. Mutations in the areas N-terminal to and within  $\alpha$ -helix 1, still largely allow for the binding of FOXC1 to the FOXC1 binding site, and play a role in organizing the FHD in such a manner that FOXC1 is localized exclusively to the nucleus. Mutation in  $\alpha$ -helix 3 clearly can alter the DNA binding specificity of FOXC1 and again play some role in the general organization of FOXC1 such that nuclear localization is efficient. The net effect of all the missense mutations and A, E, K, conversions is a transactivation deficiency. The residues studied herein, with the possible exclusion of some residues in the helix 4 region, all appear to be required for full FOXC1 activation of a reporter construct. These amino acids may be required for proper structural formation or maintenance of the FHD, or may be required for the protein-protein interactions that occur as RNA polymerase II assembles at the transcriptional start.

These studies demonstrate the functional importance of not only individual amino acids within the FHD of FOXC1, but also demonstrate how the  $\alpha$ -helix 1 and  $\alpha$ -helix 3 secondary structures in the FHD are involved in FOXC1 function. Helix 1 appears to be involved in the organization of the FHD in such a

manner that FOXC1 can be translocated to or retained within the nucleus and is transcriptionally active. Helix 3 appears to be involved in organization of the FHD so that FOXC1 nuclear translocation or retention occurs and FOXC1 is transcriptionally competent; it also plays a major role in controlling FOXC1-DNA interactions.

A third intent of these studies was, in collaboration with computational biologists, to develop a model in which the effect of amino acid alterations within the FHD could be predicted. This goal is not yet realized. What was found by our collaboration was that current models could predict which amino acids were structurally important within the FHD, although the predictions need refining. For example, the insertion of charged amino acids at positions I87 and I91 were predicted to perturb the structure of the FHD to a large extent. It is likely that the FHD of FOXC1 I87A, E, or K is disrupted to such an extent that FOXC1 is no longer stable. However, given that FOXC1 I91A, E, or K still retain DNA binding activity it would appear that the FHD is grossly native in these molecules, contrary to modeling predictions. Fortunately, this work does provide a body of molecular information that could be utilized in the future by computational biologists to develop models with better predictive value.

The real value of these studies comes not only from furthering our understanding of FOXC1 function but also from extending our understanding of the FHD itself. Except for the studies of FOXC1 described herein, no other molecular analysis had been done to test the biochemical consequences of mutations of any FOX genes. The analysis of the missense mutations confirmed

that the sequence changes identified in FOXC1 are not simply rare polymorphisms but are indeed *bona fide* disease-causing mutations. To date, the only analysis of mutations in FHDs has been the previously mentioned studies of temperature sensitive mutations in wing 2 of FOXA1 (Stevens et al. 2000) and analysis of the *dysgenic lens* missense mutations in *Foxe3* (Ormestad et al. 2002). This work is by far the largest and most in depth analysis of FHD mutations for any member of the FOX transcription factor family.

Given the high degree of conservation between FHD domains within the FOX family with respect to the three dimensional topology (Carlsson and Mahlapuu 2002; Clark et al. 1993; Jin et al. 1999; van Dongen et al. 2000; Weigelt et al. 2001), this combination of biological and computational analysis is a framework which will allow for predictive modeling of changes within the FHDs for not only members of the C class of FOX proteins, but also FHDs of other FOX classes.

## Experimental Procedures

### *Plasmid construction and mutagenesis*

*FOXCI* cDNA (a gift of Dr. Peter Carlsson) was repaired at the 3' end so that the *FOXCI* cDNA encoded the entire *FOXCI* open reading frame. The *FOXCI* cDNA was then subcloned into *EcoRI* – *XbaI* sites in the pcDNA4 His/Max B™ plasmid (Invitrogen). The high G-C content of *FOXCI* precluded mutagenesis of the entire cDNA so an additional cloning step was required. For mutagenesis reactions a fragment of *FOXCI* from nucleotides 106 – 777 was PCR-amplified and cloned into pGEM T Easy using primers 5' -ggc tac acc gcc atg c-3' (forward) and 5' -gct ctc gat ctt ggg cac-3' (reverse). This segment of *FOXCI* was then mutagenized in the pGEM T Easy vector, using the Quickchange™ mutagenesis kit (Stratagene) and appropriate primers following the manufacturer's protocol, with the addition of 5% DMSO (Table 7). For P79T and I91T degenerate oligonucleotides were employed to create the A, E, and K conversions in addition to the T conversion (Table 8). Degenerate oligonucleotides were also used to construct the other A, E, K, conversions (Table 8). Mutagenized PCR products containing the appropriate codons were selected. Potential mutant constructs were sequenced using an automated sequencer (Li-COR). An *ApaI*-*RsrII* fragment from the mutagenized construct was then cloned back into the *FOXCI* pcDNA4 His/Max B construct.

GAL4 fusion proteins were constructed by subcloning entire *FOXCI* open reading frames from the *FOXCI* pcDNA4 His/Max plasmids into *EcoRI/XbaI* sites in the pGAL DB vector.

**Table 7.** Primers used for site directed mutagenesis.

<b>Amino Acid Change</b>	<b>Forward, 5' – 3'</b>	<b>Reverse, 5' – 3'</b>
<b>P79L</b>	caaggacatggtgaagctgccctatagctacatc	gatgtagctatagggcagcttcaccatgtccttg
<b>S82T</b>	ggtgaagccgccctatacctacatcgcgctcacc	ggtgatgagcgcgatgtaggatagggcggctcacc
<b>L86F</b>	tatagctacatcgcttcatcaccatggccatc	gatggccatggtgatgaaagcgatgtagctata
<b>L86P</b>	tatagctacatcgcgccatcaccatggccatc	gatggccatggtgatggcgcgatgtagctata.
<b>I87M</b>	gctacatcgcgctcatgaccatggccatccag	ctggatggccatggtcatgagcgcgatgtagc
<b>I91S</b>	ctcatcaccatggccagccaggaacggccggac	gtccggggcgttctggctggccatggtgatgag
<b>F112S</b>	ccagttcatcatggaccgctccccctctaccggg	cccggtagaagggggagcggccatgatgaactgg
<b>I126M</b>	ggctggcagaacagcatgcgccacaacctctcg	cgagaggttgaggccatgctgttctgccagcc
<b>R127H</b>	tggcagaacagcatcaccacaacctctcgctc	gagcgagaggttggtggatgctgttctgccca
<b>S131L</b>	ccgccacaacctctgctcaacgagtgcttcg	cgaagcactcgttgagcaagaggttgaggcg

Primers used to convert the indicated amino acid position to the indicated change.

**Table 8.** Primers used for degenerate site directed mutagenesis.

<b>Amino Acid Change</b>	<b>Forward, 5' – 3'</b>	<b>Reverse, 5' – 3'</b>
<b>P79</b> A,E,K,T	aaggacatggtgaagRYgcctatagctacac	gatgtagctatagggcMKcttcacatgtcctt
<b>L86</b> A,E,K,T	tatagctacatcgcgRYcatcacatggccac	gatggccatggtgatgMKcgcgatgtagctata
<b>I87</b> A,E,K,T	agctacatcgcgctcRYcaccatggccatccag	ctggatggccatggtgMKgagcgcgatgtagct
<b>I91</b> A,E,K,T	ctcatcacatggccRYccagaacgccccggac	gtccggggcggttctggMKggccatggtgatgag
<b>I126</b> A,E,K,T	ggctggcagaacagcRYccgccacaacctctcg	cgagaggttgtggcggMKgctgttctccagcc
<b>R127</b> A,E,K,T	tggcagaacagcatcRYccacaacctctcgctc	gagcgagaggttgtggMKgatgctgttctgcca

Primers used to convert the indicated amino acid position to an alanine, glutamate, lysine, or threonine residue. Sequences are written 5' to 3'. R is G or A, Y is C or A, M is G or T, and K is C or T.

### *Cell transfection and Co-transfection Assays*

All cells were grown in DMEM + 10% fetal bovine serum at 37°C with 5% CO<sub>2</sub>. 100 mm plates of COS-7 cells were transfected at 80% confluence with 2 µg of plasmid DNA using 20 µl of FuGene6™ transfection reagent (Roche) as directed by the manufacturer. For FOXC1/Lac Z co-transfection assays 1 µg each of pcDNA4 His/Max Lac Z and pcDNA4 His/Max FOXC1 or pcDNA4 His/Max FOXC1 I87M were co-transfected into COS-7 cells. After 48 hours, proteins were extracted and analyzed by western analysis. For immunofluorescence, COS-7 cells were grown on coverslips in 6-well plates and transfected with 1 µg of plasmid DNA using 3 µl of FuGene6. For transactivation assays, HeLa cells were grown in 6-well plates and transfected with 3 µl of FuGene6 using plasmid quantities listed below.

### *Protein Extraction and Western Analysis*

48 hours post transfection, cells were washed with PBS and harvested by scraping. Cells were pelleted, resuspended in lysis buffer (20 mM HEPES pH 7.6, 150 mM NaCl, 0.5 mM DTT, 25% glycerol, 2.5 mM PMSF, 10 µg/µl Aprotinin, 9 µg/µl Leupeptin, 10 µg/µl Pepstatin A) at 4°C, and lysed by gentle sonication on ice. After centrifugation at 13,000 x g for 5 minutes at 4°C, supernatants were transferred to a microfuge tube and resolved by SDS-PAGE. Resolved proteins were transferred onto nitrocellulose for Western analysis. Western analysis was done using the mouse anti-Xpress™ antibody as the

primary antibody at dilutions of 1:5000, and a goat anti-mouse conjugated to horseradish peroxidase secondary antibody at dilutions of 1:5000.

### *Immunofluorescence*

All immunofluorescence procedures were done at room temperature. 24 hours after transfection cells were washed three times with PBS, fixed using 2% paraformaldehyde/PBS for 10 minutes, and washed three times again in PBS. Cells were permeabilized using 0.05% TritonX-100/PBS for 10 minutes then washed three times with PBS. A 5% bovine serum albumin (BSA)/PBS solution was then applied and the cells blocked for 1 hour. The cells were then washed three times with a 1% BSA/PBS solution and incubated for 1 hour with a 1:400 solution of the anti-Xpress antibody in 1% BSA/PBS. Following incubation, the cells were washed three times with the 1% BSA/PBS solution and incubated for 1 hour with a 1:400 solution of an anti-mouse Cy3-conjugated secondary antibody (Jackson Immunolaboratories) in 1% BSA/PBS. The cells were then washed with 1% BSA/PBS, mounted using mounting media containing DAPI, and coverslips sealed using nailpolish.

### *Northern Analysis*

48 hours post transfection, COS-7 cells were washed with PBS and RNA extracted using TRIzol (GibcoBRL) reagent. The RNA was size separated and quantities equalized on a 1X MOPS, pH 7.4, 0.66M formaldehyde (BDH), agarose gel and transferred to Hybond (Amersham). The Hybond blot was

hybridized with [<sup>32</sup>P]-dCTP labelled pcDNA4 His/Max B, linearized with *EcoRI*. A second hybridization of the blot was done with a [<sup>32</sup>P]-dCTP labelled PCR product from the 5' FOXC1 (from nucleotides 20 to 233). Control hybridization for loading amounts was done with [<sup>32</sup>P]-dCTP labelled S26.

#### *Electrophoretic Mobility Shift Assay (EMSA)*

COS-7 cell extracts containing recombinant FOXC1 were equalized by western analysis. Reactions were brought up to volume using untransfected COS-7 cell extract. Protein extracts were incubated with 1.3 mM DTT, 5 µg sheared salmon sperm DNA, 1 µg poly dIdC (Sigma), and 10,000-20,000 cpm of [<sup>32</sup>P]-dCTP labelled double stranded DNA containing the FOXC1 binding site (forward: 5'-gatccaaagtaataaacaacaga - 3', reverse: 5' - gatctctgttgtttattactttg - 3'). Reactions were incubated at room temperature for 15 minutes after which 3 µl of 50% glycerol was added. 6% polyacrylamide Tris-Glycine-EDTA gels were prerun for 15 minutes and EMSAs subjected to electrophoresis at room temperature for 50 minutes. Binding specificity EMSAs were performed as described above with the addition of the [<sup>32</sup>P]-dCTP labelled double stranded DNA oligonucleotides listed in Table 3.

#### *Dual Luciferase Assay*

The CMV promoter of pGL3 (Promega) was replaced with a Herpes Simplex Virus Thymidine Kinase (TK) promoter from pRLTK (Promega) cloned into the *Bgl* II-*Hind* III sites of pGL3. Six copies of the FOXC1 binding sites

(underline indicates core 9 base pair FOXC1 binding site, forward: 5' -cta gcc aaa gta aat aaa caa cag caa agt aaa taa aca aca gg - 3'; reverse: 5'- cta gcc tgt tgt tta ttt act ttg ctg ttg ttt att tac ttt gg - 3') were then cloned into the *EcoRI*-*NheI* sites, 5' to the TK promoter. HeLa cells were then transfected with 50 ng of the pGL3 TK construct, 1 ng of the Renilla control vector and 500 ng of a given FOXC1 pcDNA4 HIS/Max construct. Transfected cells were grown for 48 hours. The dual luciferase assays were performed using the Promega Dual Luciferase Assay kit according to the manufacturer's instructions (Promega).

The GAL4-FOXC1 assays were performed as above but were done in COS-7 cells using 1 ng pRL, 50 ng G5 reporter plasmid, and 500 ng of the GAL4-FOXC1 plasmid.

#### *Phosphorylation prediction*

Analysis was done using the NETPHOS Prediction Server (<http://www.cbs.dtu.dk/services/NetPhos/>).

#### *DNA modeling*

DNA modeling was done using the DNAtools model.it® prediction server ([http://www3.icgeb.trieste.it/~dna/model\\_it.html](http://www3.icgeb.trieste.it/~dna/model_it.html)).

## References

- Abdelhak S, Kalatzis V, Heilig R, Compain S, Samson D, Vincent C, Weil D, Cruaud C, Sahly I, Leibovici M, Bitner-Glindzicz M, Francis M, Lacombe D, Vigneron J, Charachon R, Boven K, Bedbeder P, Van Regemorter N, Weissenbach J, Petit C (1997) A human homologue of the *Drosophila* eyes absent gene underlies branchio- oto-renal (BOR) syndrome and identifies a novel gene family. *Nat Genet* 15:157-64.
- Alward WL, Semina EV, Kalenak JW, Heon E, Sheth BP, Stone EM, Murray JC (1998) Autosomal dominant iris hypoplasia is caused by a mutation in the Rieger syndrome (RIEG/PITX2) gene. *Am J Ophthalmol* 125:98-100.
- Assa-Munt N, Mortishire-Smith RJ, Aurora R, Herr W, Wright PE (1993) The solution structure of the Oct-1 POU-specific domain reveals a striking similarity to the bacteriophage lambda repressor DNA-binding domain. *Cell* 73:193-205.
- Berry FB, Saleem RA, Walter MA (2002) FOXC1 transcriptional regulation is mediated by N- and C-terminal activation domains and contains a phosphorylated transcriptional inhibitory domain. *J Biol Chem* 277:10292-7.
- Blixt A, Mahlapuu M, Aitola M, Pelto-Huikko M, Enerback S, Carlsson P (2000) A forkhead gene, FoxE3, is essential for lens epithelial proliferation and closure of the lens vesicle. *Genes Dev* 14:245-54.
- Brickman JM, Clements M, Tyrell R, McNay D, Woods K, Warner J, Stewart A, Beddington RS, Dattani M (2001) Molecular effects of novel mutations in

- Hesx1/HESX1 associated with human pituitary disorders. *Development* 128:5189-99.
- Burgess R, Cserjesi P, Ligon KL, Olson EN (1995) Paraxis: a basic helix-loop-helix protein expressed in paraxial mesoderm and developing somites. *Dev Biol* 168:296-306.
- Carlsson P, Mahlapuu M (2002) Forkhead transcription factors: key players in development and metabolism. *Dev Biol* 250:1-23.
- Chen S, Wang QL, Xu S, Liu I, Li LY, Wang Y, Zack DJ (2002) Functional analysis of cone-rod homeobox (CRX) mutations associated with retinal dystrophy. *Hum Mol Genet* 11:873-84.
- Cirillo LA, Lin FR, Cuesta I, Friedman D, Jarnik M, Zaret KS (2002) Opening of compacted chromatin by early developmental transcription factors HNF3 (FoxA) and GATA-4. *Mol Cell* 9:279-89.
- Cirillo LA, McPherson CE, Bossard P, Stevens K, Cherian S, Shim EY, Clark KL, Burley SK, Zaret KS (1998) Binding of the winged-helix transcription factor HNF3 to a linker histone site on the nucleosome. *Embo J* 17:244-54.
- Cirillo LA, Zaret KS (1999) An early developmental transcription factor complex that is more stable on nucleosome core particles than on free DNA. *Mol Cell* 4:961-9.
- Clark KL, Halay ED, Lai E, Burley SK (1993) Co-crystal structure of the HNF-3/fork head DNA-recognition motif resembles histone H5. *Nature* 364:412-20.

- De Haro L, Janknecht R (2002) Functional analysis of the transcription factor ER71 and its activation of the matrix metalloproteinase-1 promoter. *Nucleic Acids Res* 30:2972-9.
- D'Elia AV, Tell G, Paron I, Pellizzari L, Lonigro R, Damante G (2001) Missense mutations of human homeoboxes: A review. *Hum Mutat* 18:361-74.
- Donoviel DB, Hadjantonakis AK, Ikeda M, Zheng H, Hyslop PS, Bernstein A (1999) Mice lacking both presenilin genes exhibit early embryonic patterning defects. *Genes Dev* 13:2801-10.
- Fei Y, Hughes TE (2000) Nuclear trafficking of photoreceptor protein crx: the targeting sequence and pathologic implications. *Invest Ophthalmol Vis Sci* 41:2849-56.
- Gajiwala KS, Burley SK (2000) Winged helix proteins. *Curr Opin Struct Biol* 10:110-6.
- Gould DB, Mears AJ, Pearce WG, Walter MA (1997) Autosomal dominant Axenfeld-Rieger anomaly maps to 6p25. *Am J Hum Genet* 61:765-8.
- Green MC (1970) The developmental effects of congenital hydrocephalus (ch) in the mouse. *Developmental Biology* 23:585-608
- Gruneberg H (1943) Congenital hydrocephalus in the mouse, a case of spurious pleiotropism. *Journal of Genetics* 45:1-21
- Guarente L, Nye JS, Hochschild A, Ptashne M (1982) Mutant lambda phage repressor with a specific defect in its positive control function. *Proc Natl Acad Sci U S A* 79:2236-9.

- Hawley DK, McClure WR (1983) The effect of a lambda repressor mutation on the activation of transcription initiation from the lambda PRM promoter. *Cell* 32:327-33.
- Hellqvist M, Mahlapuu M, Blixt A, Enerback S, Carlsson P (1998) The human forkhead protein FREAC-2 contains two functionally redundant activation domains and interacts with TBP and TFIIB. *J Biol Chem* 273:23335-43.
- Hessabi B, Ziegler P, Schmidt I, Hessabi C, Walther R (1999) The nuclear localization signal (NLS) of PDX-1 is part of the homeodomain and represents a novel type of NLS. *Eur J Biochem* 263:170-7.
- Hiemisch H, Monaghan AP, Schutz G, Kaestner KH (1998) Expression of the mouse Fkh1/Mf1 and Mfh1 genes in late gestation embryos is restricted to mesoderm derivatives. *Mech Dev* 73:129-32.
- Hiemisch H, Schutz G, Kaestner KH (1998) The mouse Fkh1/Mf1 gene: cDNA sequence, chromosomal localization and expression in adult tissues. *Gene* 220:77-82.
- Hochschild A, Irwin N, Ptashne M (1983) Repressor structure and the mechanism of positive control. *Cell* 32:319-25.
- Hong HK, Lass JH, Chakravarti A (1999) Pleiotropic skeletal and ocular phenotypes of the mouse mutation congenital hydrocephalus (ch/Mf1) arise from a winged helix/forkhead transcriptionfactor gene. *Hum Mol Genet* 8:625-37.
- Honkanen RA, Nishimura DY, Swiderski RE, Bennett SR, Hong S, Kwon YH, Stone EM, Sheffield VC, Alward WL (2003) A family with Axenfeld-

- Rieger syndrome and Peters Anomaly caused by a point mutation (Phe112Ser) in the FOXC1 gene. *Am J Ophthalmol* 135:368-75.
- Jakobiec F (1982) *Ocular Anatomy, Embryology, and Teratology*. Harper and Row Publishers, Philadelphia
- Jerome LA, Papaioannou VE (2001) DiGeorge syndrome phenotype in mice mutant for the T-box gene, Tbx1. *Nat Genet* 27:286-91.
- Jin C, Marsden I, Chen X, Liao X (1999) Dynamic DNA contacts observed in the NMR structure of winged helix protein-DNA complex. *J Mol Biol* 289:683-90.
- Johnston MC, Noden DM, Hazelton RD, Coulombre JL, Coulombre AJ (1979) Origins of avian ocular and periocular tissues. *Exp Eye Res* 29:27-43.
- Kaiser-Kupfer MI (1989) Neural crest origin of trabecular meshwork cells and other structures of the anterior chamber. *Am J Ophthalmol* 107:671-2.
- Kaufmann E, Knochel W (1996) Five years on the wings of fork head. *Mech Dev* 57:3-20.
- Kawase C, Kawase K, Taniguchi T, Sugiyama K, Yamamoto T, Kitazawa Y, Alward WL, Stone EM, Nishimura DY, Sheffield VC (2001) Screening for mutations of Axenfeld-Rieger syndrome caused by FOXC1 gene in Japanese patients. *J Glaucoma* 10:477-82.
- Kidson SH, Kume T, Deng K, Winfrey V, Hogan BL (1999) The forkhead/winged-helix gene, Mf1, is necessary for the normal development of the cornea and formation of the anterior chamber in the mouse eye. *Dev Biol* 211:306-22.

- Kodandapani R, Pio F, Ni CZ, Piccialli G, Klemsz M, McKercher S, Maki RA, Ely KR (1996) A new pattern for helix-turn-helix recognition revealed by the PU.1 ETS- domain-DNA complex. *Nature* 380:456-60.
- Koizumi K, Lintas C, Nirenberg M, Maeng JS, Ju JH, Mack JW, Gruschus JM, Odenwald WF, Ferretti JA (2003) Mutations that affect the ability of the vnd/NK-2 homeoprotein to regulate gene expression: transgenic alterations and tertiary structure. *Proc Natl Acad Sci U S A* 100:3119-24.
- Komatireddy S, Chakrabarti S, Mandal AK, Reddy AB, Sampath S, Panicker SG, Balasubramanian D (2003) Mutation spectrum of FOXC1 and clinical genetic heterogeneity of Axenfeld-Rieger anomaly in India. *Mol Vis* 9:43-8.
- Konig P, Rhodes D (1997) Recognition of telomeric DNA. *Trends Biochem Sci* 22:43-7.
- Kozlowski K, Walter MA (2000) Variation in residual PITX2 activity underlies the phenotypic spectrum of anterior segment developmental disorders. *Hum Mol Genet* 9:2131-9.
- Krebs LT, Xue Y, Norton CR, Shutter JR, Maguire M, Sundberg JP, Gallahan D, Closson V, Kitajewski J, Callahan R, Smith GH, Stark KL, Gridley T (2000) Notch signaling is essential for vascular morphogenesis in mice. *Genes Dev* 14:1343-52.
- Kulak SC, Kozlowski K, Semina EV, Pearce WG, Walter MA (1998) Mutation in the RIEG1 gene in patients with iridogoniodysgenesis syndrome. *Hum Mol Genet* 7:1113-7.

- Kume T, Deng K, Hogan BL (2000) Minimal phenotype of mice homozygous for a null mutation in the forkhead/winged helix gene, *Mf2*. *Mol Cell Biol* 20:1419-25.
- Kume T, Deng K, Hogan BL (2000) Murine forkhead/winged helix genes *Foxc1* (*Mf1*) and *Foxc2* (*Mfh1*) are required for the early organogenesis of the kidney and urinary tract. *Development* 127:1387-95.
- Kume T, Deng KY, Winfrey V, Gould DB, Walter MA, Hogan BL (1998) The forkhead/winged helix gene *Mf1* is disrupted in the pleiotropic mouse mutation congenital hydrocephalus. *Cell* 93:985-96.
- Kume T, Jiang H, Topczewska JM, Hogan BL (2001) The murine winged helix transcription factors, *Foxc1* and *Foxc2*, are both required for cardiovascular development and somitogenesis. *Genes Dev* 15:2470-82.
- Labbe E, Silvestri C, Hoodless PA, Wrana JL, Attisano L (1998) *Smad2* and *Smad3* positively and negatively regulate TGF beta-dependent transcription through the forkhead DNA-binding protein *FAST2*. *Mol Cell* 2:109-20.
- Lai CS, Fisher SE, Hurst JA, Vargha-Khadem F, Monaco AP (2001) A forkhead-domain gene is mutated in a severe speech and language disorder. *Nature* 413:519-23.
- Lehmann OJ, Ebenezer ND, Ekong R, Ocaka L, Mungall AJ, Fraser S, McGill JI, Hitchings RA, Khaw PT, Sowden JC, Povey S, Walter MA, Bhattacharya SS, Jordan T (2002) Ocular developmental abnormalities and glaucoma

associated with interstitial 6p25 duplications and deletions. *Invest Ophthalmol Vis Sci* 43:1843-9.

Lehmann OJ, Ebenezer ND, Jordan T, Fox M, Ocaka L, Payne A, Leroy BP, Clark BJ, Hitchings RA, Povey S, Khaw PT, Bhattacharya SS (2000) Chromosomal duplication involving the forkhead transcription factor gene FOXC1 causes iris hypoplasia and glaucoma. *Am J Hum Genet* 67:1129-35.

Li M, Moyle H, Susskind MM (1994) Target of the transcriptional activation function of phage lambda cI protein. *Science* 263:75-7.

Libby RT, Smith RS, Savinova OV, Zabaleta A, Martin JE, Gonzalez FJ, John SW (2003) Modification of ocular defects in mouse developmental glaucoma models by tyrosinase. *Science* 299:1578-81.

Lindsay EA, Vitelli F, Su H, Morishima M, Huynh T, Pramparo T, Jurecic V, Ogunrinu G, Sutherland HF, Scambler PJ, Bradley A, Baldini A (2001) Tbx1 haploinsufficiency in the DiGeorge syndrome region causes aortic arch defects in mice. *Nature* 410:97-101.

Lines MA, Kozlowski K, Walter MA (2002) Molecular genetics of Axenfeld-Rieger malformations. *Hum Mol Genet* 11:1177-84.

Ma L, Golden S, Wu L, Maxson R (1996) The molecular basis of Boston-type craniosynostosis: the Pro148-->His mutation in the N-terminal arm of the MSX2 homeodomain stabilizes DNA binding without altering nucleotide sequence preferences. *Hum Mol Genet* 5:1915-20.

- Mears AJ, Jordan T, Mirzayans F, Dubois S, Kume T, Parlee M, Ritch R, Koop B, Kuo WL, Collins C, Marshall J, Gould DB, Pearce W, Carlsson P, Enerback S, Morissette J, Bhattacharya S, Hogan B, Raymond V, Walter MA (1998) Mutations of the forkhead/winged-helix gene, FKHL7, in patients with Axenfeld-Rieger anomaly. *Am J Hum Genet* 63:1316-28.
- Mears AJ, Mirzayans F, Gould DB, Pearce WG, Walter MA (1996) Autosomal dominant iridogoniodygenesis anomaly maps to 6p25. *Am J Hum Genet* 59:1321-7.
- Merscher S, Funke B, Epstein JA, Heyer J, Puech A, Lu MM, Xavier RJ, Demay MB, Russell RG, Factor S, Tokooya K, Jore BS, Lopez M, Pandita RK, Lia M, Carrion D, Xu H, Schorle H, Kobler JB, Scambler P, Wynshaw-Boris A, Skoultschi AI, Morrow BE, Kucherlapati R (2001) TBX1 is responsible for cardiovascular defects in velo-cardio-facial/DiGeorge syndrome. *Cell* 104:619-29.
- Mirzayans F, Gould DB, Heon E, Billingsley GD, Cheung JC, Mears AJ, Walter MA (2000) Axenfeld-Rieger syndrome resulting from mutation of the FKHL7 gene on chromosome 6p25. *Eur J Hum Genet* 8:71-4.
- Moore MW, Klein RD, Farinas I, Sauer H, Armanini M, Phillips H, Reichardt LF, Ryan AM, Carver-Moore K, Rosenthal A (1996) Renal and neuronal abnormalities in mice lacking GDNF. *Nature* 382:76-9.
- Muller CW (2001) Transcription factors: global and detailed views. *Curr Opin Struct Biol* 11:26-32.

- Nishimura DY, Searby CC, Alward WL, Walton D, Craig JE, Mackey DA, Kawase K, Kanis AB, Patil SR, Stone EM, Sheffield VC (2001) A spectrum of FOXC1 mutations suggests gene dosage as a mechanism for developmental defects of the anterior chamber of the eye. *Am J Hum Genet* 68:364-72.
- Nishimura DY, Swiderski RE, Alward WL, Searby CC, Patil SR, Bennet SR, Kanis AB, Gastier JM, Stone EM, Sheffield VC (1998) The forkhead transcription factor gene FKHL7 is responsible for glaucoma phenotypes which map to 6p25. *Nat Genet* 19:140-7.
- Ormestad M, Blixt A, Churchill A, Martinsson T, Enerback S, Carlsson P (2002) Foxe3 haploinsufficiency in mice: a model for Peters' anomaly. *Invest Ophthalmol Vis Sci* 43:1350-7.
- Overdier DG, Porcella A, Costa RH (1994) The DNA-binding specificity of the hepatocyte nuclear factor 3/forkhead domain is influenced by amino-acid residues adjacent to the recognition helix. *Mol Cell Biol* 14:2755-66.
- Palmer CG, Bader P, Slovak ML, Comings DE, Pettenati MJ (1991) Partial deletion of chromosome 6p: delineation of the syndrome. *Am J Med Genet* 39:155-60.
- Panicker SG, Sampath S, Mandal AK, Reddy AB, Ahmed N, Hasnain SE (2002) Novel mutation in FOXC1 wing region causing Axenfeld-Rieger anomaly. *Invest Ophthalmol Vis Sci* 43:3613-6.
- Pfaffle RW, DiMattia GE, Parks JS, Brown MR, Wit JM, Jansen M, Van der Nat H, Van den Brande JL, Rosenfeld MG, Ingraham HA (1992) Mutation of

- the POU-specific domain of Pit-1 and hypopituitarism without pituitary hypoplasia. *Science* 257:1118-21.
- Pierrou S, Enerback S, Carlsson P (1995) Selection of high-affinity binding sites for sequence-specific, DNA binding proteins from random sequence oligonucleotides. *Anal Biochem* 229:99-105.
- Pierrou S, Hellqvist M, Samuelsson L, Enerback S, Carlsson P (1994) Cloning and characterization of seven human forkhead proteins: binding site specificity and DNA bending. *Embo J* 13:5002-12.
- Plaja A, Vidal R, Soriano D, Bou X, Vendrell T, Mediano C, Pueyo JM, Labrana X, Sarret E (1994) Terminal deletion of 6p: report of a new case. *Ann Genet* 37:196-9
- Priston M, Kozlowski K, Gill D, Letwin K, Buys Y, Levin AV, Walter MA, Heon E (2001) Functional analyses of two newly identified PITX2 mutants reveal a novel molecular mechanism for Axenfeld-Rieger syndrome. *Hum Mol Genet* 10:1631-8.
- Qian X, Costa RH (1995) Analysis of hepatocyte nuclear factor-3 beta protein domains required for transcriptional activation and nuclear targeting. *Nucleic Acids Res* 23:1184-91.
- Raymond V, Dubois S, Rodrigure M, Couture F, Anctil J, Cote G, Amyot M, Blondeau P, Bergeron E, Walter M, Morissette J (2001) Chromosomal duplication at the IRID1 locus on 6p25 associated with wide variability of the glaucoma phenotype. *American Journal of Human Genetics*. Vol. Supplemental 2632

- Sasaki H, Hogan BL (1993) Differential expression of multiple fork head related genes during gastrulation and axial pattern formation in the mouse embryo. *Development* 118:47-59.
- Semina EV, Reiter R, Leysens NJ, Alward WL, Small KW, Datson NA, Siegel-Bartelt J, Bierke-Nelson D, Bitoun P, Zabel BU, Carey JC, Murray JC (1996) Cloning and characterization of a novel bicoid-related homeobox transcription factor gene, RIEG, involved in Rieger syndrome. *Nat Genet* 14:392-9.
- Shields MB (1983) Axenfeld-Rieger syndrome: a theory of mechanism and distinctions from the iridocorneal endothelial syndrome. *Trans Am Ophthalmol Soc* 81:736-84
- Smith RS, Zabaleta A, Kume T, Savinova OV, Kidson SH, Martin JE, Nishimura DY, Alward WL, Hogan BL, John SW (2000) Haploinsufficiency of the transcription factors FOXC1 and FOXC2 results in aberrant ocular development. *Hum Mol Genet* 9:1021-32.
- Stevens K, Cirillo L, Zaret KS (2000) Creating temperature-sensitive winged helix transcription factors. Amino acids that stabilize the DNA binding domain of HNF3. *J Biol Chem* 275:30471-7.
- Suzuki T, Takahashi K, Kuwahara S, Wada Y, Abe T, Tamai M (2001) A novel (Pro79Thr) mutation in the FKHL7 gene in a Japanese family with Axenfeld-Rieger syndrome. *Am J Ophthalmol* 132:572-5.
- Swiderski RE, Reiter RS, Nishimura DY, Alward WL, Kalenak JW, Searby CS, Stone EM, Sheffield VC, Lin JJ (1999) Expression of the Mfl gene in

developing mouse hearts: implication in the development of human congenital heart defects. *Dev Dyn* 216:16-27.

Takahashi Y, Koizumi K, Takagi A, Kitajima S, Inoue T, Koseki H, Saga Y (2000) *Mesp2* initiates somite segmentation through the Notch signalling pathway. *Nat Genet* 25:390-6.

Topczewska JM, Topczewski J, Shostak A, Kume T, Solnica-Krezel L, Hogan BL (2001) The winged helix transcription factor *Foxc1a* is essential for somitogenesis in zebrafish. *Genes Dev* 15:2483-93.

Topczewska JM, Topczewski J, Solnica-Krezel L, Hogan BL (2001) Sequence and expression of zebrafish *foxc1a* and *foxc1b*, encoding conserved forkhead/winged helix transcription factors. *Mech Dev* 100:343-7.

Ulyanov NB, Bauer WR, James TL (2002) High-resolution NMR structure of an AT-rich DNA sequence. *J Biomol NMR* 22:265-80.

van Dongen MJ, Cederberg A, Carlsson P, Enerback S, Wikstrom M (2000) Solution structure and dynamics of the DNA-binding domain of the adipocyte-transcription factor FREAC-11. *J Mol Biol* 296:351-9.

Vitelli F, Taddei I, Morishima M, Meyers EN, Lindsay EA, Baldini A (2002) A genetic link between *Tbx1* and fibroblast growth factor signaling. *Development* 129:4605-11.

Weigel D, Jackle H (1990) The fork head domain: a novel DNA binding motif of eukaryotic transcription factors? *Cell* 63:455-6.

- Weigelt J, Climent I, Dahlman-Wright K, Wikstrom M (2001) Solution structure of the DNA binding domain of the human forkhead transcription factor AFX (FOXO4). *Biochemistry* 40:5861-9.
- Winnier GE, Kume T, Deng K, Rogers R, Bundy J, Raines C, Walter MA, Hogan BL, Conway SJ (1999) Roles for the winged helix transcription factors MF1 and MFH1 in cardiovascular development revealed by nonallelic noncomplementation of null alleles. *Dev Biol* 213:418-31.
- Yamagishi H, Maeda J, Hu T, McAnally J, Conway SJ, Kume T, Meyers EN, Yamagishi C, Srivastava D (2003) Tbx1 is regulated by tissue-specific forkhead proteins through a common Sonic hedgehog-responsive enhancer. *Genes Dev* 17:269-81.
- Yeo CY, Chen X, Whitman M (1999) The role of FAST-1 and Smads in transcriptional regulation by activin during early *Xenopus* embryogenesis. *J Biol Chem* 274:26584-90.
- Zhou S, Zawel L, Lengauer C, Kinzler KW, Vogelstein B (1998) Characterization of human FAST-1, a TGF beta and activin signal transducer. *Mol Cell* 2:121-7.
- Zhou Y, Kato H, Asanoma K, Kondo H, Arima T, Kato K, Matsuda T, Wake N (2002) Identification of FOXC1 as a TGF-beta1 responsive gene and its involvement in negative regulation of cell growth. *Genomics* 80:465-72.
- Zurcher VL, Golden WL, Zinn AB (1990) Distal deletion of the short arm of chromosome 6. *Am J Med Genet* 35:261-5.